Discovery and Optimization of Pyrrolopyrimidine Derivatives as Selective Disruptors of the Perinucleolar Compartment, a Marker of Tumor Progression toward Metastasis

Kevin J. Frankowski[a,b,*], Samarjit Patnaik[c,*], Chen Wang[d], Noel Southall[c], Dipannita Dutta[c], Soumita De[e], Dandan Li[e], Christopher Dextras[c], Yi-Han Lin[c], Marthe Bryant-Connah[c], Danielle Davis[c], Feijun Wang[b], Leah M. Wachsmuth[c], Pranav Shah[c], Jordan Williams[c], Md Kabir[c], Edward Zhu[c], Bolormaa Baljinnyam[c], Amy Wang[c], Xin Xu[c], John Norton[d], Marc Ferrer[c], Steve Titus[c], Anton Simeonov[c], Wei Zheng[c], Lesley A. Mathews Griner[c], Ajit Jadhav[c], Jeffrey Aubé[a,b], Mark J. Henderson[c], Udo Rudloff[e], Frank J. Schoenen[a], Sui Huang[d,*], Juan J. Marugan[c,*]

[a]KU Specialized Chemistry Center, University of Kansas, 2034 Becker Drive, Lawrence, KS 66047.

[b]Center for Integrative Chemical Biology and Drug Discovery, UNC Eshelman School of Pharmacy, University of North Carolina at Chapel Hill, Chapel Hill, NC 27599.

[c]National Center for Advancing Translational Sciences, National Institutes of Health, 9800 Medical Center Drive, Rockville, MD 20850.

[d]Department of Cell and Molecular Biology, Northwestern University, Chicago, IL 60611.

[e]Rare Tumor Initiative, Pediatric Oncology Branch, National Cancer Institute, National Institutes of Health, 10 Center Drive, Bethesda, MD 20892.

Abstract

The perinucleolar compartment (PNC) is a dynamic subnuclear body found at the periphery of the nucleolus. The PNC is enriched with RNA transcripts and RNA-binding proteins, reflecting different states of genome organization. PNC prevalence positively correlates with cancer progression and metastatic capacity, making it a useful marker for metastatic cancer progression. A high-throughput, high-content assay was developed to identify novel small molecules that selectively reduce PNC prevalence in cancer cells. We identified and further optimized a pyrrolopyrimidine series able to reduce PNC prevalence in PC3M cancer cells at submicromolar concentrations without affecting cell viability. SAR exploration of the structural

elements necessary for activity resulted in the discovery of several potent compounds. Analysis of *in vitro* drug-like properties led to the discovery of the bioavailable analogue, metarrestin, which has shown potent antimetastatic activity with improved survival in rodent models and is currently being evaluated in a first-in-human Phase 1 clinical trial.

Graphical Abstract
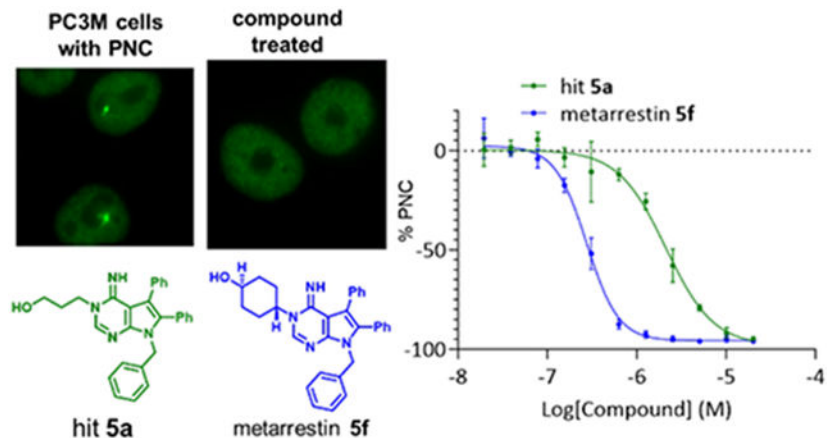
Introduction

Cancer remains the second-leading cause of death in the United States with metastasis, the process by which primary tumors disseminate throughout the body to secondary sites, as the foremost cause of mortality for >90% of cancer patients.[1, 2] Over the past decades, extensive efforts have gone into understanding the underlying mechanisms of metastasis; however, many of the key factors and requirements for metastatic transformation and tumor progression remain largely unknown, thus making specific anti-metastatic drug development difficult.[3-9]

The search for therapeutic tools specifically impacting the metastatic processes has led to the discovery and advancement of matrix metalloproteinase inhibitors (MMPIs), bisphosphonates, and antiangiogenesis agents to the clinic.[9-12] However, each has had limited clinical success, and currently, there is no approved treatment that selectively targets metastatic progression. Given both the clinical need and the complexity of metastatic disease mechanisms, we decided to pursue a previously unexplored approach and focused on phenotypic markers of genome organization that reflect cellular genomic state characteristics unique to metastatic cancer cells. One such marker identifying cancer cells competent to metastasize is the perinucleolar compartment (PNC).[13] The PNC, similar to other ribonucleoprotein particles (RNPs), seems to be associated with specific cellular states, is a membrane-less, highly dynamic subnuclear body that is driven by polymerase I transcription

known to be upregulated in metastasis and liquid–liquid phase separation (LLPS). Recently, Yap and colleagues have identified the long non-coding RNA (lncRNA) strRNA57, a 10-kb Pol I rDNA intergenic spacer transcript that contains several hundred binding motifs for the ubiquitously expressed heterogeneous nuclear ribonucleoproteins (hnRNP) polypyrimidine tract-binding protein 1 (PTBP1), as an essential element for PNC formation and PNC maintenance in cancer cells.[14] The PNC structure forms only in cancer cells, but not in normal, non-transformed cells —including embryonic stem cells.[15] PNC prevalence (the percentage of cells with at least one PNC) positively associates with disease progression in several solid-organ cancers and negatively associates with patient outcomes.[16, 17] PNC prevalence increases with disease progression for breast, ovarian, and colorectal cancers, and reaches near 100% in distant metastases.[16, 17] A high PNC prevalence in early stage breast cancer associates with poor patient outcomes.[17] The close association of PNC with metastatic capabilities of cancer cells in vitro and in vivo makes PNC prevalence a robust surrogate marker for cancer metastasis. Thus, PNC reduction may be used as a phenotypic marker to identify novel therapeutic compounds that may interfere with essential genome organization processes required for metastasis and may induce changes that lead to the prevention and inhibition of cancer metastasis.

Here, we disclose our work identifying and developing novel compounds that reduce PNC prevalence at concentrations where cell viability is not affected. We detail a medicinal chemistry optimization campaign around a pyrrolopyrimidine series that ultimately led to the discovery of the clinical candidate metarrestin (NCATS-SM0590, Figure 1). Metarrestin's selectivity to arrest cancer versus normal cell growth, ability to block metastasis in multiple *in vivo* metastatic models, lack of overt toxicity, and favorable PK profile, as previously demonstrated, facilitated the FDA approval toward its current evaluation in a first-in-human Phase I trial to investigate its safety and clinical activity in subjects with metastatic solid tumors.[18, 19]

Results and Discussion

Screening and Hit Triage

To identify novel, PNC-disrupting small molecules we performed a high-throughput screening (HTS) campaign of the NIH Molecular Libraries Small Molecule Repository (MLSMR), testing 140,800 compounds for reduction of PNC prevalence using a high-content assay (HCA) that utilized PC3M cells that stably expressed a GFP (green fluorescent protein)-PTB (polypyrimidine track binding) protein for detection of the PNC.[20] The PTB protein is a RNA-binding protein involved in many aspects of RNA metabolism, and is an essential structural component of the PNC.[14, 21] The stable expression of GFP-PTB allows for one-step detection of PNC prevalence making it amenable for high-content screening. A lncRNA with hundreds of PTBP1-specific motifs known to sequester a substantial fraction of PTBP1 has recently been shown to be an essential component of PNC formation and maintenance. Cells were incubated with compounds for 16 hours, fixed with paraformaldehyde, and treated with Hoechst 33342 (Thermofischer Scientific) to stain the cell nucleus. Plates were imaged on an IN Cell™ Analyzer 1000 (GE Healthcare Life Sciences) automated microscope using a 20X objective, a standard FITC filter set, with

an exposure time of ~100-150 msec/well. The PNC prevalence was determined using the Multitarget Analysis Module present in the IN Cell™ Workstation software (V3.5).[21] Signal-to-background was on average 15-fold, and Z' factor was on average 0.6, demonstrating a robust high-content screening assay. This effort identified 4,338 compounds that reduced PNC prevalence below 5% (vehicle treated wells were at about 50-60%). After these compounds were retested, 121 (1.1%) compounds reconfirmed their activity in the screening assay using a higher stringency cutoff on a minimum number of cells in the well to avoid cytotoxic compounds. Subsequently, new samples of 119 compounds were tested in a 12-point titration from 50 μM to 25 nM in triplicate, which led to 93 active compounds. Structural analysis classified the active compounds into 25 clusters and 25 singletons. The effect of compounds on cell viability after 24 h treatment was measured using the ATPlite™ luminescence assay for cellular ATP levels. Using this cell viability data, the HTS-active compounds were further categorized into three compound classes: 26 compounds with no decrease in ATP, 18 with strong decrease in ATP (i.e., −80% or more), and 49 with weak decrease in ATP (ca. −30 to −79%). A caspase 3/7 assay was used as an orthogonal measure of cytotoxicity. Furthermore, a DNA-displacement PicoGreen assay was utilized to exclude possible DNA intercalators previously known to have a PNC-disassembling effect as part of their genotoxic and cytotoxic activity. Finally, representative compounds from twelve chemical classes were analyzed for activity in a BellBrooks Labs® tumor cell migration assay. This extensive characterization yielded two high-priority chemotypes, CID 790407 (AC_{50} of 1.98 μM) and CID 5152963 (AC_{50} of 0.83 μM), that were active in the PNC HCA and the invasion assay, but inactive in all other secondary cytotoxicity/viability assays. It was critical that the novel PNC modulators had no impact on cell viability so that the sought anti-metastatic effect are separated from any genotoxic or cell killing function. Notably, only two chemotypes, CID 790407 and 5152963 were progressed to medicinal chemistry optimization (Figure 2).

Structure–Activity Relationship (SAR) Studies

Of the two candidates from the HTS campaign, we first optimized the thiophene hit compound (CID 790407, Figure 2) that emerged from the screening with an AC_{50} of 1.98 μM in the HCA. Several analogues were synthesized, in which we systematically explored possible replacements of the thiophene and the *meta*-pyridyl groups, as well as substitutions around them. A further number of alternatives to the amide linker between the aryl groups were also synthesized. However, all analogues proved to be inactive and the thiophene series was not pursued further.

In parallel to the ultimately unsuccessful exploration of the thiophene chemotype, we started a complementary effort to expand the SAR around the pyrrolopyrimidine hit compound (CID 5152963, Figure 2). We developed a robust synthetic approach that allowed us to access a wide range of analogues and modify the groups attached to both nitrogen- and carbon- positions of the scaffold. Our approach is exemplified by the two general synthetic routes that, with slight modifications allowed access to most of the analogues in this study (Schemes 1 and 2). The ketone-containing analogue **5n** was accessed via oxidation of the hydroxy analogue **5f** (Scheme 3). We exploited the Knoevenagel condensation approach for pyrrole construction developed by Roth and Eger.[22] The aminopyrroles **2**

were converted to the ethyl formimidates **3**, which could then be cyclized to the final pyrrolopyrimidine derivatives **5** upon heating with the appropriate amine in methanol.[23] The monophenylpyrrole analogue synthesis utilized an analogous approach starting from chlorobenzophenone **6** and using the protocol developed by Yumoto *et al.*[24] The amino pyrrole **8** was converted to the formimidate **9** and then alkylated with benzyl bromide to give the penultimate intermediate **10**. Final pyrrolopyrimidine derivatives **11** were again obtained from heating with the appropriate amine in methanol. Using these two related synthetic routes, we were able to construct the vast majority of analogues in this SAR study. The analogues were screened in the high-content assay for PNC disassembly using the same PC3M-PTB-GFP reporter cell line that was used in the screen (Tables 1-7). The image analysis was done using the IN Cell™ Analyzer 1000 and later with the Opera Phenix Plus High-Content Screening System (Perkin Elmer) after 24 h incubation with analogues. As with other phenotypic screens, the observed compound activity in the PNC disassembly assay is a combination of target potency and compound physicochemical properties that facilitate cellular penetration and requisite localization. In an effort to correlate physical properties of analogues with observed PNC reduction activity, we estimated the lipophilicity (cLogP) of all analogues and experimentally determined the permeability of most analogues in PAMPA (Parallel artificial membrane permeability assay from Pion Inc.). While no global correlations were found, specific activity–liposphilicity or permeability associations of potential interest are discussed below along with the observed SAR trends. We also assessed the stability of most analogues for degradation to isolated CD1 mouse liver microsomes (MLM) and identified a couple notable trends between functional groups and observed stability, as detailed in the SAR discussion below.

We began our SAR investigation of this scaffold by varying the chain length of the *N*-3 hydroxypropyl group of the HTS hit **5a** and found that while the smaller ethyl analogue **5b** was over twice as potent, the butyl and pentyl analogues (**5c** and **5d**, respectively) were slightly less potent than **5a**. Capping the free hydroxyl as in the methyl ether **5e** reduced the potency of **5b** over ten-fold (9.31 μM). Constraining the conformation of the alkyl chain as a cyclohexyl ring (analogue **5f**) afforded a dramatic increase in potency (ca. 9-fold, 0.20 μM). We initially synthesized the analogue with the hydroxyl in the *trans* configuration and later tested the *cis*-configuration analogue **5g**, which was surprisingly less potent in the PNC reduction assay (ca. four-fold, 0.83 μM). The reduced activity of **5g** reveals the nuanced relationship between hydroxy conformation and PNC activity. The stereoisomeric analogues **5f** and **5g** possessed identical cLogP values and high PAMPA permeability values, therefore, the potency reduction most likely arises from reduced interaction of the *trans* isomer with the molecular target. Both the *trans* and *cis* isomers possessed excellent stability to liver microsomes (120 mins and 52.3 mins for **5f** and **5g**, respectively), which contributed to the decision on the preclinical development of **5f**. The 1,2-substituted constitutional isomer **5h** was 2.5-fold less potent compared to the 1,4-substituted compound **5f**. Insertion of a methylene linker between the cyclohexane ring and the *N*-3 position on the pyrimidine scaffold resulted in further reduced potency (**5i**, 2.00 μM vs. **5h**, 0.51 μM). The methylene linked cyclohexanol **5i** was found to possess low stability in liver microsomes (2.4 mins). The alternative methylene insertion between the cyclohexane ring and the hydroxyl group was also detrimental, though less drastically (**5j**, 0.93 μM vs. **5h**, 0.51 μM). Notably, all

analogues from this series (**5a** to **5j**) that were evaluated in PAMPA and found to possess excellent permeability. The branched linear hydroxy chain analogues **5k** and **5l** lost all PNC reduction activity (>20 μM), though both **5k** and **5l** also bore an additional phenyl group as well. The structurally similar analogues **5k** and **5l** possessed nearly identical cLogP values, however **5k** possessed low PAMPA permeability while **5l** modest permeability (606 × 10⁻⁶ cm/sec). This observation highlights the limitations in using simple, calculated metrics such as cLogP to stand in for experimental values. Both analogues also possessed reduced liver microsome stability compared to earlier analogues (except **5i**), likely related to the addition phenyl group. In contrast to the open-chain exemplar **5e** above, capping the hydroxycyclohexyl as the methyl ether analogue **5m** possessed comparable potency (0.25 μM) to **5f**. Both the cyclohexanone analogue **5n** and the tetrahydropyran analogue **5o** also possessed comparable potency (0.30 μM) to the *trans*-hydroxycyclohexane analogue **5f**, however both **5n** and **5o** possessed slightly lower stability to MLM. Together the retention of potency for analogues **5m**–**5o** demonstrate that a free hydroxy moiety is not critical for PNC reduction activity. The range of cLogP values (3.94–5.06) for the comparably potent analogues **5f** and **5m**–**5o** indicate that these functional groups may warrant further investigation or modification. The methylene-tethered tetrahydropyran **5p** was drastically less potent (10.86 μM) than **5o** or even the methylene-tethered analogue **5i**. The methylene-tethered tetrahydrofuran analogues **5q** and **5r** possessed only modest potency (10.86 μM and 9.31 μM, respectively). Further contraction of ring size, as in the oxetane analogue **5s**, resulted in loss of all PNC reduction potency and a very low observed PAMPA permeability. We also explored other tethered functional groups, such as the diethylacetal analogue **5t**, which possessed only very low activity (23.4 μM). Nitrogen-containing groups were also explored on the *N*-3 pyrimidine sidechains, with the *N*-4-pyridylaminoethyl analogue **5u**, *N*,*N*-dimethylaminoethyl analogue **5w**, and *N*-benzyl-4-piperidinyl analogue **5y** affording modestly potent analogues (2.95 to 6.59 μM). Other nitrogen-containing analogues (i.e., **5v**, **5x** and **5z**) were less potent (12.59 to >20 μM). Interestingly, the primary amine **5v** was markedly less potent than the dimethyl tertiary amines **5w** and **5x** The low PAMPA permeability and cLogP of **5v** might contribute to the drastic reduction in potency. Analogue **5x** possessed unexpected stability in MLM for an amine-containing molecule ($T_{1/2}$ 120 mins). In a singular example, the 3,4-dimethoxyphenethyl analogue **5aa** possessed only marginal potency (25.12 μM) and further aryl-containing analogues were not explored.

We also synthesized a series of *N*-3 position-substituted analogues where the *N*-7 benzyl was replaced with *N*-7 phenethyl (**5bb** to **5jj**). Many of the analogues reproduced the trends observed in the *N*-7 benzyl series discussed above. Like its *N*-7 benzyl counterpart **5c**, the *N*-3 hydroxybutyl analogue **5cc** lost potency (c.a. three-fold) and liver microsome stability compared to the ethyl analogue **5bb**. The *trans*-1,4-substituted compound *5dd*, analogous to **5f**, was also the most potent of the phenethyl series with an AC_{50} of 0.34 μM. A similar trend in potency reduction upon insertion of a methylene linker between the cyclohexane ring and the *N*-3 position on the pyrimidine ring was also observed for this series as demonstrated by **5ee** (2.72 μM). Analogous to analogue **5i**, this functional group was again associated with marked reduction in liver microsome stability. In contrast to the previous trend in the benzyl series, the tetrahydropyran analogue **5ff** exhibited an almost three-fold reduction in potency (0.96 μM) and over eight-fold reduction in liver microsome

stability (14.5 mins) compared to the *trans*-hydroxycyclohexane analogue **5dd**. Tethering the tetrahydropyran group to a methylene resulted in a further potency loss (**5gg**, 10.00 μM). The methylene tetrahydrofuran analogues **5hh** and **5ii** possessed only moderate potency (10.86 and 7.94 μM, respectively) and poor liver microsome stability (6.9 and 8.4 mins, prespectively). The nitrogen-containing analogue **5jj** was the least potent of the series (12.59 μM), the same potency to the corresponding *N*-7 benzyl analogue **5x**.

In addition to the *N*-7 phenethyl analogues, we also explored other alternative *N*-7 pyrrole substituents. We evaluated three different *para*-substitutions, as shown in Table 4, at the *N*-7 pyrrole benzyl moiety: an electron donating methoxy (**5kk**–**5pp**), and electron withdrawing trifluoromethoxy (**5qq**–**5uu**) and sulfonamide groups (**5vv**–**5xx**). The prior structure–activity trends identified largely held when applied across these *para*-substituted benzyl analogues; within each subset the tetrahydropyran analogues and the *trans* 4-hydroxycylohexane analogues were most potent. The *para*-methoxybenzyl substituent afforded similar potencies to the benzyl and phenethyl counterparts; as observed by comparing the *trans*-4-hydroxycylohexane analogues **5mm**, **5ee** and **5f**. Notably, the permeability and liver microsome stability of **5mm** was equaled that of **5f**. On the other hand, *para*-trifluoromethoxybenzyl and *para*-sulfonamidobenzyl afforded appreciably less potent compounds. Of the *para*-sulfonamidobenzyl analogues **5vv**–**5xx**, the tetrahydropyran analogue **5ww** possessed the greatest potency (1.18 μM). The cLogP values for these analogues were markedly lower (2.19–2.81) than other analogues, highlighting the striking effect of the polar primary sulfonamide group on physicochemical properties; this set of compounds also had low permeability with negligible values in the PAMPA assay..

In contrast, *N*-7 alkyl groups afforded analogues of generally low potency (**5yy** to **5ddd**, Table 5), with the interesting exception of the *N*-3 tetrahydropyran analogue combined with the pyrrole *N*-methylene cyclopropyl group (**5ccc**, 0.83 μM). The liver microsome stability of **5ccc** (68.0 mins) was also more favorable than the other cyclopropyl analogues explored. The cyclopropyl analogues **5bbb**–**5ddd** possessed a range of activity (0.83–34.35 μM) and fairly consistent cLogP values (3.49–4.11) and high permeability, which indicated that the differences in potency are more likely due to interactions with the target.

We concurrently investigated the effect of replacing the *C*-5 and *C*-6 phenyl groups (Table 6). Replacing both phenyl groups with either *para*-methoxyphenyl or 3,4-methylenedioxyphenyl resulted in analogues (**5eee** to **5lll**, Table 6) with negligible activity. We attempted to reduce the molecular weight and aromatic content of the series through phenyl replacement with hydrogen or alkyl groups. Replacement of the *C*-6 phenyl group with hydrogen afforded only inactive analogues with poor liver microsome stability (**11a** to **11d**, Table 6). Similarly, replacement of both phenyl groups with either methyl groups or a four-carbon tether resulted in a complete loss of potency (**5mmm** to **5rrr**, Table 6). The methyl-subsituted pyrrole analogues **5mmm** to **5ooo** possessed the lowest cLogP values of any analogues tested (1.59–1.91), however the PAMPA permeability ranged widely from negligible (**5nnn**) to highly permeable (**5ooo**). True cellular permeability is more complex than the eperimental PAMPA permeability and while it is tempting to extrapolate the drop in cLogP values with a possible decrease in cell permeability, the inactivity of

all other phenyl group replacments (i.e., analogues **5eee** to **5lll**, **11a** to **11d** and **5ooo** to **5rrr**) likely reflects the critical role of the unsubstituted phenyls on the pyrrole ring. With the exception of the hyroxypropyl analogue **5ppp**, the phenyl–alkyl modification retained suitable liver microsome stability. Though the SAR efforts on phenyl replacement were far from comprehensive, this survey of phenyl replacements highlights the challenges of reducing the aromatic content in this series. Select inactive analogues may be useful as inactive control compounds, most notably the analogues **11a** and **11b**. The synthetic intermediates **2a**, **3a**, and **4f**, *enroute* to **5f** (metarrestin), were also evaluated for their PNC inhibitory activity and found to be inactive (Table 7).

During the above SAR investigations, we realized that while stable under ambient conditions, the *N*-3 substituted (amidine) analogues (Tables 2-6) could be forced to undergo a Dimroth rearrangement to the fully aromatic isomers under high-pressure heating with water and a cosolvent (Scheme 4). Our typical conditions were a 1:3 ratio of water:isopropanol under microwave irradiation at 150 °C for two hours, a modification of the protocol developed by Fischer and Misun on the Dimroth rearrangement of pyrrolopyrimidines.[25] In order to distinguish between the starting analogues and the Dimroth rearranged isomers, we sought a spectroscopic identification method. While the NMR spectra for the isomers were consistently very similar, we were able to identify characteristic IR absorption bands corresponding to the starting and Dimroth-rearranged pyrrolopyrimidine isomers (ca. 1620 and 1590 cm^{-1}, respectively). We examined a small series of Dimroth-rearranged isomer analogues derived from active analogues (**13a**–**13b**, Table 7), which were uniformly inactive in reducing PNC prevalence. Though completely inactive in the PNC disassembly assay, the construction of these analogues allowed us to confidently affirm the structural identity of the analogues in Tables 2-6. Even more importantly, the Dimroth rearrangement provided ready access to isomeric, inactive control compounds for mechanism-of-action and other studies.

The SAR campaign detailed above, and the most noteworthy general trends identified for this chemical series are summarized in Figure 3. We observed that substitution at the *N*-3 and *N*-7 positions was amenable to variation, while replacement of the *C*-5 and *C*-6 phenyl groups —even with substituted phenyl groups— was highly detrimental to PNC disassembling activity. At the *N*-3 position, a range of hydroxyl and ether-bearing groups afforded potent analogues, though the potency was highly sensitive to the configuration and steric considerations. Even certain nitrogen-containing side chains were tolerated at this site. The *N*-7 position accommodated a range of aryl-containing sidechains attached via a one- or two-carbon tether length. Purely aliphatic side chains generally afforded low-potency analogues, with the notable exception of the cyclopropyl analogue **5ccc**. All the pyrrolopyrimidine analogues could undergo a Dimroth rearrangement to afford fully aromatic though inactive constitutional isomers, which reinforces the specific steric and configuration requirements for this series.

In addition to PNC inhibitory activity, we screened all analogues in Tables 1-7 for cell viability (CellTiterGlo™ luminescence assay from Promega) and detected marginal effects on ATP levels after 24 h, the time point at which we examined for PNC reduction. This was important to differentiate the PNC reduction phenotype from general cytotoxicity. In

addition, we incubated the compounds for 48 h and discovered that some analogues were associated with reductions of ATP levels at the highest concentration tested (10 μM). PNC reduction along with viability at 24 and 48 h concentration-response curves for select compounds are showcased in Figure 4. **5f** (metarrestin) shows a ~38-fold window between PNC reduction and 48 h viability. The window is smaller for the hit and much narrower for positive controls camptothecin and doxorubicin, highlighting the potential for these pyrrolopyrimidine PNC inhibitors to serve as a new generation of more selective cancer therapeutics compared to genotoxic chemotherapeutics with their associated liabilities of narrow therapeutic windows and—not infrequently—deleterious side effects.

Extended characterization of key analogues

As mentioned above, a key strategy in our SAR campaign was to establish a window between PNC disassembly and cytotoxicity. As PNC disassembly was assumed to correlate with antimetastatic activity, it was desirable to study concentration-dependent compound effects on cell proliferation and migration *in vitro* as a surrogate for later *in vivo* activity. Such a strategy has been shown to guide the interpretation of *in vivo* studies where we would look at reduction of metastatic tumor burden while monitoring primary tumor growth. To that end, we used the Incucyte® platform to examine proliferation of live PC3M-PTB-GFP cells where the reduction of PNC prevalence was used to drive the SAR campaign. The plot in Figure 5 shows the % confluence of PC3M-PTB-GFP cells with 11-point dilution of **5f** (metarrestin) and compares it with hit **5a** and inactive analogue **11b**. Cell growth was measured every four hours for a period of 130 h. For low concentrations (<100 nM), both hit **5a** and **5f** show similar modest concentration-dependent delay of cell proliferation, still being able to reach confluency. However, at concentrations >100 nM, we observe **5f** starts to show a greater capacity to inhibit cell proliferation than hit **5a**; this is pronounced at 10 μM (orange curves). Both compounds **5a** and **5f** exhibit slight cytotoxicity at the highest concentration of 20 μM. The inactive control **11b** hardly showed any concentration-dependent effects on cell proliferation with a modest effect at 20 μM.

Thus, at single-digit micromolar concentrations, **5f** (metarrestin) induces growth arrest in cancer cells with high PNC prevalence in the range of 48–72 hours without promoting cell apoptosis, having no effect on the growth of normal cells or early-stage cancer cells with no detectable PNC prevalence.[17] In our hands, this observed selective cytostatic effect seems to be irreversible after several days of exposure to **5f** (metarrestin), leaving the cells in a senescent-like stage.

We also evaluated hit **5a** and lead **5f** in the NCI-60 panel (Supplementary Information, Figures S1 and S2), a collection of 60 human cancerous cell lines used by the National Cancer Institute for the development and screening of novel anticancer drugs. This panel allows the evaluation of compounds in 60 cell lines representing leukemia, melanoma, non-small-cell lung carcinoma, and cancers of the brain, ovary, breast, colon, kidney, and prostate. Concentration-dependent growth inhibition was observed (1 μM) across all cell lines; at the highest concentration (100 μM), we observed cell death in all cell lines. Thus, the chemical series appears to inhibit growth across advanced cancer cell lines at concentrations that overlap with PNC reduction activity. An analysis with the COMPARE

algorithm,[26] which compares activity in the NCI-60 panel to previously tested molecules, suggested that the hit **5a** and lead **5f** (metarrestin) have a novel mode of action. We have demonstrated that **5f** (metarrestin) is involved in the modulation of the RNA Polymerase I activity and nucleolus assembly in advanced cancer cells, a previously not employed anti-cancer mechanism.[18] Metarrestin-selective inhibition of polymerase 1 transcription and pre-RNA synthesis in cancer cells with high PNC prevalence suggests that inhibition of ribosomal function and protein synthesis in metastatic cells promotes growth arrest and eventually an irreversible senescent-like stage.

Since the PNC is located at the periphery of the nucleolus, we have investigated and reported its effects on the nucleolar structure of cancer cells with high PNC prevalence and observed that **5f** (metarrestin) shrinks nucleolar volume, disrupts nucleolar ultrastructure, and ultimately alters ribosomal distribution in cells.[18] Having developed the SAR against the PNC disassembly, we wanted to check if key elements of the SAR would track with effects on nucleolar volume and integrity. To that end, we compared hit **5a**, **5f** (metarrestin) and the inactive analog **11b** for their ability to reduce nucleolar volume in PC3M cells. While the inactive analog did not influence nucleolar integrity and morphology, both **5a** and **5f** were able to reduce nucleolar volume (volume of bright spots in Figure 6B) in a concentration-response manner with similar potencies (Figure 6A). Images of the nucleoli (bright spots) in the nucleus (diffuse faint blue) after treatment with **5f** (metarrestin) and inactive control **11b** at 1 and 30 μM are shown in Figure 6B. A closer look at the nucleolar architecture was conducted with **5f** (metarrestin) and the inactive analog **11b** by examining their effect on the RNA-synthesis marker RP-194 and ribosomal pre-assembly regulator NOPP140 (Figure 6C). The diffuse distribution off RP-194 and NOPP140 which was observed in the DMSO and **11b**-treated cells was disrupted with **5f** (metarrestin) treatment which, instead, showcased a punctate distribution of these markers in the nucleolus. Thus, with this limited set of compounds, we think that SAR observed in PNC disassembly translates to overarching effects on the nucleolus structure.

To assess potential off-target interactions with biological targets, the lead compound **5f** (metarrestin) was screened against 44 GPCR- and CNS-relevant targets in the Psychoactive Drug Screening Program's comprehensive binding-affinity panel (Table 8). With the exception of the sigma 2 receptor, **5f** did not possess sub-micromolar affinity for any of the targets. This assessment for potential off-target effects correlates well with the observed tolerability of **5f** (metarrestin) in subsequent animal studies.[18,27,28] To investigate potential interference with oxidative metabolism pathways, we previously reported the effect of **5f** on a panel of CYP enzymes.[28]

Analysis of drug-like properties

Focusing closer on four potent PNC inhibitors with AC_{50} 300 nM (**5f**, **5n**, **5o**, and **5dd**) we decided to evaluate their drug-like properties and compare them with hit **5a**. While all compounds appeared to have high passive permeability as determined via PAMPA, analogues **5f** and **5dd** had better aqueous kinetic solubility and stability in MLM (Table 9) than the rest.
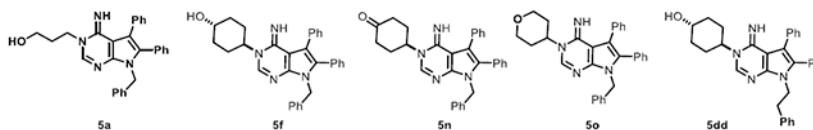
Hit **5a** was initially chosen as a benchmark for pharmacokinetic evaluation of the chemical series. After a single 50 mpk dose was administered via intraperitoneal injection (IP) in male C57BL/6 mice, plasma concentrations were monitored for 48 h (Figure 7). The hit was able to achieve a C_{max} of 9.90 μM with an AUC_{48h} of 26.0 hr*μM and terminal $T_{1/2}$ of 4.1 h, which indicate that the initial 50 mpk dose was in excess of that required to reach therapeutically relevant levels. Subsequently analogue **5f** (metarrestin), with the best combination of microsome stability and aqueous solubility was evaluated at two ascending IP doses of 5 and 25 mpk. At a 25 mpk dose, **5f** (metarrestin) afforded high drug levels in the plasma with a C_{max} of 6.2 μM at 30 minutes and a C_{last} as high as 0.5 μM at 48 hours; this dose has been used for multiple dose studies with no observable toxicity and pronounced efficacy in reducing metastatic tumor burden in three different models.[18] A low 5 mpk IP dose also provided a C_{max} of 0.91 μM and average concentrations of 146 and 23 nM at 12 and 24 h, respectively. Figure 7 summarizes the concentration vs. time curves for **5f** (metarrestin) and Table 10 summarizes calculated PK parameters. We have recently reported the details of the formulation and PK dosing of **5f** (metarrestin) in wild-type and autochthonous KPC (Pdx1-Cre;LSL-KrasG12D/+;Tp53R172H/+) mice, the latter of which is a murine pancreatic cancer mouse model mimicking drug distribution of human disease.[27] We have also reported the metabolism and pharmacokinetics of **5f** (metarrestin) in multiple species.[28] These studies indicate that **5f** (metarrestin) has a characteristic slow clearance in multiple species and we expect to see a similar profile in phase I human clinical trials (ClinicalTrials.gov Identifier: NCT04222413).

Conclusion

In summary, our HTS campaign successfully identified compounds that reduced the prevalence of PNC through the utilization of a high-content assay that used a GFP–PTB transgene for the detection of, and changes to, the PNC, a marker of genome organization associated with metastasis, in PC3M cancer cells. Of the compounds identified, two non-cytotoxic hits were chosen for further SAR development and optimization. The chemical synthesis of 78 analogues around the pyrrolopyrimidine hit, **5a**, led to the identification of several compounds with IC_{50} <500 nM in the high-content PNC assay without affecting cytotoxicity, unlike previous PNC disassemblers with pronounced genotoxic activity. Further evaluation of the biological actions of optimized molecules disclosed their capacity to downregulate ribosomal biogenesis and induce irreversible growth arrest selectively in cancer cells with high PNC prevalence. Analysis of *in vitro* drug-like properties led to selection of **5f** (metarrestin) for pharmacokinetic evaluation which showed extended coverage in the plasma well beyond its IC_{50}. These observations catalyzed the evaluation of **5f** (metarrestin) in several rodent models of metastasis where it was efficacious in inhibiting metastatic progression and promoting survival. The efficacy in rodent models then provided rationale for further preclinical characterization and development, leading to IND

filing and the investigation of **5f** (metarrestin) as a phase I human clinical trial candidate (NCT04222413).

Experimental

High-Content Assay for PNC Detection

This assay measures reduction of PNC prevalence in living cells. Detection and quantification is enabled by the expression of a green fluorescent protein (GFP) tagged polypyrimidine-tract-binding protein (PTBP), which is enriched in the PNC several-hundred-fold compared to the nucleus. We previously reported a robust system to monitor PNC prevalence using a PC3M cell line that stably expresses GFP–PTB,[21] thus eliminating PNC detection via immunofluorescent staining. Cells expressing the fusion proteins possess comparable cell morphology and cell growth to their endogenous counterparts. Details of the GFP–PTB transgene screening assay have been previously reported and provide further information on theimage analysis, selection of PNC-positive and -negative objects, and hit prioritization.[21]

In brief, PC3M cells with GFP–PTB at a density of 75-90% confluency in T175 flasks were harvested using 7 mL TrypLE Express cell dissociation reagent. After dissociation (5 minutes room temperature incubation) 10 mL of complete media was added to the TrypLE/cell suspension. The liquid was transferred to a 50 mL conical tube and cells were pelleted at 1000 RPM for 5 min. Supernatant was removed and cells were resuspended to a final density of 150–200 cells/μL in complete media. Cells were plated in 5 μL volume (750–1000 cells/well) into 1536 well Black uclear Aurora Low Base plates and allowed to recover and adhere at 37 °C in a humidified 5% CO_2 incubator for 4 hours. Compounds were transferred to the plates using a 1536-well pintool. Camptothecin positive control (59 μM final) was added to column 2 and 1:3 dilutions of camptothecin was added to column 3. DMSO negative controls were present in columns 1 and 4. After a 16 hour incubation in the 37 °C incubator, cells were fixed by the addition of 4 μL of 6% EM grade paraformaldehyde (containing 0.1% triton X 100) directly to the cells. The plates were incubated at room temperature for 20 minutes. The liquid was removed using a 32 channel Kalypsys aspirator and the fixed cells were washed twice with 5 μL PBS followed by a final addition of 5 μL PBS containing 1 μg/ml Hoechst 33342. Fixed plates were sealed and stored at 4 °C until imaged were imaged on the InCell 1000 automated microscope using a 20 x objective, a standard FITC filter set, no camera binning, and an exposure time of ~100–150 msec/well. PNC prevalence was quantitated with the MTA algorithm.

For the data displayed in SAR tables in this manuscript, the assay was performed in 386-well format and the images were acquired using the Opera Phenix Plus High-Content Screening System (Perkin Elmer). PNC spots were analyzed and counted in Columbus Software. PC3M nuclei with PNC spots 3 and >0 are counted positive. PNC prevalence % = (Nuclei with PNC positive spots/Total nuclei) × 100. Compounds were analyzed after 24 h incubation at concentrations ranging from 20 μM to 19.5 nM, 11-points in 1:2 dilution, in triplicate except where indicated otherwise. % Activity is normalized as percent change in PNC with DMSO = 0% activity, 0% PNC = −100% activity; **5f** (metarrestin) is used as the

as positive control in each plate. Representative images after 24 h with DMSO and 9.2 μM of **5f** are provided in the Supporting Information (Figure S-3).

ATP Assay

PC3M cells with GFP–PTB were grown as mentioned above and plated in 5 μL volume (2000 cells/well) into 1536-well white solid bottom plates, allowed to recover and adhere at 37 °C in a humidified 5% CO_2 incubator for 4 hours. Compound libraries (23 nL in DMSO) were transferred to the plates in duplicate using a 1536 well pintool. After a 24 h or 48 h incubation in the 37 °C incubator, all wells were treated with 3 μL of ATPLite™ (Perkin Elmer) reagent using a multidrop combi dispenser. Bubbles that formed during dispensing were removed by spinning the plates for one minute at 1500 RPM on a tabletop centrifuge. Luminescencent signal was detected on a Viewlux CCD based imager (PerkinElmer) with a clear filter and a 30 second integration time.

BellBrooks® Labs Tumor Cell Migration Assay

We employed the BellBrook Labs® tumor cell migration assay to evaluate the effect of compounds on 3-dimensional tumor migration using a standard screening-sized plate with an array of embedded microchannels.

We used PC3M cells (analogous to the PNC reduction assay) to evaluateinvasion through 3D fibrillar collagen in the Iuvo Single Microchannel Plate. Ten compound concentrations were tested to provide a range of exposure levels. 820 nL of 3-dimensional type I collagen (1 mg/mL) was prefilled into the plate channels through the input port. Following gelation, PC3M cells (approximately 2,000 cells) were seeded into the output port using growth media (Roswell Park Memorial Institute (RPMI) medium + 10% (fetal bovine serum) FBS with antibiotics) in a volume of 5 μL. The plates were incubated at 37 °C for five days inside a humidified container (Bioassay dish, Corning) with daily media changes (including test compounds). The cells were then fixed and stained with Hoechst 33342. Imaging with 4x objective under epifluorescence, allowed thereliable detection of cells across the 140 μm height range of the microchannel. The range of ten test compound concentrations were obtained by serial dilutions of a factor of 3 to afford test compound concentrations ranging from 50 μM or 100 μM to 2.5 nM. All assays were conducted in the presence of 0.1% DMSO. Four replicates were performed for all test concentrations. Four concentration-response curves were performed per plate, as well as 16 negative-control channels (no compound) and 16 positive-control channels (50 μM blebbistatin). Each image was systematically cropped along the right edge of the channel. Cell counts were obtained using the 'count nuclei' function on Metamorph (Molecular Devices) andon-linear regression analysis was performed with GraphPad Prism.

PC3M Caspase 3/7 Assay

To perform the Apo-ONE® Homogeneous caspase-3/7 Assay, the buffer and caspase 3/7 substrate (rhodamine 110, bis-(N-CBZL- aspartyl-L-glutamyl-L-valyl-L-aspartic acid amide; Z-DEVD-R110)) are mixed and added to the sample. Upon sequential cleavage and removal of the DEVD peptides by caspase-3/7 activity and excitation at 499 nm, the rhodamine 110 leaving group becomes intensely fluorescent with an emission maximum at

521 nm. The media and cell culture reagents were purchased from Invitrogen (Carlsbad, CA), and Caspase Glo 3/7 came from Promega.

Cells from the highly metastatic PC3M-GFP reporter cell line (Professor Sui Huang, Northwestern University) were plated in 5 μL volume (2000 cells/well) into 1536 well white solid bottom plates and allowed to recover and adhere at 37 °C in a humidified 5% CO_2 incubator for 4 hours. Compound libraries (23 nL of 12.5 uM in columns 5–48) were transferred to the plates in duplicate using a 1536 well pintool. Camptothecin positive control (59 μM final) was added to column 2 and 1:3 dilutions of camptothecin were added to column 3. DMSO negative controls were present in columns 1 and 4. 4. After a 24-hour incubation in the 37 °C incubator, all wells were treated with 3 μL of Caspase Glo 3/7 reagent using a multidrop combi dispenser (ThermoFisher). Bubbles that formed during dispensing were removed by spinning the plates for 1 minute at 1500 RPM on a table top centrifuge. Plates were incubated at room temperature for 5 minutes. Luminescencent signal was detected on a Viewlux CCD based imager (PerkinElmer) with a clear filter and a 30 second integration time.

PicoGreen® Assay

A supercoiled plasmid (pBR322) was diluted to 200 ng/mL in TE and 2 μL was dispensed into 1536 well black plates Multidrop Combi (ThermoFisher). 23 μL of compounds dissolved in 100% DMSO were transferred using a pintool (12-point dose response from 28 nM to 57 μM in 1:2 dilutions) and incubated in the presence of DNA for 30 minutes at room temperature. A baseline signal was measured using an Envision PMT based plate reader using a 488 nm excitation filter and a 520 nm emission filter. The PicoGreen dye (Invitrogen) was diluted in TE and 2 μL/well was dispensed to the 1536 well plate using a Multidrop Combi. Plates were incubated at 37 °C for 10 minutes prior to being read on the Envision plate reader Ex488/Em520. 100 ng/mL of propidium iodide was used as the positive intercalation control.

Nucleolar disassembly assay

PC-3M cells were cultured in RPMI 1640 medium (Thermofisher) with 10% FBS (Invitrogen) and 100 units/mL of penicillin and streptomycin (Thermofisher) and trypsinized at 70% confluence. Cells (100 μL/well) were seeded at density of 2×10^5 cells/mL in glass-bottom 96 well plate (Corning, cat# 4586) overnight at 37 °C, 5% CO_2. To evaluate nucleolar disassembly, media was replaced with 100 μL RMPI media containing compound or 1% DMSO and incubated 24 hr at 37 °C, 5% CO_2. Nucleolar staining was performed following protocol recommended in Nucleolar-ID® Green Detection Kit (Cat #: ENZ-51009-500). Hoechst 33342 (Thermofisher # H3570) was used for staining nucleus. Images were captured using Zeiss 780 confocal microscope. Three separate images for each treatment conditions were analyzed using Image J software. The number of automatically counted bright objects (green fluorescent objects) was normalized to the number of Hoechst-stained nuclei. For relative comparison, the fluorescence ratio for vehicle-treated cells was set to 100.

Immunofluorescence assays

Immunofluorescence analysis was carried out using Zeiss LSM 880 confocal microscope. 50,000 PC3M cells were seeded onto 8-well chamber slides. Cells were treated with 1 μM of **5f** (metarrestin) or **11b** for 1h at 37 °C followed by fixation with 4% paraformaldehyde for 15 min, permeabilization with 0.3% Triton X-100 for 5 min and blocking with 3% BSA in PBS for 1 h. After blocking, cells were incubated with primary antibodies against RPA194 (sc48385) at dilution 1:200 and NOP140 (sc-374033) at dilution 1:100 overnight at 4 °C. Cells were washed then stained with secondary antibodies for 1 h at rt, followed by additional washing and the addition of mounting medium (H-1200 Vectashield) with DAPI. Images were taken at 63× magnification, and three separate images for each treatment group containing about 200 cells were analyzed using ImagePro software (Media Cybernetics). The number of automatically counted bright objects (fluorescence of secondary antibodies for specific proteins) was normalized to the number of DAPI stained nuclei.

Incucyte® Assay

PC3M-PTB1-GFP cells were cultured in DMEM supplemented with 10% FBS and 1% penicillin/streptomycin and dissociated at 70% confluence. 40 μL of PC3M-PTB1-GFP cells at a density of 1.25×10^4 cells/ml were seeded in tissue-culture-treated 384-well plates (Corning, cat#3712) and incubated overnight at 37 °C, 5% CO_2. 40 μL of DMEM containing compound were added to the wells with cells such that 11 final compound concentrations from 10 nM to 20 μM could be evaluated. Plates were placed in the Incucyte® Zoom (Essen), and brightfield photographs were taken every four hours for approximately 130 h. Incucyte® ZOOM Software was used to measure percent confluence.

Multi-time Point Mouse Microsomal Stability Assay

A substrate depletion method was chosen to determine in vitro $T_{1/2}$. The assay (384-well format) consisted of two parts; a robotic system for incubation and sample clean up and an integrated LC/MS method to calculate the percent remaining of parent compound. The assay incubation system consisted of 0.5 mg/mL microsomal protein (male CD-1 microsomes; Catalog# M1000; Xenotech LLC), 1.0 μM drug concentration, and NADPH regeneration system (containing 0.650 mM NADP+, 1.65 mM glucose 6-phosphate, 1.65 mM $MgCl_2$, and 0.2 unit/mL G6PDH) in 100 mM phosphate buffer at pH 7.4. The incubation was carried out at 37 °C for 60 min. Sample aliquots were taken at 0, 5, 10, 15, 30 and 60 min. The reaction was quenched by adding acetonitrile containing 0.28 μM albendazole (internal standard). After a 20 min centrifugation at 3000 rpm, the supernatant was transferred to an analysis plate before the samples were analyzed by LC/MS. Data analysis was performed as described previously.[29, 30]

Parallel Artificial Membrane Permeability Assay (PAMPA)

The stirring double-sink PAMPA method (patented by pION Inc.) was employed to determine the permeability of compounds via PAMPA as published before.[31] The PAMPA lipid membrane consisted of an artificial membrane of a proprietary lipid mixture and dodecane (Pion Inc.), optimized to predict gastrointestinal tract passive permeability. The lipid was immobilized on a plastic matrix of a 96-well "donor" filter plate placed below

a 96-well "acceptor" plate. pH 7.4 solution was used in both donor and acceptor wells. The test articles, stocked in 10 mM DMSO solutions, were diluted to 0.05 mM in aqueous buffer (pH 7.4), and the concentration of DMSO was 0.5% in the final solution. During the 30-minute permeation period at room temperature, the test samples in the donor compartment were stirred using the Gutbox technology (Pion Inc.) to reduce the aqueous boundary layer. The test article concentrations in the donor and acceptor compartments were measured using a UV plate reader (Nano Quant, Infinite® 200 PRO, Tecan Inc., Männedorf, Switzerland). Permeability calculations were performed using Pion Inc. software and were expressed in units of 10-6cm/s. Compounds with low or weak UV signal we analyzed using high resolution LC/MS (Thermo QExactive). The three controls used were ranitidine (low permeability), dexamethasone (moderate permeability) and verapamil (high permeability).

Mouse Pharmacokinetic Studies

Studies were conducted by ChemPartner. Fed male C57BL/6 mice or female BALB/c mice (sourced from Si Bei Fu LaboratoryAnimal Technology Co. Ltd.), approximately 6–8 weeks of age and weight of approximately 25–30 g, were dosed with analogs **5e** and **5f**. **5f** was formulated in 10% NMP + 20% PEG400 + 70% (25%HP-β-CD in Water) at 5 mg/mL for the 50 mpk study; it was formulated in 5% NMP + 20% PEG400 + 75% (10%HP-β-CD in Water) at 0.5 and 1 mg/mL for the 5 and 10 mpk studies respectively. **5e** was formulated in 10% DMAC+5% Solutol HS 15+ 85% Saline at 5 mg/mL for the 50 mpk study. The formulations were prepared prior to dosing a cohort of N=24 mice. Plasma was collected from N=3 mice per time point postdose. The animal was anesthetized with isoflurane and restrained manually at the designated time points. Approximately 120 μL of blood samples were taken from the animals into K2EDTA tube via retro-orbital puncture. Blood sample was put on ice and centrifuged to obtain plasma sample (2000 g, 5 min under 4°C) within 15 minutes. Plasma samples were then quickly frozen, and kept at −80°C until analyzed by LC/MS/MS. Animals were also monitored during the in-life phase by once daily cageside observations; no adverse clinical signs were noted.

Use of Animal Subjects

All animal studies included as part of this manuscript were performed in accordance with institutional guidelines as defined by Institutional Animal Care and Use Committee (IACUC).

General Synthesis and Compound Analysis Experimental Details

All reagents were used as received from commercial sources. Acetonitrile, toluene, CH_2Cl_2 and THF were purified using the Innovative Technology PureSolv solvent purification system using two alumina columns. The ^1H and ^{13}C NMR spectra were recorded on a 400 MHz Bruker Avance spectrometer equipped with a broadband observe probe and a 500 MHz Bruker AVIII spectrometer equipped with a dual cryoprobe, respectively. Chemical shifts are reported in parts per million and were referenced to residual proton solvent signals. ^{13}C multiplicities (where reported) were determined with the aid of an APT pulse sequence, differentiating the signals for methyl (CH_3) and methyne (CH) carbons as "d" from methylene (CH_2) and quarternary (C) carbons as "u". The infrared (IR) spectra were

acquired as thin films using a universal ATR sampling accessory on a Thermo Fisher Nicolet iS5 FT-IR spectrometer and the absorption frequencies are reported in cm^{-1}. Melting points were determined on a Stanford Research Systems Optimelt automated melting point system interfaced through a PC and are uncorrected. Microwave syntheses were conducted in a Biotage Initiator constant temperature microwave synthesizer. Flash column chromatography separations were performed using the Teledyne Isco CombiFlash Rf using RediSep Rf silica gel columns.

TLC was performed on Analtech UNIPLATE silica gel GHLF plates (gypsum inorganic hard layer with fluorescence). TLC plates were developed using iodine vapor or ceric ammonium molybdate stain, as required. Automated preparative RP HPLC purification was performed using an Agilent 1200 Mass-Directed Fractionation system (Prep Pump G1361 with gradient extension, make-up pump G1311A, pH modification pump G1311A, HTS PAL autosampler, UV-DAD detection G1315D, fraction collector G1364B, and Agilent 6120 quadrapole spectrometer G6120A). HRMS determinations were analyzed with a ThermoFisher Q Exactive HF-X (ThermoFisher, Bremen, Germany) mass spectrometer coupled with a Waters Acquity H-class liquid chromatograph system. Samples were introduced via a heated electrospray source ionization (HESI) at a flow rate of 0.6 mL/min. Electrospray source conditions were set as: spray voltage 3.0 kV, sheath gas (nitrogen) 60 arb, auxillary gas (nitrogen) 20 arb, sweep gas (nitrogen) 0 arb, nebulizer temperature 375 °C, capillary temperature 380 °C, RF funnel 45 V. The mass range was set to 150–2000 m/z. All measurements were recorded at a resolution setting of 120,000. The preparative chromatography conditions included a Waters X-Bridge C_{18} column (19×150 mm, 5 μm, with 19×10-mm guard column), elution with a water and acetonitrile gradient, which increases 20% in acetonitrile content over 4 min at a flow rate of 20 mL/min (modified to pH 9.8 through addition of NH_4OH by auxiliary pump), and sample dilution in DMSO. The preparative gradient, triggering thresholds, and UV wavelength were selected according to the analytical RP HPLC analysis of each crude sample. The analytical method used an Agilent 1200 RRLC system with UV detection (Agilent 1200 DAD SL) and mass detection (Agilent 6224 TOF). The analytical method conditions included a Waters Aquity BEH C_{18} column (2.1×50 mm, 1.7 μm) and elution with a linear gradient of 5% acetonitrile in pH 9.8 buffered aqueous ammonium formate to 100% acetonitrile at 0.4 mL/min flow rate. Compound purity was measured on the basis of peak integration (area under the curve) from UV/Vis absorbance (at 214 nm), and compound identity was determined on the basis of HRMS analysis. All compounds used for assays or biological studies possessed HPLC purity >95%. The analytical HPLC system used is a dedicated instrument for assessing compound purity and routinely detects impurities as low as 0.1%. Any compounds with a measured HPLC purity of 100% were thus conservatively assigned a purity of "> 99.5%". Any compounds purified by automated preparative RP HPLC purification utilized the same solvent gradient and column material used in the analytical conditions to minimize the possibility of undetected impurities carrying over from the purification run.

All final compounds were inspected for functional groups known to contribute PAINS liabilities, and none were found.

General Procedure A: one-pot, three-component synthesis of *N*-substituted aminopyrroles 2.—The modified Voigt reaction/Knoevenagel condensation sequence was carried out following the procedure of Roth and Eger.[1] Thus, hydroxyketone **1**, the primary amine (1.5 equiv) and concentrated HCl (0.01 mL/mmol benzoin) were heated at reflux for 2–3 hours and the mixture removed from the heat source. To the still warm mixture was added malononitrile (2.0 equiv) in DMF (0.13 mL/mmol malononitrile). The reaction mixture was stirred for 12 to 16 h, while the temperature cooled to rt, affording the crude pyrrole as a solid mass. The solid was partitioned between water and CH_2Cl_2 and the aqueous layer extracted with additional CH_2Cl_2 (2 ×50 mL). The combined organics were dried with Na_2SO_4 and the solvent removed in vacuo to afford the pyrrole product, which was suitable for further use without purification.

General Procedure B: alternative, one-pot, three-component synthesis of *N*-substituted aminopyrroles 2.—The modified Voigt reaction/Knoevenagel condensation sequence was carried out via a modification on the procedure of Mezheritskii and coworkers.[2] Thus, hydroxyketone **1**, the primary amine (1.0 equiv) and trifluoroacetic acid (0.05 equiv) in toluene (2 M for benzoin) were heated at reflux using a Dean–Stark trap until approximately one equivalent of water had been collected. The mixture was cooled to rt and the toluene removed in vacuo. The residue was dissolved in ethanol (4 M) and malononitrile (2.0 equiv, unless otherwise noted) was added portionwise to maintain the reaction at reflux. The reaction mixture was stirred for an additional 2 h, while the temperature cooled to rt. Water was added to the reaction and the precipitate collected by filtration to afford the pyrrole product, which was suitable for further use without purification.

General Procedure C: conversion of aminopyrroles 2 to pyrroloformimidates 3.—A solution of the aminopyrrole and triethylorthoformate (10 equiv, unless otherwise noted) were heated at 70 °C for 14–19 h and cooled to rt. The reaction was diluted with CH_2Cl_2, concentrated directly onto celite and purified by silica chromatography to afford the pure product.

General Procedure D: nucleophilic amine addition to pyrroloformidates 3 and subsequent pyrimidine cyclization.—A mixture of pyrroloformimidate **3** or **10** and amine component (1.0–4.0 equiv) in MeOH (the greater of 2 mL or 15 mL/mmol **3**) were heated at 65 °C for 15–20 h. Solvent was removed *in vacuo* and the residue purified by either silica gel flash chromatography or mass-directed, reverse-phase, preparative HPLC (MDF purification) to afford the pyrrolpyrimidine product.

General Procedure E: modified nucleophilic amine addition (with base additive) to pyrroloformidates 3 and subsequent pyrimidine cyclization.—A mixture of pyrroloformimidate **3**, amine component (2.0–5.0 equiv) and added base (1.0–3.0 equiv) in MeOH (the greater of 2 mL or 15 mL/mmol **3**) were heated at 65 °C for 15–20 h. Solvent was removed *in vacuo* and the residue purified by either silica gel flash chromatography or mass-directed fraction collection, reverse-phase, preparative HPLC (MDF purification) to afford the pyrrolpyrimidine product.

Synthesis of Pyrroloformimidate Intermediates 3

Ethyl (*E*)-*N*-(1-benzyl-3-cyano-4,5-diphenyl-1*H*-pyrrol-2-yl)formimidate (3a).—

This intermediate was synthesized as previously reported.[3]

Ethyl (*E*)-*N*-(3-cyano-1-phenethyl-4,5-diphenyl-1H-pyrrol-2-yl)formimidate (3b).

—2-Amino-1-phenethyl-4,5-diphenyl-1H-pyrrole-3-carbonitrile **2b**[4] (1.980 g, 5.45 mmol) and triethylorthoformate (13.61 mL, 82.00 mmol, 15.0 equiv) were reacted according to General Procedure C for 19 h to afford **3b** as an ochre solid (1.53 g, 3.65 mmol, 67% yield). ^{1}H NMR (400 MHz, CDCl$_3$) δ 1.42 (t, *J* = 7.1 Hz, 3H), 2.70 (t, *J* = 7.3 Hz, 2H), 4.08 (t, *J* = 7.3 Hz, 2H), 4.35 (q, *J* = 7.1 Hz, 2H), 6.85 (dd, *J* = 2.9, 6.5 Hz, 2H), 7.13–7.27 (m, 12H), 7.37 (dd, *J* = 2.0, 5.0 Hz, 3H), 8.16 (s, 1H); ^{13}C NMR (101 MHz, CDCl$_3$) δ 14.1, 36.5, 44.9, 63.1, 78.7, 118.0, 123.1, 126.5, 126.7, 128.0, 128.2, 128.3, 128.5, 128.7, 128.7, 129.0, 131.1, 131.2, 132.9, 137.9, 144.2, 158.2; IR 2207, 1627, 1603 cm^{-1}.

Ethyl (*E*)-*N*-(3-cyano-1-(4-methoxybenzyl)-4,5-diphenyl-1H-pyrrol-2-yl)formimidate 3c.—

2-Amino-1-(4-methoxybenzyl)-4,5-diphenyl-1H-pyrrole-3-carbonitrile **2c**[5] (1.990 g, 5.24 mmol) and triethylorthoformate (8.73 mL, 52.4 mmol, 10.0 equiv) were reacted according to General Procedure C for 28 h to afford **3c** as a yellow sticky solid (0.70 g, 1.61 mmol, 31% yield). R_f = 0.74 (50% EtOAc in hexanes); ^{1}H NMR (400 MHz, CDCl$_3$) δ 1.36 (t, *J* = 7.1 Hz, 3H), 3.76 (s, 3H), 4.33 (q, *J* = 7.1 Hz, 2H), 5.01 (s, 2H), 6.72–6.85 (m, 4H), 7.07–7.12 (m, 2H), 7.13–7.36 (complex, 9H); ^{13}C NMR (101 MHz, CDCl$_3$) δ 14.0, 46.3, 55.2, 63.3, 79.0, 113.8, 118.0, 123.1, 126.6, 127.9, 128.2, 128.3, 128.5, 129.0, 129.7, 131.0, 131.3, 132.9, 143.9, 158.4, 158.8; IR (neat) 2207, 1627, 1511, 1459 cm^{-1}.

2-Amino-4,5-diphenyl-1-(4-(trifluoromethoxy)benzyl)-1*H*-pyrrole-3-carbonitrile (2d).—

Benzoin (3.89 g, 18.3 mmol), 4-(trifluoromethoxy)benzylamine (3.50 g, 18.3 mmol, 1.0 equiv) and malononitrile (3.63 g, 54.9 mmol, 3.0 equiv) were reacted according to General Procedure B to afford the pyrrole **2d** as light brown solid (4.79 g, 11.1 mmol, 60% yield). ^{1}H NMR (400 MHz, CDCl$_3$) δ 3.89 (br s, 2H), 4.92 (s, 2H), 7.00–7.35 (complex, 14H). ^{13}C NMR (101 MHz, CDCl$_3$) δ 46.3, 76.5, 117.3, 120.2 (q, *J* = 226.9 Hz), 121.7, 125.6, 126.5, 127.4, 128.2, 128.3, 128.7, 128.8, 130.7, 131.0, 132.9, 134.8, 145.6, 148.8; ^{19}F NMR (376 MHz, CDCl$_3$) δ –57.9. IR (neat) 2200, 1629, 1555, 1257 cm^{-1}.

Ethyl (*E*)-*N*-(3-cyano-1-(4-(trifluoromethoxy)benzyl)-4,5-diphenyl-1H-pyrrol-2-yl)formimidate (3d).—

2-Amino-1-(4-(trifluoromethoxy)benzyl)-4,5-diphenyl-1H-pyrrole-3-carbonitrile **2d** (7.89 g, 18.20 mmol) and triethylorthoformate (30.3 mL, 182.0 mmol, 10.0 equiv) were reacted according to General Procedure C for 28 h to afford formimidate **3d** as an orange, sticky solid (1.80 g, 3.68 mmol, 20% yield). R_f = 0.80 (50% EtOAc in hexanes); ^{1}H NMR (400 MHz, CDCl$_3$) δ 1.33 (t, *J* = 7.1 Hz, 3H), 4.29 (q, *J* = 7.1 Hz, 2H), 5.07 (s, 2H), 6.90 (d, *J* = 8.6 Hz, 2H), 7.04–7.11 (m, 4H), 7.14–7.37 (complex, 9H); ^{13}C NMR (101 MHz, CDCl$_3$) δ 13.9, 46.2, 63.4, 79.2, 117.8, 120.4 (q, *J* = 258.5 Hz), 121.0, 123.4, 126.7, 128.1, 128.2, 128.4, 128.5, 128.6, 129.0, 130.7, 131.2, 132.7, 136.3, 143.7, 148.3, 158.5; IR (neat) 2208, 1628, 1508, 1459 cm^{-1}.

4-((2-Amino-3-cyano-4,5-diphenyl-1H-pyrrol-1-yl)methyl)benzenesulfonamide (2e).—Benzoin (1.003 g, 4.73 mmol), 4-aminomethylbenzenesulfonamide (0.880 g, 4.73 mmol, 1.0 equiv) and malononitrile (0.625 g, 9.46 mmol, 2.0 equiv) were reacted according to General Procedure B to afford the pyrrole **2e** as a reddish brown solid (0.770 g, 1.80 mmol, 38% yield). R_f = 0.17 (50% EtOAc in hexanes); mp = 151–189 °C (dec); ^{1}H NMR (400 MHz, DMSO-d6) δ 5.06 (s, 2 H), 6.22 (s, 2 H), 7.05 (d, J = 8.8 Hz, 2 H), 7.10-7.17 (complex, 5 H), 7.23 (m, 2 H), 7.28 (m, 3 H), 7.33 (s, 2 H), 7.74 (d, J = 8.4 Hz, 2 H); ^{13}C NMR (101 MHz, DMSO-d6, APT pulse sequence) δ d (CH, CH$_3$) 107.0, 125.8, 126.2, 126.4, 127.9, 128.0, 128.5, 131.0; u (C, CH$_2$) 67.0, 117.9, 120.2, 123.6, 130.8, 133.5, 141.1, 142.8, 148.7; IR 2193, 1616, 1601, 1545 cm^{-1}; HRMS calcd for $C_{24}H_{21}N_4O_2S$ [M + H]$^+$ 429.1385, found 429.1377; HPLC purity 44.3%.

(*E*)-Ethyl *N*-(3-cyano-4,5-diphenyl-1-(4-sulfamoylbenzyl)-1*H*-pyrrol-2-yl)formimidate (3e)—4-((2-amino-3-cyano-4,5-diphenyl-1H-pyrrol-1-yl)methyl)benzenesulfonamide **2e** (552 mg, 1.29 mmol) was reacted according to General Procedure C to afford the formimidate **3e** as a light orange solid (325 mg, 0.671 mmol, 52% yield). R_f = 0.45 (50% EtOAc in hexanes); mp = 87–92 °C; ^{1}H NMR (400 MHz, CDCl$_3$) δ 1.29 (t, J = 7.2 Hz, 3 H), 4.23 (q, J = 7.2 Hz, 2 H), 5.10 (s, 2 H), 5.13 (s, 2 H), 7.03 (m, 4 H), 7.13-7.31 (complex, 8 H), 7.80 (d, J = 8.8 Hz, 2 H), 8.55 (s, 1 H); ^{13}C NMR (101 MHz, CDCl$_3$, APT pulse sequence) δ d (CH, CH$_3$) 13.9, 126.6, 126.7, 127.0, 128.2, 128.5, 128.6, 128.9, 131.0, 158.6; u (C, CH$_2$) 46.4, 63.4, 117.6, 123.4, 128.4, 130.3, 132.4, 141.0, 142.6, 143.7; IR 2208, 1627 cm^{-1}; HRMS calcd for $C_{27}H_{25}N_4O_3S$ [M + H]$^+$ 485.1647, found 485.1648; HPLC purity 92.6%.

2-Amino-1-(cydohexylmethyl)-4,5-diphenyl-1*H*-pyrrole-3-carbonitrile (2f).—Benzoin (425.6 mg, 2.005 mmol), cyclohexylmethanamine (227.0 mg, 2.005 mmol, 1.0 equiv) and malononitrile (265 mg, 4.01 mmol, 2.0 equiv) were reacted according to General Procedure B to afford the pyrrole **2f** as a purple solid (0.4235 g, 1.191 mmol, 59% yield). ^{1}H NMR (400 MHz, CDCl$_3$) δ 0.66 (q, J = 12.3 Hz, 2H), 0.99-1.10 (m, 2H), 1.39-1.52 (m, 3H), 1.53-1.68 (m, 4H), 3.56 (d, J = 7.2 Hz, 2H), 3.97 (s, 2H), 7.08-7.21 (m, 7H), 7.31–7.36 (m, 3H); ^{13}C NMR (101 MHz, CDCl$_3$) δ 25.6, 26.0, 30.5, 37.9, 49.4, 75.8, 117.8, 120.8, 125.7, 126.2, 128.0, 128.1, 128.6, 128.7, 131.5, 131.5, 133.2, 145.5. IR 1447, 1503, 1552, 1629, 2197 cm^{-1}.

(*E*)-Ethyl *N*-(3-cyano-1-(cyclopropylmethyl)-4,5-diphenyl-1*H*-pyrrol-2-yl)formimidate (3f).—2-amino-1-(cyclohexylmethyl)-4,5-diphenyl-1H-pyrrole-3-carbonitrile **2f** (0.3987 g, 1.122 mmol) was reacted according to General Procedure C to afford the formimidate product **3f** as colorless crystals (0.2897 g, 0.704 mmol, 63% yield). ^{1}H NMR (400 MHz, CDCl$_3$) δ 0.61–0.70 (m, 2H), 0.98–1.05 (m, 2H), 1.43 (t, J = 7.1 Hz, 3H), 1.48-1.66 (m, 4H), 3.74 (d, J = 7.0 Hz, 2H), 4.39 (q, J = 7.1 Hz, 2H), 7.10–7.23 (m, 7H), 7.24–7.42 (m, 3H), 8.50 (s, 1H); ^{13}C NMR (101 MHz, CDCl$_3$) δ 14.1, 25.6, 26.1, 30.5, 38.5, 49.4, 63.2, 117.3, 118.2, 122.8, 126.4, 128.1, 128.5, 129.0, 131.3, 131.4, 133.0, 137.2, 144.0, 158.0; IR 1241, 1465, 1507, 1633, 2208 cm^{-1}.

2-Amino-1-(cyclopropylmethyl)-4,5-diphenyl-1*H*-pyrrole-3-carbonitrile (2g).—
Benzoin (4.54 g, 21.37 mmol), aminomethylcyclopropane (1.52 g, 21.37 mmol, 1.0 equiv) were reacted according to the general procedure B to afford the pyrrole **2g** as a brown solid (2.22 g, 7.08 mmol, 33% yield). ^{1}H NMR (400 MHz, CDCl$_3$) δ 0.03 (dd, J = 0.8, 4.8 Hz, 2 H), 0.03 (dd, J = 1.2, 8.0 Hz, 2 H), 0.88 (m, 1 H), 3.58 (d, J = 6.0 Hz, 2 H), 4.14 (br s, 2 H), 7.10–7.22 (complex, 7 H), 7.32–7.34 (m, 3 H); ^{13}C NMR (101 MHz, CDCl$_3$, APT pulse sequence) δ d (CH, CH$_3$) 10.9, 126.2, 128.0, 128.1, 128.57, 128.60, 131.5; u (C, CH$_2$) 4.2, 47.5, 117.7, 120.9, 125.2, 131.4, 133.3, 145.6; IR 2193, 1616, 1601, 1545 cm^{-1}; HRMS calcd for C$_{24}$H$_{21}$N$_4$O$_2$S [M + H]$^+$ 429.1385, found 429.1377.

(*E*)-Ethyl *N*-(3-cyano-1-(cyclopropylmethyl)-4,5-diphenyl-1*H*-pyrrol-2-yl)formimidate (3g).—2-Amino-1-(cyclopropylmethyl)-4,5-diphenyl-1*H*-pyrrole-3-carbonitrile **2g** (4.92 g, 15.70 mmol) was reacted according to General Procedure C to afford the formimidate product **3g** as a light brown oil (1.60 g, 4.33 mmol, 28% yield). R$_f$ = 0.65 (25% EtOAc in hexanes); ^{1}H NMR (400 MHz, CDCl$_3$) δ 0.01 (d, J = 5.6 Hz, 2 H), 0.34 (d, J = 7.2 Hz, 2 H), 0.85 (m, 1 H), 1.14 (t, J = 7.2 Hz, 3 H), 3.74 (d, J = 6.8 Hz, 2 H), 4.38 (q, J = 7.2 Hz, 2 H), 7.12–7.25 (complex, 7 H), 7.34 (d, J = 2.8 Hz, 2 H), 7.39–7.45 (m, 1 H), 8.52 (s, 1 H); ^{13}C NMR (101 MHz, CDCl$_3$, APT pulse sequence) δ d (CH, CH$_3$) 11.6, 14.1, 126.4, 128.1, 128.2, 128.6, 128.9, 131.3, 158.2; u (C, CH$_2$) 3.9, 47.6, 63.3, 78.7, 118.1, 122.9, 128.0, 131.3, 132.9, 143.6; IR 2210, 1722, 1632 cm^{-1}; HRMS calcd for C$_{24}$H$_{24}$N$_3$O [M + H]$^+$ 370.1919, found 370.1918.

2-Amino-1-benzyl-4,5-bis(4-methoxyphenyl)-1H-pyrrole-3-carbonitrile (2h).—
4,4'-2-Hydroxy-1,2-bis(4-methoxyphenyl)ethan-1-one (5.02 g, 18.44 mmol) and benzyl amine (2.96 g, 27.66 mmol, 1.5 equiv) were reacted according to General Procedure A to afford the pyrrole product **2h** as a light brown solid (3.10 g, 7.57 mmol, 41% yield). R$_f$ = 0.47 (40% EtOAc in hexanes); mp = 219–223 °C; ^{1}H NMR (400 MHz, CDCl$_3$) δ 3.76 (s, 3 H), 3.77 (s, 3 H), 4.89 (s, 2 H), 6.78 (m, 4 H), 7.07 (m, 4 H), 7.19 (m, 2 H), 7.31 (m, 1 H), 7.37 (m, 2 H); ^{13}C NMR (101 MHz, CDCl$_3$, APT pulse sequence) δ d (CH, CH$_3$) 55.2, 113.7, 114.1, 125.8, 127.9, 129.2, 129.7, 132.3; u (C, CH$_2$) 46.8, 117.7, 120.4, 123.1, 124.8, 136.2, 145.4, 158.1, 159.4, 159.8, 169.3; IR 2199, 1608, 1519 cm^{-1}; HRMS calcd for C$_{26}$H$_{24}$N$_3$O$_2$ [M + H]$^+$ 410.1869, found 410.1872.

(*E*)-Ethyl N-(1-benzyl-3-cyano-4,5-bis(4-methoxyphenyl)-1*H*-pyrrol-2-yl)formimidate (3h).—Pyrrole **2h** (1.19 g, 2.91 mmol) was reacted according to General Procedure C to afford the formimidate **3h** as a viscous, yellow oil (1.10 g, 2.36 mmol, 81% yield). R$_f$ = 0.42 (25% EtOAc in hexanes); ^{1}H NMR (400 MHz, CDCl$_3$) δ 1.29 (t, J = 7.2 Hz, 3 H), 3.74 (s, 3 H), 3.77 (s, 3 H), 4.25 (dq, J = 0.8, 6.8 Hz, 2 H), 5.02 (s, 2 H), 6.76 (m, 4 H), 6.89 (dd, J = 1.6, 8.0 Hz, 2 H), 6.97 (d, J = 8.8 Hz, 2 H), 7.16-7.26 (complex, 5 H), 8.49 (s, 1 H); ^{13}C NMR (101 MHz, CDCl$_3$, APT pulse sequence) δ d (CH, CH$_3$) 13.9, 55.1, 113.7, 113.6, 113.9, 126.4, 127.2, 128.4, 130.0, 132.4, 158.1; u (C, CH$_2$) 46.8, 63.1, 118.2, 122.6, 123.0, 125.4, 127.8, 137.7, 143.4, 158.1, 159.4; IR 2208, 1632, 1519 cm^{-1}; HRMS calcd for C$_{28}$H$_{28}$N$_3$O$_3$ [M + H]$^+$ 466.2131, found 466.2148.

2-Amino-4,5-bis(benzo[*d*][1,3]dioxol-5-yl)-1-benzyl-1*H*-pyrrole-3-carbonitrile (2i)—251-002. Piperoin (2.13 g, 7.09 mmol), benzyl amine (0.760 g, 7.09 mmol) and malononitrile (0.937 g, 14.18 mmol, 2.0 equiv) were reacted according to General Procedure B to afford the pyrrole product **2i** as a light brown solid (1.52 g, 3.47 mmol, 49% yield). ^{1}H NMR (400 MHz, CDCl$_3$) δ 3.82 (s, 2H), 4.89 (s, 2H), 5.90 (s, 2H), 5.95 (s, 2H), 6.60 (d, *J* = 1.4 Hz, 1H), 6.63 (dd, *J* = 8.0, 1.6 Hz, 1H), 6.71 (d, *J* = 1.8 Hz, 2H), 6.73 (d, *J* = 2.2 Hz, 1H), 6.81 (dd, *J* = 8.1, 1.7 Hz, 1H), 7.05 (d, *J* = 7.2 Hz, 2H), 7.32 (d, *J* = 7.2 Hz, 1H), 7.37 (t, *J* = 7.3 Hz, 2H). ^{13}C NMR (101 MHz, CDCl$_3$) δ 46.8, 75.9, 100.8, 101.2, 108.3, 108.6, 109.3, 111.3, 117.4, 120.7, 122.3, 124.2, 124.8, 125.1, 125.8, 127.1, 128.0, 129.3, 136.0, 145.4, 146.2, 147.4, 147.7, 147.8. IR (neat) 2199, 1629, 1555, 1504, 1237 cm^{-1}.

(*E*)-Ethyl N-(1-benzyl-3-cyano-4,5-bis(4-methoxyphenyl)-1*H*-pyrrol-2-yl)formimidate (3i).—Pyrrole **2i** (388.0 mg, 0.887 mmol) was reacted according to General Procedure C to afford the formimidate **3i** as a viscous, yellow oil (228.0 mg, 0.462 mmol, 52% yield). ^{1}H NMR (400 MHz, CDCl$_3$) δ 1.30 (td, *J* = 7.1, 2.0 Hz, 3H), 4.26 (qd, *J* = 7.1, 1.8 Hz, 2H), 5.02 (s, 2H), 5.89 (d, *J* = 2.2 Hz, 2H), 5.95 (d, *J* = 2.2 Hz, 2H), 6.50 (s, 1H), 6.53 (dd, *J* = 7.9, 2.2 Hz, 1H), 6.66 – 6.74 (m, 3H), 6.75 – 6.83 (m, 1H), 6.88 (d, *J* = 7.2 Hz, 2H), 7.13 – 7.32 (m, 3H), 8.47 (s, 1H). ^{13}C NMR (101 MHz, CDCl$_3$) δ 13.9, 46.8, 63.2, 79.0, 100.8, 101.2,108.3, 108.4, 109.5, 111.4, 117.9, 122.6, 122.9, 124.1, 125.2, 126.4, 126.7, 127.3, 127.7, 128.5, 137.6, 143.5, 146.4, 147.4, 147.6, 147.7, 158.3. IR (neat) 2208, 1630, 1504, 1477, 1238 cm^{-1}

2-Amino-4-phenyl-1*H*-pyrrole-3-carbonitrile (8).—To a solution of malononitrile (1.133 g, 17.15 mmol, equiv) in methanol (20 mL) and sodium hydroxide solution (4 mL, 48% by weight) was added the phthalimide **7**[6] (3.50 g, 13.2 mmol). The reaction was stirred at rt for 3 h then diluted with water (75 mL) and filtered. The precipitate was washed with water (2 × 25 mL), dissolved in CH$_2$Cl$_2$, dried with N$_2$SO$_4$ and evaporated to afford the previously reported pyrrole[7] as a brown solid (1.50 g, 8.19 mmol, 62% yield). that was used without further purification. ^{1}H NMR (400 MHz, DMSO-d6) δ 5.75 (br s, 2H), 6.53 (s, 1H), 7.14–7.24 (m, 1H), 7.28–7.39 (m, 2H), 7.50–7.62 (m, 2H); ^{13}C NMR (101 MHz, DMSO-d6, APT pulse sequence) δ d (CH, CH$_3$) 108.7, 125.0, 125.8, 128.6; u (C, CH$_2$) 118.8, 121.6, 134.3, 149.8.

Ethyl (*E*)-N-(3-cyano-4-phenyl-1*H*-pyrrol-2-yl)formimidate (9).—2-Amino-4-phenyl-1*H*-pyrrole-3-carbonitrile **8** (0.717 g, 3.91 mmol) was reacted according to General Procedure C to afford the formimidate product **9** as a tan solid (0.783 g, 3.27 mmol, 84% yield). ^{1}H NMR (400 MHz, acetone-d6) δ 1.39 (t, *J* = 7.1 Hz, 3H), 4.38 (qd, *J* = 0.8, 7.1 Hz, 2H), 7.03 (d, *J* = 1.7 Hz, 1H), 7.25–7.33 (m, 1H), 7.38–7.47 (m, 2H), 7.64–7.74 (m, 2H), 8.45 (s, 1H); ^{13}C NMR (101 MHz, acetone-d6, APT pulse sequence) δ d (CH, CH$_3$) 113.8, 126.8, 127.5, 129.6, 159.4; u (C, CH$_2$) 63.8, 118.1, 126.0, 134.7, 152.2.

Ethyl (E)-*N*-(1-benzyl-3-cyano-4-phenyl-1*H*-pyrrol-2-yl)formimidate (10).—Ethyl (*E*)-N-(3-cyano-4-phenyl-1*H*-pyrrol-2-yl)formimidate **9** (471 mg, 1.97 mmol), potassium carbonate (544 mg, 3.94 mmol, 2.0 equiv) and benzyl bromide (438 mg, 2.56 mmol, 1.3 equiv) were combined in acetone (15 mL) and stirred at 65 °C for 19 h. The reaction was

adsorbed onto Celite and purified by flash chromatography to afford the *N*-benzyl pyrrole as a light yellow solid (486 mg, 1.48 mmol, 75% yield). ^{1}H NMR (400 MHz, acetone-d6) δ 1.38 (t, *J* = 7.1 Hz, 3H), 4.43 (qd, *J* = 0.8, 7.1 Hz, 2H), 5.20 (s, 2H), 7.13 (s, 1H), 7.25–7.49 (complex, 9H), 7.57–7.81 (m, 1H), 8.51 (s, 1H); ^{13}C NMR (101 MHz, acetone-d6, APT pulse sequence) δ d (CH, CH$_3$) 14.4, 117.3, 126.8, 127.7, 128.4, 128.6, 129.6, 129.6, 159.8; u (C, CH$_2$) 49.9, 64.1, 118.3, 125.2, 134.4, 138.5, 145.4; HRMS calcd for C$_{21}$H$_{20}$N$_3$O [M + H]$^+$ 330.1601, found 330.1613.

2-Amino-1-benzyl-4,5-dimethyl-1*H*-pyrrole-3-carbonitrile (2j).—3-Hydroxybutan-2-one (6.38 g, 72.4 mmol) and benzyl amine (7.76 g, 72.4 mmol, 1.0 equiv) were reacted according to General Procedure B using zinc chloride (0.987 g, 7.24 mmol, 0.1 equiv) in place of trifluoroacetic acid to afford the previously reported pyrrole product[8] **2j** as an orange–brown solid (12.30 g, 54.6 mmol, 75% yield). ^{1}H NMR (400 MHz, CDCl$_3$) δ 2.03 (s, 3H), 2.06 (s, 3H), 3.59 (br s, 2H), 4.93 (s, 2H), 7.01 (d, *J* = 7.3 Hz, 2H), 7.29–7.39 (m, 3H). ^{13}C NMR (101 MHz, CDCl$_3$) δ 9.5, 10.0, 46.0, 113.6, 117.6, 119.2, 125.8, 127.8, 129.1, 136.3, 143.1.

Ethyl (*E*)-*N*-(1-benzyl-3-cyano-4,5-dimethyl-1*H*-pyrrol-2-yl)formimidate (3j).—Pyrrole **2j** (1.75 g, 7.77 mmol) was reacted according to General Procedure C to afford the formimidate **3j** as a viscous, yellow oil (0.7768 g, 2.76 mmol, 36% yield). R$_f$ = 0.61 (25% EtOAc in hexanes); ^{1}H NMR (400 MHz, CDCl$_3$) δ 1.30 (t, *J* = 7.1 Hz, 3H), 1.97 (s, 3H), 2.07 (s, 3H), 4.25 (q, *J* = 7.1 Hz, 2H), 5.05 (s, 2H), 7.00 (d, *J* = 7.4 Hz, 2H), 7.27 (dq, *J* = 7.3, 14.0 Hz, 3H), 8.43 (s, 1H); ^{13}C NMR (101 MHz, CDCl$_3$, APT pulse sequence) δ d (CH, CH$_3$) 9.8, 9.9, 14.0, 126.3, 127.4, 128.7, 157.4; u (C, CH$_2$) 46.1, 63.0, 116.0, 118.1, 122.6, 137.5, 141.6.

2-Amino-1-phenethyl-4,5,6,7-tetrahydro-1*H*-indole-3-carbonitrile (2k).—2-Hydroxcyclohexaone (2.23 g, 19.5 mmol) and benzyl amine (2.37 g, 19.5 mmol, 1.0 equiv) were reacted according to General Procedure B using zinc chloride (0.266 g, 1.95 mmol, 0.1 equiv) in place of trifluoroacetic acid to afford the pyrrole product **2k** as an orange-brown solid (2.26 g, 8.52 mmol, 44% yield). ^{1}H NMR (400 MHz, CDCl$_3$) δ 1.62-1.87 (m, 4H), 2.28 (t, *J* = 5.6 Hz, 2H), 2.44 (t, *J* = 5.7 Hz, 2H), 2.88 (t, *J* = 6.6 Hz, 2H), 3.11 (s, 2H), 3.85 (t, *J* = 6.5 Hz, 2H), 7.01 (d, *J* = 6.9 Hz, 2H), 7.24-7.31 (m, 3H); ^{13}C NMR (101 MHz, CDCl$_3$) δ 21.2, 21.5, 22.9, 22.9, 36.5, 44.2, 74.9, 116.3, 117.7, 122.1, 127.1, 128.9, 128.9, 138.0, 143.4.

Ethyl (*E*)-*N*-(3-cyano-1-phenethyl-4,5,6,7-tetrahydro-1*H*-indol-2-yl)formimidate (3k).—Pyrrole **2k** (1.74 g, 6.56 mmol) was reacted according to General Procedure C to afford the formimidate **3k** as a viscous, colorless oil (0.9844 g, 3.06 mmol, 47% yield). R$_f$ = 0.62 (25% EtOAc in hexanes); ^{1}H NMR (400 MHz, CDCl$_3$) δ 1.35 (t, *J* = 7.1 Hz, 3H), 1.60–1.77 (m, 4H), 2.23 (td, *J* = 2.8, 5.0, 5.6 Hz, 2H), 2.48 (td, *J* = 1.7, 5.9 Hz, 2H), 2.84 (t, *J* = 7.0 Hz, 2H), 3.94 (t, *J* = 7.1 Hz, 2H), 4.24 (qd, *J* = 0.8, 7.1 Hz, 2H), 6.89–7.02 (m, 2H), 7.10–7.39 (m, 3H), 8.11 (s, 1H); ^{13}C NMR (101 MHz, CDCl$_3$, APT pulse sequence) δ d (CH, CH$_3$) 14.2, 126.7, 128.5, 128.9, 156.9; u (C, CH$_2$) 14.2, 21.3, 21.6, 22.9, 23.0, 36.8, 44.2, 62.8, 118.1, 118.3, 125.3, 138.3, 141.9.

Synthesis and Characterization of Pyrrolopyrimidine Final Analogues

3-(7-Benzyl-4-imino-5,6-diphenyl-4,7-dihydro-3*H*-pyrrolo[2,3-*d*]pyrimidin-3-yl)propan-1-ol (5a).—Formimidate **3a** (1.5000 g, 3.70 mmol) and 3-aminopropanol (0.5560 g, 7.40 mmol, 2.0 equiv) were reacted according to General Procedure D and purified by flash chromatography to afford **5a** as a white solid (1.1872 g, 2.73 mmol, 74% yield). ^{1}H NMR (CDCl$_3$) δ 1.91 (ddt, J = 4.6, 7.6, 11.3 Hz, 2H), 3.53 (t, J = 5.5 Hz, 2H), 4.20 (t, J = 5.8 Hz, 2H), 5.29 (s, 2H), 6.94 (dd, J = 2.1, 7.5 Hz, 2H), 7.02–7.07 (m, 2H), 7.17–7.27 (complex, 11H), 7.69 (s, 1H); ^{13}C NMR (101 MHz, CDCl$_3$) δ 33.7, 43.0, 46.2, 56.6, 102.9, 118.1, 126.8, 127.0, 127.3, 128.1, 128.2, 128.4, 128.5, 130.4, 130.5, 131.1, 133.4, 133.6, 137.7, 143.2, 145.5, 157.1; IR (neat) 1622, 1561, 1484 cm^{-1}; HRMS calcd for C$_{28}$H$_{27}$N$_4$O [M + H]$^+$ 435.2179, found 435.2190; HPLC purity = 97.9%.

2-(7-Benzyl-4-imino-5,6-diphenyl-4,7-dihydro-3*H*-pyrrolo[2,3-d]pyrimidin-3-yl)ethan-1-ol (5b).—Formimidate **3a** (30.0 mg, 0.074 mmol) and 2-aminoethanol (6.8 mg, 0.111 mmol, 1.5 equiv) were reacted according to General Procedure D and purified by flash chromatography to afford **5b** as a tan solid (29.1 mg, 0.069 mmol, 93% yield). ^{1}H NMR (400 MHz, CDCl$_3$) δ 3.92–4.04 (m, 2H), 4.20–4.48 (m, 2H), 5.30 (s, 2H), 6.85–6.96 (m, 2H), 6.97–7.07 (m, 2H), 7.15–7.33 (complex, 11H), 7.73 (s, 1H); ^{13}C NMR (101 MHz, CDCl$_3$) δ 10.2, 27.0, 46.8, 56.2, 71.9, 100.6, 117.2, 127.1 (× 2C), 128.0, 128.6, 128.6, 128.7, 128.7, 129.3, 129.4, 130.2, 130.8, 131.1, 133.1, 136.1, 138.3, 144.4; HRMS calcd for C$_{27}$H$_{25}$N$_4$O [M + H]$^+$ 421.2023, found 421.2018; HPLC purity = 97.5%.

4-(7-Benzyl-4-imino-5,6-diphenyl-4,7-dihydro-3*H*-pyrrolo[2,3-*d*]pyrimidin-3-yl)butan-1-ol (5c).—Formimidate **3a** (40.0 mg, 0.099 mmol) and 4-aminobutanol (17.6 mg, 0.198 mmol, 2.0 equiv) were reacted according to General Procedure D and purified by flash chromatography to afford **5c** as a tan solid (37.5 mg, 0.084 mmol, 85% yield). ^{1}H NMR (400 MHz, DMSO-d_6) δ 1.43 (dt, J = 13.6, 6.6 Hz, 2H), 1.71 (p, J = 8.0, 7.5 Hz, 2H), 3.38–3.44 (m, 2H), 3.96 (t, J = 7.2 Hz, 2H), 5.24 (s, 2H), 6.85 (d, J = 6.8 Hz, 2H), 7.11 (dd, J = 7.3, 2.0 Hz, 2H), 7.15–7.36 (complex, 11H), 8.00 (s, 1H). ^{13}C NMR (101 MHz, DMSO-d_6) δ 24.9, 29.5, 45.3, 46.1, 60.5, 102.6, 117.2, 126.4, 126.9, 127.1, 128.1, 128.2, 128.2, 128.4, 130.3, 130.4, 130.8, 131.8, 134.0, 137.9, 142.4, 147.1, 154.4; IR (neat) 1656, 1617, 1546, 1495 cm^{-1}; HRMS calcd for C$_{29}$H$_{29}$N$_4$O [M + H]$^+$ 449.2336, found 449.2350; HPLC purity = 98.2%.

5-(7-Benzyl-4-imino-5,6-diphenyl-4,7-dihydro-3*H*-pyrrolo[2,3-*d*]pyrimidin-3-yl)pentan-1-ol (5d).—Formimidate **3a** (40.0 mg, 0.099 mmol) and 5-aminopentanol (20.4 mg, 0.198 mmol, 2.0 equiv) were reacted according to General Procedure D and purified by flash chromatography to afford **5d** as a tan solid (45.1 mg, 0.097 mmol, 98% yield). ^{1}H NMR (500 MHz, CDCl$_3$) δ 1.52 (p, J = 7.1 Hz, 2H), 1.62 (p, J = 6.4 Hz, 2H), 1.88 (p, J = 7.9 Hz, 2H), 1.98 (s, 1H), 3.63 (t, J = 5.7 Hz, 2H), 4.08–4.22 (m, 2H), 5.31 (s, 2H), 6.88–6.98 (m, 2H), 7.05 (d, J = 7.6 Hz, 2H), 7.21–7.29 (m, 11H), 7.78 (s, 1H). ^{13}C NMR (126 MHz, CDCl$_3$, APT pulse sequence) δ d (CH, CH$_3$) 126.7, 127.2, 127.4, 128.2, 128.3, 128.5, 128.5, 130.4, 130.9, 145.2; u (C, CH$_2$) 22.6, 28.2, 31.8, 46.2, 48.7, 61.5, 102.5, 117.8, 130.0, 133.1, 134.2, 137.4, 143.6, 154.4; IR 1625, 1563, 1496 cm^{-1}; HRMS calcd for C$_{30}$H$_{31}$N$_4$O [M + H]$^+$ 463.2492, found 463.2492; HPLC purity = 95.2%.

7-Benzyl-3-(2-methoxyethyl)-5,6-diphenyl-3,7-dihydro-4*H***-pyrrolo[2,3-*d*]pyrimidin-4-imine (5e).—**Formimidate **3a** (40.0 mg, 0.099 mmol) and 2-methoxyethan-1-amine (14.9 mg, 0.198 mmol, 2.0 equiv) were reacted according to General Procedure D and purified by flash chromatography to afford **5e** as a tan solid (32.4 mg, 0.075 mmol, 75% yield). ^{1}H NMR (CDCl$_3$) δ 3.34 (s, 3H), 3.71 (dd, *J* = 4.3, 5.3 Hz, 2H), 4.22 (t, *J* = 4.8 Hz, 2H), 5.28 (s, 2H), 6.93–6.97 (m, 2H), 7.02–7.06 (m, 2H), 7.16–7.27 (m, 11H), 7.75 (s, 1H); ^{13}C NMR (101 MHz, CDCl$_3$, APT pulse sequence) δ d (CH, CH$_3$) 59.0, 126.8, 126.9, 127.2, 128.0, 128.2, 128.3, 128.5, 130.5, 131.1, 146.8; u (C, CH$_2$) 46.1, 47.3, 69.8, 103.3, 118.1, 130.7, 132.8, 133.9, 137.9, 143.1, 155.3; HRMS calcd for C$_{28}$H$_{27}$N$_4$O [M + H]$^+$ 435.2179, found 435.2201; HPLC purity > 99.5%.

trans*-4-(7-Benzyl-4-imino-5,6-diphenyl-4,7-dihydro-3H***-pyrrolo[2,3-*d*]pyrimidin-3-yl)cyclohexan-1-ol (5f).—**The analogue **5f** (metarrestin) was prepared as previously reported.[9]

cis*-4-(7-Benzyl-4-imino-5,6-diphenyl-4,7-dihydro-3H***-pyrrolo[2,3-*d*]pyrimidin-3-yl)cyclohexan-1-ol (5g).—**Formimidate 3**a** (53.5 mg, 0.132 mmol), *cis*--4-aminocyclohexan-1-ol hydrochloride (100.0 mg, 0.659 mmol, 5.0 equiv) and sodium methoxide (21.4 mg, 0.40 mmol, 3 equiv) were reacted according to General Procedure E and purified by flash chromatography followed by MDF purification to afford **5g** as an off-white solid (25.3 mg, 0.053 mmol, 40% yield). ^{1}H NMR (400 MHz, CDCl$_3$) 1.67–1.92 (complex, 6H), 1.96–2.08 (m, 2H), 4.01 (t, *J* = 2.7 Hz, 1H), 5.03 (t, *J* = 12.5 Hz, 1H), 5.21 (s, 2H), 6.84–6.90 (m, 2H), 6.94–6.99 (m, 2H), 7.08–7.21 (complex, 11H), 7.88 (s, 1H); ^{13}C NMR (101 MHz, CDCl$_3$, APT pulse sequence) δ d (CH, CH$_3$) 52.9, 64.2, 126.9, 127.0, 127.3, 128.1, 128.2, 128.4, 128.5, 130.6, 131.1, 143.0; u (C, CH$_2$) 36.7, 44.5, 26.3, 32.4, 46.1, 102.8, 118.0, 130.5, 133.4, 133.6, 137.8, 142.8, 155.0; HRMS calcd for C$_{31}$H$_{31}$N$_4$O [M + H]$^+$ 475.2492, found 475.2501; HPLC purity = 99.1%.

trans*-2-(7-Benzyl-4-imino-5,6-diphenyl-4,7-dihydro-3H***-pyrrolo[2,3-*d*]pyrimidin-3-yl)cyclohexan-1-ol (5h).—**251-9-1 Formimidate **3a** (142 mg, 0.35 mmol) and *trans*-2-aminocyclohexan-1-ol (81 mg, 0.70 mmol, 2.0 equiv) were reacted according to General Procedure D and purified by MDF purification to afford **5h** as an off-white solid (42.6 mg, 0.090 mmol, 26% yield). ^{1}H NMR (400 MH, CDCl$_3$) δ 1.20–1.55 (m, 3H), 1.67–1.88 (m, 3H), 2.05 (dt, *J* = 2.8, 12.2 Hz, 1H), 2.19 (dd, *J* = 3.8, 12.7 Hz, 1H), 3.67 (td, *J* = 4.5, 10.4 Hz, 1H), 4.99 (ddd, *J* = 3.5, 10.3, 13.4 Hz, 1H), 5.26, 5.30 (ABq, *J*$_{AB}$ = 15.8 Hz, 2H), 6.93–6.98 (m, 2H), 7.02–7.06 (m, 2H), 7.14–7.38 (complex, 11H), 7.86 (s, 1H); ^{13}C NMR (101 MHz, CDCl$_3$, APT pulse sequence) δ d (CH, CH$_3$) 41.0, 59.6, 75.7, 126.8, 126.9, 127.3, 128.1, 128.2, 128.3, 128.5, 130.5, 131.1, 142.6; u (C, CH$_2$) 24.5, 25.8, 31.9, 36.4, 46.1, 103.1, 118.0, 130.5, 133.3, 133.7, 137.8, 142.7, 159.0; HRMS calcd for C$_{31}$H$_{31}$N$_4$O [M + H]$^+$ 475.2492, found 475.2496; HPLC purity = 99.7%.

trans*-2-((7-Benzyl-4-imino-5,6-diphenyl-4,7-dihydro-3H***-pyrrolo[2,3-*d*]pyrimidin-3-yl)methyl)cyclohexan-1-ol (5i).—**Formimidate **3a** (60.0 mg, 0.149 mmol) and *trans*-2-(aminomethyl)cyclohexan-1-ol (38.2 mg, 0.296 mmol, 2.0 equiv) were reacted according to General Procedure D and purified by MDF

purification to afford **5i** as an off-white solid (61.4 mg, 0.126 mmol, 84% yield). ^{1}H NMR (400 MHz, CDCl₃) δ 1.13–1.36 (m, 5H), 1.64–1.80 (m, 3H), 1.99 (d, *J* = 11.7 Hz, 1H), 3.18 (td, *J* = 4.2, 10.2 Hz, 1H), 3.90 (dd, *J* = 2.4, 14.7 Hz, 1H), 4.58 (dd, *J* = 4.4, 14.4 Hz, 1H), 5.30, 5.32 (ABq, J_{AB} = 15.7 Hz, 2H), 6.89–6.98 (m, 2H), 7.02–7.09 (m, 2H), 7.15–7.34 (m, 11H), 7.75 (s, 1H); ^{13}C NMR (101 MHz, CDCl₃, APT pulse sequence) δ d (CH, CH₃) 46.2, 69.9, 126.9, 127.3, 127.4, 128.3, 128.4, 128.5, 128.6, 130.5, 131.0, 146.1; u (C, CH₂) 24.9, 25.6, 29.3, 34.5, 46.2, 50.5, 102.4, 117.8, 130.0, 133.1, 134.4, 137.3, 143.7, 155.7; HRMS calcd for $C_{32}H_{33}N_4O$ [M + H]⁺ 489.2649, found 489.2657; HPLC purity = 96.8%.

trans-2-((7-Benzyl-4-imino-5,6-diphenyl-4,7-dihydro-3*H*-pyrrolo[2,3-*d*]pyrimidin-3-yl)methyl)cyclohexyl)methanol (5j).—Formimidate **3a**

(99.0 mg, 0.244 mmol), *trans*-2-(aminomethyl)cyclohexan-1-ol
(60.6 mg, 0.366 mmol, 1.5 equiv) and sodium methoxide (26.4
mg, 0.488 mmol, 2.0 equiv) were reacted according to General Procedure D and purified by MDF purification to afford **5j** as a tan solid (53.5 mg, 0.109 mmol, 45% yield). ^{1}H NMR (500 MHz, CDCl₃) δ 1.29–1.65 (m, 3H), 1.72–1.96 (m, 5H), 2.05–2.11 (m, 1H), 3.26 (dd, *J* = 1.8, 12.2 Hz, 1H), 3.46 (dd, *J* = 2.4, 12.2 Hz, 1H), 4.92 (ddd, *J* = 3.7, 11.2, 12.6 Hz, 1H), 5.29, 5.29 (ABq, J_{AB} = 12.7 Hz, 2H), 6.91–6.98 (m, 2H), 7.01–7.10 (m, 2H), 7.17–7.29 (m, 11H), 7.83 (s, 1H); ^{13}C NMR (126 MHz, CDCl₃, APT pulse sequence) δ d (CH, CH₃) 46.6, 53.6, 126.8, 127.0, 127.3, 128.21, 128.24, 128.4, 128.5, 130.5, 131.1, 142.8; u (C, CH₂) 25.7, 26.2, 28.9, 33.3, 46.1, 62.1, 102.5, 118.0, 130.3, 133.4, 133.6, 137.7, 142.7, 157.3; HRMS calcd for $C_{32}H_{33}N_4O$ [M + H]⁺ 489.2649, found 489.2652; HPLC purity = 99.6%.

(*S*)-2-(7-Benzyl-4-imino-5,6-diphenyl-4,7-dihydro-3*H*-pyrrolo[2,3-*d*]pyrimidin-3-yl)-3-phenylpropan-1-ol (5k).—Formimidate **3a** (81.3 mg, 0.20 mmol), potassium *tert*-

butoxide (45.0 mg, 0.40 mmol, 2.0 equiv) and (*S*)-2-amino-3-phenylpropan-1-ol (60.6 mg, 0.40 mmol, 2.0 equiv) were reacted according to General Procedure D and purified by flash chromatography to afford **5k** as a sticky yellow solid (89.1 mg, 0.17 mmol, 87% yield). ^{1}H NMR (400 MHz, CDCl₃) δ 3.24 (dd, *J* = 5.6, 14.0 Hz, 1H), 3.56 (dd, *J* = 9.6, 14.0 Hz, 1H), 3.98 (dd, *J* = 5.2, 12.4 Hz, 1H), 4.05 (d, *J* = 8.4 Hz, 1H), 4.30 (br s, 1H), 5.17 (d, *J* = 15.6 Hz, 1H), 5.26 (d, *J* = 16.0 Hz, 1H), 6.56 (br s, 1H), 6.86-6.88 (m, 2H), 7.03-7.05 (m, 2H), 7.17-7.31 (complex, 16H); ^{13}C NMR (101 MHz, CDCl₃) δ 33.8, 36.8, 46.1, 63.8, 102.9, 118.0, 126.6, 126.7, 127.0, 127.2, 128.05, 128.12, 128.4, 128.6, 129.0, 130.3, 130.5, 131.0, 133.3, 133.6, 137.7, 138.4, 142.9, 155.9; IR (neat) 1622, 1495, 1355 cm⁻¹; [α]$_D$ = −271.3 (c 0.028, chloroform); HRMS calcd for $C_{34}H_{31}N_4O$ [M + H]⁺ 511.2492, found 511.2517; HPLC purity = 99.0%.

(1*S*,2*R*)-2-(7-Benzyl-4-imino-5,6-diphenyl-4,7-dihydro-3*H*-pyrrolo[2,3-*d*]pyrimidin-3-yl)-1-phenylpropan-1-ol (5l).—Formimidate **3a** (40.0

mg, 0.099 mmol) and (1*S*,2*R*)-2-amino-1-phenylpropan-1-ol (29.9
mg, 0.198 mmol, 2.0 equiv) were reacted according to
General Procedure D and purified by flash chromatography to afford **5l** as a tan solid (27.5 mg, 0.054 mmol, 54% yield). ^{1}H NMR (400 MHz, CD₃OD) δ 1.29 (d, *J* = 5.8 Hz, 3H), 3.22 (dt, *J* = 3.2, 1.6 Hz, 1H), 4.93 (s, 1H), 5.20 (s, 1H), 5.24 (br s, 1H), 6.69–6.81 (m, 2H), 6.95 (d, *J* = 6.9 Hz, 2H), 7.02–7.28 (complex, 14H), 7.38 (d, *J* = 7.4 Hz, 2H), 7.97 (s, 1H). [13]C

NMR (101 MHz, CD$_3$OD) δ 14.0, 46.9, 55.4, 75.4, 104.0, 119.3, 127.3, 127.7, 128.2, 128.3, 128.4, 129.2, 129.2, 129.3, 129.4, 129.4, 131.7, 131.8, 132.2, 134.7, 135.2, 139.2, 143.4, 143.8, 157.8. IR (neat) 1722, 1622, 1558, 1264 cm^{-1}; [α]$_D$ = +186.3 (c 1.3, chloroform); HRMS calcd for C$_{34}$H$_{31}$N$_4$O [M + H]$^+$ 511.2492, found 511.2505; HPLC purity = 97.1%.

7-Benzyl-3-((trans)-4-methoxycyclohexyl)-5,6-diphenyl-3,7-dihydro-4H-pyrrolo[2,3-d]pyrimidin-4-imine (5m).—

Formimidate **3a** (96.0 mg, 0.237 mmol) and (trans)-4-methoxycyclohexylamine (61.2 mg, 0.474 mmol, 2.0 equiv) were reacted according to General Procedure D and purified by MDF purification to afford **5m** as an off-white solid (22.0 mg, 0.045 mmol, 19% yield). ^{1}H NMR (CDCl$_3$, 500 MHz) δ 1.41–1.55 (m, 2H), 1.63 (qd, J = 3.1, 12.7 Hz, 2H), 2.14 (dd, J = 2.9, 12.2 Hz, 2H), 2.22 (d, J = 11.5 Hz, 2H), 3.23 (tt, J = 4.1, 10.9 Hz, 1H), 3.37 (s, 3H), 5.08 (ddd, J = 3.6, 8.6, 12.2 Hz, 1H), 5.27 (s, 2H), 6.96 (dd, J = 1.6, 8.0 Hz, 2H), 7.02–7.08 (m, 2H), 7.15–7.30 (complex, 11H), 7.75 (s, 1H); ^{13}C NMR (126 MHz, CDCl$_3$, APT pulse sequence) δ d: 51.7, 56.0, 78.5, 126.8, 126.8, 127.3, 128.0, 128.2, 128.3, 128.5, 130.6, 131.1, 142.5; u: 30.5, 31.2, 46.0, 103.3, 118.3, 130.6, 132.7, 133.9, 138.0, 142.3, 155.5; HRMS calcd for C$_{32}$H$_{33}$N$_4$O [M + H]$^+$ 489.2649, found 489.2649; HPLC purity = 99.8%.

4-(7-Benzyl-4-imino-5,6-diphenyl-4,7-dihydro-3H-pyrrolo[2,3-d]pyrimidin-3-yl)cyclohexan-1-one (5n).—

A 20 mL oven-dried reaction vial was cooled with dry nitrogen and charged with 4 Å molecular sieves (1.0 g), followed by **5f** (metarrestin) (200 mg, 0.421 mmol), DMSO and Burgess reagent (131 mg, 0.548 mmol, 1.3 equiv). Although the substrate **5f** did not appear to completely dissolve, the reaction was stirred at rt for 2 h. LCMS analysis showed <10% conversion with predominantly substrate **5f** remaining. Water was added and the reaction extracted with EtOAc; the organic layer was dried (MgSO$_4$), filtered, concentrated and purified by flash chromatography and then preparative thin-layer chromatography to provide **5n** (11 mg, 0.023 mmol, 6% yield). ^{1}H NMR (400 MHz, CDCl$_3$) δ 2.05 (dq, J = 12.8, 4.5 Hz, 2H), 2.36–2.45 (m, 2H), 2.50–2.60 (m, 1H), 2.60–2.73 (m, 2H), 5.28 (s, 2H), 5.53–5.68 (m, 1H), 6.94–6.99 (m, 2H), 7.02–7.08 (m, 2H), 7.18–7.31 (complex, 11H), 7.75 (s, 1H); LCMS calc. for C$_{32}$H$_{29}$N$_4$O [M + H]$^+$ 473.6, found 473.0; HPLC purity >99.5%.

7-Benzyl-5,6-diphenyl-3-(tetrahydro-2H-pyran-4-yl)-3,7-dihydro-4H-pyrrolo[2,3-d]pyrimidin-4-imine (5o).—

Formimidate **3a** (40.0 mg, 0.099 mmol) and 4-aminotetrohydropyran (20.0 mg, 0.198 mmol, 2.0 equiv) were reacted according to General Procedure D and purified by flash chromatography to afford **5o** as a white solid (34.1 mg, 0.074 mmol, 75% yield). ^{1}H NMR (CDCl$_3$, 401 MHz) δ 1.87–2.03 (complex, 4 H), 3.62 (t, J = 11.6 Hz, 2 H), 4.11 (dd, J = 4.0, 11.4 Hz, 2 H), 5.28 (s, 2 H), 5.32–5.40 (m, 1 H), 6.49 (br s, 1 H), 6.96 (dd, J = 2.0, 8.0 Hz, 2 H), 7.05 (dd, J = 1.6, 8.0 Hz, 2 H), 7.17–7.26 (complex, 11 H), 7.81 (s, 1 H); ^{13}C NMR (101 MHz, CDCl$_3$, APT pulse sequence) δ d: 49.9, 126.9, 127.0, 127.4, 128.2, 128.3, 128.4, 128.7, 130.7, 131.2, 142.7; u: 33.0, 46.2, 67.8, 103.2, 118.4, 130.7, 133.1, 134.0, 138.0, 142.4, 155.4; HRMS calcd for C$_{30}$H$_{29}$N$_4$O [M + H]$^+$ 461.2336, found 461.2334; HPLC purity = 98.4%.

7-Benzyl-5,6-diphenyl-3-((tetrahydro-2*H*-pyran-4-yl)methyl)-3,7-dihydro-4*H*-pyrrolo[2,3-*d*]pyrimidin-4-imine (5p).—Formimidate **3a** (148 mg, 0.365 mmol) (tetrahydro-2H-pyran-4-yl)methanamine (84 mg, 0.730 mmol, 2.0 equiv) were reacted according to General Procedure D and purified by flash chromatography to afford **5p** as a tan solid (150.6 mg, 0.317 mmol, 87% yield).
^{1}H NMR (400 MHz, CDCl$_3$) δ 1.41 (qd, J = 4.4, 12.1 Hz, 2H), 1.57–1.72 (m, 2H), 2.28–2.46 (m, 1H), 3.24–3.46 (m, 2H), 3.92–4.03 (m, 2H), 4.26 (d, J = 7.4 Hz, 2H), 5.36 (s, 2H), 6.87–6.94 (m, 2H), 7.04–7.09 (m, 2H), 7.17–7.38 (complex, 11H), 7.91 (s, 1H), 8.57 (s, 1H); ^{13}C NMR (101 MHz, CDCl$_3$, APT pulse sequence) δ d (CH, CH$_3$) 33.0, 127.0, 127.7, 128.0, 128.5, 128.6, 128.9, 129.0, 130.4, 130.9, 145.1; u (C, CH$_2$) 30.0, 46.6, 55.3, 67.3, 101.4, 117.4, 129.2, 132.1, 136.5, 136.6, 144.8, 153.0; HRMS calcd for C$_{31}$H$_{31}$N$_4$O [M + H]$^+$ 475.2492, found 475.2500; HPLC purity > 99.5%.

7-Benzyl-5,6-diphenyl-3-((tetrahydrofuran-3-yl)methyl)-3,7-dihydro-4*H*-pyrrolo[2,3-*d*]pyrimidin-4-imine (5q).—Formimidate **3a** (104.0 mg, 0.256 mmol) (tetrahydrofuran-3-yl)methanamine (51.9 mg, 0.513 mmol, 2.0 equiv) were reacted according to General Procedure D and purified MDF purification to afford **5q** as an off-white solid (74.7 mg, 0.162 mmol, 63% yield). ^{1}H NMR (500 MHz, CDCl$_3$) δ 1.67–1.77 (m, 1H), 2.09 (dtd, J = 5.4, 8.0, 13.2 Hz, 1H), 2.99–3.14 (m, 1H), 3.65 (dd, J = 4.7, 9.0 Hz, 1H), 3.72–3.82 (m, 2H), 3.96 (td, J = 5.4, 8.2 Hz, 1H), 4.10 (dd, J = 8.0, 13.8 Hz, 1H), 4.19 (dd, J = 7.1, 13.8 Hz, 1H), 5.31 (s, 2H), 6.90–6.96 (m, 2H), 7.03–7.08 (m, 2H), 7.17–7.31 (complex, 11H), 7.81 (s, 1H), 8.62 (br s, 1H); ^{13}C NMR (126 MHz, CDCl$_3$, APT pulse sequence) δ d (CH, CH$_3$) 37.4, 126.8, 127.3, 127.5, 128.3, 128.4, 128.5, 128.6, 130.4, 131.0, 145.4; u (C, CH$_2$) 29.6, 37.4, 46.3, 51.0, 67.5, 70.4, 102.4, 117.8, 129.9, 133.0, 134.5, 137.3, 143.6, 154.3; HRMS calcd for C$_{30}$H$_{29}$N$_4$O [M + H]$^+$ 461.2336, found 461.2345; HPLC purity = 99.6%.

7-Benzyl-5,6-diphenyl-3-((tetrahydrofuran-2-yl)methyl)-3,7-dihydro-4l-pyrrolo[2,3-*d*]pyrimidin-4-imine (5r).—Formimidate **3a** (40.0 mg, 0.099 mmol) and (tetrahydrofuran-2-yl)methanamine (20.0 mg, 0.198 mmol, 2.0 equiv) were reacted according to General Procedure D and purified by MDF purification to afford **5r** as a white solid (17.4 mg, 0.038 mmol, 38% yield). ^{1}H NMR (400 MHz, CDCl$_3$) δ 1.62 (ddt, J = 7.5, 8.6, 12.4 Hz, 1H), 1.91 (pd, J = 2.3, 7.0 Hz, 2H), 2.02–2.15 (m, 1H), 3.67–3.81 (m, 2H), 3.88 (dt, J = 6.8, 8.4 Hz, 1H), 4.33 (qd, J = 2.6, 7.5 Hz, 1H), 4.51 (dd, J = 2.6, 13.8 Hz, 1H), 5.27 (s, 2H), 6.92–6.98 (m, 2H), 7.01–7.06 (m, 2H), 7.15–7.28 (m, 11H), 7.80 (s, 1H); ^{13}C NMR (101 MHz, CDCl$_3$, APT pulse sequence) δ d (CH, CH$_3$) 76.4, 126.7, 126.9, 127.2, 127.9, 128.1, 128.2, 128.5, 130.6, 131.1, 146.8; u (C, CH$_2$) 25.9, 28.9, 46.1, 50.4, 68.0, 103.3, 118.2, 130.8, 132.6, 134.0, 138.0, 143.0, 155.8; HRMS calcd for C$_{30}$H$_{29}$N$_4$O [M + H]$^+$ 461.2336, found 461.2356; HPLC purity = 98.8%.

7-Benzyl-3-(oxetan-2-ylmethyl)-5,6-diphenyl-3,7-dihydro-4*H*-pyrrolo[2,3-*d*]pyrimidin-4-imine (5s).—Formimidate **3a** (35.0 mg, 0.075 mmol) oxetan-3-ylmethanamine (9.8 mg, 0.113 mmol, 1.5 equiv) were reacted according to General Procedure D and purified MDF purification to afford **5s** as a tan solid (30.2 mg, 0.068 mmol, 90% yield). ^{1}H NMR (500 MHz, CDCl$_3$) δ 2.45–2.53 (m, 1H), 3.44 (dd, J =

8.3, 13.7 Hz, 1H), 3.60 (ddd, J = 1.5, 4.8, 13.7 Hz, 1H), 3.66 (dd, J = 6.5, 11.6 Hz, 1H), 3.76 (dd, J = 5.2, 11.6 Hz, 1H), 4.34 (dd, J = 8.8, 13.1 Hz, 1H), 4.59–4.67 (m, 1H), 5.35, 5.35 (ABq, J_{AB} = 12.4 Hz, 2H), 6.85–6.93 (m, 2H), 7.00–7.06 (m, 2H), 7.16–7.22 (m, 5H), 7.23–7.42 (m, 6H), 8.31 (s, 1H), 8.52 (s, 1H); ^{13}C NMR (126 MHz, CDCl$_3$, APT pulse sequence) δ d (CH, CH$_3$) 32.0, 127.1, 127.8, 128.1, 128.5, 128.6, 129.1, 129.2, 130.4, 130.9, 168.1; u (C, CH$_2$) 42.4, 46.7, 49.8, 60.3, 100.1, 116.6, 128.8, 131.6, 136.3, 137.8, 145.6, 148.3; HRMS calcd for C$_{29}$H$_{27}$N$_4$O [M + H]$^+$ 447.2179, found 447.2193; HPLC purity = 99.8%.

7-Benzyl-3-(4,4-diethoxybutyl)-5,6-diphenyl-3,7-dihydro-4*H*-pyrrolo[2,3-*d*]pyrimidin-4-imine (5t).

212-20E Formimidate **3a** (40.0 mg, 0.099 mmol) and 4,4-diethoxybutan-1-amine (31.9 mg, 0.198 mmol, equiv) were reacted according to General Procedure D and purified by flash chromatography to afford **5t** as an off-white solid (25.8 mg, 0.050 mmol, 50% yield). ^{1}H NMR (400 MHz, CDCl$_3$) δ 1.20 (t, J = 7.0 Hz, 6H), 1.72 (dt, J = 5.9, 12.0 Hz, 2H), 1.91 (tt, J = 6.0, 8.3 Hz, 2H), 3.49 (dq, J = 7.0, 9.4 Hz, 2H), 3.65 (dq, J = 7.1, 9.4 Hz, 2H), 4.04–4.14 (m, 2H), 4.52 (t, J = 5.6 Hz, 1H), 5.28 (s, 2H), 6.92–6.97 (m, 2H), 7.02–7.07 (m, 2H), 7.16–7.26 (m, 11H), 7.71 (s, 1H); ^{13}C NMR (101 MHz, CDCl$_3$, APT pulse sequence) δ d (CH, CH$_3$) 15.4, 102.9, 126.8, 126.9, 127.3, 128.0, 128.2, 128.3, 128.5, 130.5, 131.1, 145.8; u (C, CH$_2$) 24.2, 30.7, 46.1, 47.5, 61.5, 103.3, 118.1, 130.6, 133.8, 136.3, 137.9, 143.1, 155.1; HRMS calcd for C$_{33}$H$_{37}$N$_4$O$_2$ [M + H]$^+$ 521.2911, found 521.2948; HPLC purity > 99.5%.

N-(2-(7-Benzyl-4-imino-5,6-diphenyl-4,7-dihydro-3*H*-pyrrolo[2,3-*d*]pyrimidin-3-yl)ethyl)pyridm-4-amine (5u).

Formimidate **3a** (40.0 mg, 0.099 mmol) and N^1-(pyridin-4-yl)ethane-1,2-diamine (27.2 mg, 0.198 mmol, 2.0 equiv) were reacted according to General Procedure D and purified by MDF purification to afford 5u as a light brown solid (25.0 mg, 0.050 mmol, 51% yield). ^{1}H NMR (400 MHz, CDCl$_3$) δ 3.52–3.66 (m, 2H), 4.32 (t, J = 5.5 Hz, 2H), 5.29 (s, 2H), 6.35 (t, J = 5.0 Hz, 1H), 6.41 (d, J = 5.5 Hz, 2H), 6.89–6.95 (m, 2H), 7.01–7.05 (m, 2H), 7.15–7.30 (m, 10H), 7.69 (s, 1H), 8.09–8.18 (m, 2H); ^{13}C NMR (101 MHz, CDCl$_3$, APT pulse sequence) δ d (CH, CH$_3$) 107.3, 126.7, 126.9, 127.3, 128.1, 128.2, 128.3, 128.5, 130.5, 131.0, 145.5, 149.8; u (C, CH$_2$) 43.5, 46.4, 53.0, 103.2, 118.0, 130.4, 133.2, 133.7, 137.7, 142.8, 153.1, 156.7; HRMS calcd for C$_{32}$H$_{29}$N$_6$ [M + H]$^+$ 497.2448, found 497.2477; HPLC purity = 97.8%.

2-(7-Benzyl-4-imino-5,6-diphenyl-4,7-dihydro-3*H*-pyrrolo[2,3-*d*]pyrimidin-3-yl)ethan-1-amine (5v).

Formimidate **3a** (40.0 mg, 0.099 mmol) and ethane-1,2-diamine (11.9 mg, 0.198 mmol, 2.0 equiv) were reacted according to General Procedure D and purified by MDF purification to afford **5v** as a tan solid (18.8 mg, 0.045 mmol, 45% yield). ^{1}H NMR (400 MHz, CDCl$_3$) δ 3.13 (t, J = 6.4 Hz, 2H), 4.12 (t, J = 6.4 Hz, 2H), 5.28 (s, 2H), 6.95–6.93 (m, 2H), 7.05–7.03 (m, 2H), 7.27–7.18 (complex, 11H), 7.76 (s, 1H); ^{13}C NMR (101 MHz, CDCl$_3$) δ 40.4, 46.1, 50.6, 103.1, 118.0, 126.8, 127.0, 127.3, 128.07, 128.17, 128.24, 128.3, 128.4, 128.5, 130.4, 130.5, 130.8, 131.0, 133.2, 133.7, 137.7, 143.2, 146.0, 155.3; IR 1625, 1496, 1356, cm^{-1}; HRMS calcd for C$_{27}$H$_{26}$N$_5$ [M + H]$^+$ 420.2183, found 420.2178; HPLC purity = 95.1%.

2-(7-Benzyl-4-imino-5,6-diphenyl-4,7-dihydro-3*H*-pyrrolo[2,3-*d*]pyrimidin-3-yl)-*N*,*N*-dimethylethan-1-amine (5w).—Formimidate **3a** (82.1 mg, 0.20 mmol), potassium *tert*-butoxide (45.4 mg, 0.4 mmol, 2.0 equiv) and N^1,N^1-dimethylethane-1,2-diamine (35.7 mg, 0.40 mmol, 2.0 equiv) were reacted according to General Procedure E and purified by flash chromatography to afford **5w** as a sticky yellow solid (80.3 mg, 0.18 mmol, 89% yield). ^{1}H NMR (400 MHz, CDCl$_3$) δ 2.29 (s, 6H), 2.66 (t, J = 6.4 Hz, 2H), 4.09 (t, J = 6.4 Hz, 2H), 5.27 (s, 2H), 6.95–6.93 (m, 2H), 7.04–7.02 (m, 2H), 7.23–7.16 (complex, 11H), 7.72 (s, 1H); ^{13}C NMR(101 MHz, CDCl$_3$) δ 39.7, 45.6, 46.0, 57.4, 103.4, 118.1, 126.70, 126.75, 127.2, 127.9, 128.1, 128.2, 128.4, 130.5, 130.7, 131.0, 132.5, 134.0, 142.9, 146.3, 155.4; IR (neat) 1627, 1603, 1565 cm^{-1}; HRMS calcd for C$_{29}$H$_{30}$N$_5$ [M + H]$^+$ 448.2496, found 448.2512; HPLC purity > 99.5%.

2-(7-Benzyl-4-imino-5,6-diphenyl-4,7-dihydro-3*H*-pyrrolo[2,3-*d*]pyrimidin-3-yl)-*N*,*N*-dimethylpropan-1-amine (5x).—Formimidate **3a** (40.0 mg, 0.099 mmol) and N^1,N^1-dimethylpropane-1,3-diamine (20.2 mg, 0.198 mmol, 2.0 equiv) were reacted according to General Procedure D and purified by MDF purification to afford **5x** as a tan solid (30.8 mg, 0.067 mmol, 67% yield). ^{1}H NMR (400 MHz, CDCl$_3$) δ 2.11 (p, J = 6.9 Hz, 2H), 2.34 (s, 6H), 2.52 (t, J = 6.8 Hz, 2H), 4.39 (t, J = 7.0 Hz, 2H), 5.34 (s, 2H), 6.88–6.94 (m, 2H), 7.02–7.07 (m, 2H), 7.18–7.33 (m, 11H), 8.10 (s, 1H), 8.60 (s, 1H); ^{13}C NMR (101 MHz, CDCl$_3$, APT pulse sequence) δ d (CH, CH$_3$) 40.9, 44.5, 127.0, 127.6, 127.8, 128.4, 128.6, 128.9, 130.4, 131.0, 145.6, 168.8; u (C, CH$_2$) 25.3, 46.5, 47.1, 54.9, 101.6, 117.5, 129.5, 132.4, 135.8, 136.9, 144.7, 153.2; HRMS calcd for C$_{30}$H$_{32}$N5 [M + H]$^+$ 462.2652, found 462.2665; HPLC purity = 98.0%.

7-benzyl-3-(1-benzylpiperidin-4-yl)-5,6-diphenyl-3,7-dihydro-4*H*-pyrrolo[2,3-*d*]pyrimidin-4-imine (5y).—Formimidate **3a** (40.0 mg, 0.099 mmol) and 1-benzylpiperidin-4-amine (37.7 mg, 0.198 mmol, 2.0 equiv) were reacted according to General Procedure D and purified by MDF purification to afford **5y** as a tan solid (15.8 mg, 0.029 mmol, 29% yield). ^{1}H NMR (400 MHz, CDCl$_3$) δ 1.91 (qd, J = 3.8, 12.1 Hz, 2H), 1.98–2.08 (m, 2H), 2.23 (td, J = 2.4, 11.8 Hz, 2H), 3.01–3.11 (m, 2H), 3.55 (s, 2H), 5.08 (tt, J = 3.9, 12.1 Hz, 1H), 5.27 (s, 2H), 6.93–6.97 (m, 2H), 7.01–7.06 (m, 2H), 7.14–7.29 (m, 12H), 7.29–7.36 (m, 4H), 7.84 (s, 1H); ^{13}C NMR (101 MHz, CDCl$_3$) δ 31.9, 45.9, 50.9, 53.1, 62.8, 103.1, 118.2, 126.7, 127.0, 127.2, 127.9, 128.1, 128.2, 128.2, 128.4, 129.1, 130.5, 130.6, 131.0, 132.6, 133.9, 137.9, 138.1, 142.3, 142.7, 155.4; IR (neat) 1626, 1603, 1559 cm^{-1}; HRMS calcd for C$_{37}$H$_{36}$N$_5$ [M + H]$^+$ 550.2965, found 550.2999; HPLC purity = 99.5%.

7-Benzyl-5,6-diphenyl-3-(3-(4-phenylpiperazm-1-yl)propyl)-3,7-dihydro-4*H*-pyrrolo[2,3-*d*]pyrimidin-4-imine (5z).—Formimidate **3a** (40.0 mg, 0.099 mmol) and 3-(4-phenylpiperazin-1-yl)propan-1-amine (43.4 mg, 0.198 mmol, 2.0 equiv) were reacted according to General Procedure D and purified by MDF purification to afford **5z** as a tan solid (31.6 mg, 0.055 mmol, 55% yield). ^{1}H NMR (400 MHz, CDCl$_3$) δ 2.08 (t, J = 6.5 Hz, 2H), 2.46 (t, J = 6.6 Hz, 2H), 2.55–2.62 (m, 4H), 3.11–3.19 (m, 4H), 4.23 (t, J = 6.5 Hz, 2H), 5.28 (d, J = 3.6 Hz, 2H), 6.85 (tt, J = 1.0, 7.3 Hz, 1H), 6.89–6.95 (m, 4H), 7.00–7.05 (m, 2H), 7.14–7.33 (m, 13H), 7.86 (s, 1H), 8.71

(br s, 1H); ^{13}C NMR (101 MHz, CDCl$_3$, APT pulse sequence) δ d (CH, CH$_3$) 116.0, 119.7, 126.8, 127.2, 127.4, 128.3, 128.5, 128.5, 129.1, 130.5, 131.1, 146.2, 168.8; u (C, CH$_2$) 24.7, 46.2, 46.4, 49.2, 53.0, 54.5, 102.9, 117.9, 130.3, 133.4, 133.8, 137.6, 143.6, 151.3, 154.7; HRMS calcd for C$_{38}$H$_{39}$N$_6$ [M + H]$^+$ 579.3231, found 579.3257; HPLC purity > 99.5%.

7-Benzyl-3-(3,4-dimethoxyphenethyl)-5,6-diphenyl-3,7-dihydro-4*H*-pyrrolo[2,3-*d*]pyrimidin-4-imine (5aa).—Formimidate **3a** (40.0 mg, 0.099 mmol) and 2-(3,4-dimethoxyphenyl)ethan-1-amine (35.9 mg, 0.198 mmol, 2.0 equiv) were reacted according to General Procedure D and purified by flash chromatography to afford **5aa** as an off-white solid (43.1 mg, 0.080 mmol, 81% yield), ^{1}H NMR (400 MHz, CDCl$_3$) δ 3.09 (t, *J* = 6.8 Hz, 2H), 3.77 (s, 3H), 3.85 (s, 3H), 4.32 (t, *J* = 6.8 Hz, 2H), 5.26 (s, 2H), 6.70 (s, 1H), 6.72 (d, *J* = 2.0 Hz, 1H), 6.78 (d, *J* = 8.0 Hz, 1H), 6.87–6.92 (m, 2H), 7.02–7.07 (m, 2H), 7.15–7.31 (m, 11H), 7.33 (s, 1H); ^{13}C NMR (101 MHz, CDCl$_3$, APT pulse sequence) δ d (CH, CH$_3$) 55.8, 55.9, 111.4, 112.2, 121.0, 126.8, 127.2, 127.4, 128.2, 128.3, 128.5 (× 2C), 130.5, 131.1, 145.6; u (C, CH$_2$) 34.0, 46.2, 50.2, 118.0, 130.3, 130.6, 133.5, 137.7, 140.1, 143.5, 147.9, 148.0, 149.1, 154.6; HRMS calcd for C$_{35}$H$_{33}$N$_4$O$_2$ [M + H]$^+$ 541.2598, found 541.2628; HPLC purity = 99.2%.

2-(4-lmino-7-phenethyl-5,6-diphenyl-4,7-dihydro-3H-pyrrolo[2,3-*d*]pyrimidin-3-yl)ethan-1-ol (5bb).—Formimidate **3b** (124.0 mg, 0.296 mmol) and 2-aminoethanol (72.2 mg, 1.18 mmol, 4.0 equiv) were reacted according to General Procedure D and purified by flash chromatography to afford **5bb** as an off-white solid (61.0 mg, 0.140 mmol, 48% yield). ^{1}H NMR (400 MHz, CDCl$_3$) δ 2.82–3.00 (m, 2H), 3.88–4.03 (m, 2H), 4.16–4.25 (m, 2H), 4.25–4.40 (m, 2H), 6.85–6.93 (m, 2H), 6.99–7.05 (m, 2H), 7.12–7.35 (m, 11H), 7.67 (s, 1H); ^{13}C NMR (101 MHz, CDCl$_3$, APT pulse sequence) δ d (CH, CH$_3$) 126.6, 127.0, 128.2, 128.3, 128.4, 128.5, 128.8, 130.5, 130.9, 145.3; u (C, CH$_2$) 36.7, 44.5, 53.2, 63.6, 103.0, 117.6, 133.5, 133.6, 138.0 (× 2C), 143.1, 157.4; HRMS calcd for C$_{28}$H$_{27}$N$_4$O [M + H]$^+$ 435.2179, found 435.2190; HPLC purity = 97.9%.

2-(4-lmino-7-phenethyl-5,6-diphenyl-4,7-dihydro-3*H*-pyrrolo[2,3-*d*]pyrimidin-3-yl)butan-1-ol (5cc).—Formimidate **3b** (30.0 mg, 0.072 mmol) and 2-aminobutanol (19.3 mg, 0.216 mmol, 3.0 equiv) were reacted according to General Procedure D and purified by flash chromatography to afford **5cc** as an off-white solid (25.5 mg, 0.055 mmol, 77% yield). ^{1}H NMR (400 MHz, CDCl$_3$) δ 1.62 (p, *J* = 5.9 Hz, 2H), 1.95 (p, *J* = 7.1 Hz, 2H), 2.82–2.97 (m, 2H), 3.74 (t, *J* = 5.7 Hz, 2H), 3.99–4.12 (m, 2H), 4.17–4.40 (m, 2H), 6.81–6.96 (m, 2H), 7.04 (dd, *J* = 7.6, 1.8 Hz, 2H), 7.10–7.39 (complex, 11H), 7.70 (s, 1H); ^{13}C NMR (101 MHz, CDCl$_3$) δ 25.8, 27.9, 36.7, 44.3, 46.7, 61.5, 103.3, 117.6, 126.5, 126.8, 128.0, 128.2, 128.3, 128.4, 128.7, 130.4, 130.6, 130.8, 132.9, 133.7, 138.0, 142.8, 145.0, 155.3; IR (neat) 1621, 1561, 1486, 1442 cm^{-1}; HRMS calcd for C$_{30}$H$_{31}$N$_4$O [M + H]$^+$ 463.2492, found 463.2525; HPLC purity > 99.5%.

(*trans*)-4-(4-lmino-7-phenethyl-5,6-diphenyl-4,7-dihydro-3*H*-pyrrolo[2,3-*d*]pyrimidin-3-yl)cyclohexan-1-ol (5dd).—Formimidate **3b** (48.0 mg, 0.114 mmol), (*tans*)-4-amino-cyclohexanol hydrochloride (52.0 mg, 0.343 mmol, 3.0 equiv) and sodium methoxide (18.5 mg, 0.342 mmol, 3.0 equiv) were

reacted according to General Procedure E and purified by flash chromatography to afford **5dd** as an off-white solid (33.5 mg, 0.069 mmol, 60% yield). ^{1}H NMR (400 MHz, CDCl$_3$) δ 1.54–1.77 (m, 4H), 2.12 (dt, *J* = 5.3, 10.5 Hz, 4H), 2.84–2.98 (m, 2H), 3.64–3.81 (m, 1H), 4.20–4.37 (m, 2H), 5.02–5.21 (m, 1H), 6.87–6.97 (m, 2H), 7.03–7.09 (m, 2H), 7.15–7.31 (complex, 11H), 7.78 (s, 1H); ^{13}C NMR (101 MHz, CDCl$_3$, APT pulse sequence) δ d (CH, CH$_3$) 41.0, 51.9, 126.6, 127.0, 128.1, 128.3, 128.3, 128.4, 128.8, 130.5, 130.9, 142.0; u (C, CH$_2$) 30.6, 34.7, 36.8, 44.4, 103.0, 117.9, 130.6, 133.0, 133.7, 138.1, 142.3, 155.2; HRMS calcd for C$_{32}$H$_{33}$N$_4$O [M + H]$^+$ 489.2649, found 489.2650; HPLC purity = 98.8%.

(*trans*)-2-((4-lmino-7-phenethyl-5,6-diphenyl-4,7-dihydro-3*H*-pyrrolo[2,3-*d*]pyrimidin-3-yl)methyl)cyclohexan-1-ol (5ee).—Formimidate **3b** (33.0 mg, 0.079 mmol) and (*tans*)-2-(aminomethyl)cyclohexan-1-ol (20.3 mg, 0.157 mmol, 2.0 equiv) were reacted according to General Procedure D and purified by MDF purification to afford **5ee** as an off-white solid (20.3 mg, 0.068 mmol, 86% yield). ^{1}H NMR (500 MHz, CDCl$_3$) δ 1.13–1.29 (m, 3H), 1.30–1.42 (m, 1H), 1.66–1.80 (m, 3H), 1.90 (dtt, *J* = 3.2, 6.8, 10.0 Hz, 1H), 1.99–2.08 (m, 1H), 2.89 (t, *J* = 7.6 Hz, 2H), 3.25 (td, *J* = 4.2, 10.5 Hz, 1H), 4.25–4.41 (m, 3H), 4.46 (dd, *J* = 6.2, 14.8 Hz, 1H), 6.85–6.95 (m, 2H), 7.04–7.12 (m, 2H), 7.15–7.22 (complex, 5H), 7.25–7.41 (complex, 6H), 7.83 (s, 1H), 8.59 (br s, 1H); ^{13}C NMR (126 MHz, CDCl$_3$, APT pulse sequence) δ d (CH, CH$_3$) 41.0, 45.3, 126.8, 127.8, 128.5, 128.6, 128.7, 128.9, 130.4, 130.7, 145.2, 168.3; u (C, CH$_2$) 24.9, 25.5, 29.3, 34.9, 36.5, 44.7, 51.9, 101.5, 117.3, 129.6, 132.4, 135.7, 137.5, 144.4, 154.0; HRMS calcd for C$_{33}$H$_{35}$N$_4$O [M + H]$^+$ 503.2805, found 503.2803; HPLC purity = 98.6%.

7-Phenethyl-5,6-diphenyl-3-(tetrahydro-2*H*-pyran-4-yl)-3,7-dihydro-4*H*-pyrrolo[2,3-*d*]pyrimidin-4-imine (5ff).—Formimidate **3b** (92.0 mg, 0.219 mmol) and 4-aminotetraydropyran (44.4 mg, 0.439 mmol, equiv) were reacted according to General Procedure D and purified by MDF purification to afford **5ff** as an off-white solid (24.7 mg, 0.052 mmol, 24% yield). ^{1}H NMR (400 MHz, CDCl$_3$) δ 1.86–2.08 (m, 4H), 2.83–2.98 (m, 2H), 3.62 (td, *J* = 2.3, 11.6 Hz, 2H), 4.09–4.17 (m, 2H), 4.23–4.32 (m, 2H), 5.37 (tt, *J* = 4.3, 11.9 Hz, 1H), 6.88–6.94 (m, 2H), 7.03–7.09 (m, 2H), 7.15–7.33 (complex, 11H), 7.81 (s, 1H); ^{13}C NMR (101 MHz, CDCl$_3$, APT pulse sequence) δ d (CH, CH$_3$) 49.7, 126.6, 126.9, 128.0, 128.30, 128.31, 128.5, 128.8, 130.5, 130.9, 142.1; u (C, CH$_2$) 32.9, 36.9, 44.4, 67.7, 103.1, 118.0, 130.7, 132.8, 133.8, 138.1, 155.3; HRMS calcd for C$_{31}$H$_{31}$N$_4$O [M + H]$^+$ 475.2492, found 475.2496; HPLC purity = 98.3%.

7-Phenethyl-5,6-diphenyl-3-((tetrahydro-2*H*-pyran-4-yl)methyl)-3,7-dihydro-4*H*-pyrrolo[2,3-*d*]pyrimidin-4-imine (5gg).—Formimidate **3b** (45.0 mg, 0.107 mmol) and 4-(aminomethyl)tetraydropyran (18.5 mg, 0.161 mmol, 1.5 equiv) were reacted according to General Procedure D and purified by MDF purification to afford **5gg** as an off-white solid (30.6 mg, 0.0063 mmol, 58% yield). ^{1}H NMR (500 MHz, CDCl$_3$) δ 1.38 (qd, *J* = 4.5, 12.2 Hz, 2H), 1.62–1.73 (m, 2H), 2.35 (dqd, *J* = 3.5, 7.3, 11.2 Hz, 1H), 2.82–2.95 (m, 2H), 3.38 (td, *J* = 2.0, 11.8 Hz, 2H), 3.92–4.06 (m, 4H), 4.23–4.37 (m, 2H), 6.82–6.95 (m, 2H), 7.11 (m, 2H), 7.12–7.36 (complex, 11H), 7.66 (s, 1H), 8.66 (br s, 1H);; ^{13}C NMR (126 MHz, CDCl$_3$, APT pulse sequence) δ d (CH, CH$_3$) 37.4, 126.7, 127.7, 128.5, 128.5, 128.7, 128.7, 128.8, 130.4, 130.7, 144.6; u (C, CH$_2$) 29.5, 36.5, 44.7, 51.9, 67.5,

70.3, 101.8, 117.4, 129.7, 132.5, 135.4, 137.6, 144.0, 153.5; HRMS calcd for $C_{32}H_{33}N_4O$ $[M + H]^+$ 489.2649, found 489.2654; HPLC purity = 99.7%.

7-Phenethyl-5,6-diphenyl-3-((tetrahydrofuran-3-yl)methyl)-3,7-dihydro-4*H*-pyrrolo[2,3-*d*]pyrimidin-4-imine (5hh).

—Formimidate **3b** (43.0 mg, 0.102 mmol) and 3-(aminomethyl)tetrahydrofuran (10.4 mg, 0.102 mmol, 1.0 equiv) were reacted according to General Procedure D and purified by MDF purification to afford **5hh** as an off-white solid (36.4 mg, 0.077 mmol, 75% yield). ^{1}H NMR (400 MHz, CDCl$_3$) δ 1.69–1.80 (m, 1H), 2.13 (dtd, *J* = 5.4, 8.0, 13.2 Hz, 1H), 2.84–2.94 (m, 2H), 3.02–3.12 (m, 1H), 3.64 (dd, *J* = 4.5, 9.2 Hz, 1H), 3.77 (ddt, *J* = 4.0, 6.8, 8.1 Hz, 2H), 3.98 (td, *J* = 5.4, 8.3 Hz, 1H), 4.21 (dd, *J* = 8.3, 14.0 Hz, 1H), 4.32–4.46 (m, 3H), 6.82–6.95 (m, 2H), 7.07 (dd, *J* = 1.5, 8.1 Hz, 2H), 7.15–7.23 (complex, 5H), 7.25–7.42 (complex, 6H), 7.80 (s, 1H), 8.62 (br s, 1H); ^{13}C NMR (101 MHz, CDCl$_3$, APT pulse sequence) δ d (CH, CH$_3$) 33.0, 126.6, 127.2, 128.3, 128.4, 128.5, 128.5, 128.8, 130.5, 130.8, 145.4; u (C, CH$_2$) 30.4, 36.7, 44.5, 54.3, 67.5, 102.8, 117.7, 130.3, 133.3, 137.9, 143.2, 154.6, 168.6; HRMS calcd for $C_{31}H_{31}N_4O$ $[M + H]^+$ 475.2492, found 475.2488; HPLC purity = 99.8%.

7-Phenethyl-5,6-diphenyl-3-((tetrahydrofuran-2-yl)methyl)-3,7-dihydro-4*H*-pyrrolo[2,3-*d*]pyrimidin-4-imine (5ii).

—Formimidate **3b** (30.0 mg, 0.072 mmol) and 2-(aminomethyl)tetrahydrofuran (14.6 mg, 0.144 mmol, 2.0 equiv) were reacted according to General Procedure D and purified by MDF purification to afford **5ii** as tan solid (31.5 mg, 0.0664 mmol, 92% yield). ^{1}H NMR (400 MHz, CDCl$_3$) δ 1.58–1.72 (m, 1H), 1.87–1.98 (m, 2H), 2.11–2.26 (m, 1H), 2.81–3.06 (m, 2H), 3.73–3.97 (m, 3H), 4.33 (dddd, *J* = 1.7, 6.9, 8.3, 13.3 Hz, 3H), 4.81 (dd, *J* = 2.3, 14.2 Hz, 1H), 6.89 (dd, *J* = 2.0, 7.4 Hz, 2H), 7.04 (dd, *J* = 1.7, 7.8 Hz, 2H), 7.15–7.21 (complex, 5H), 7.21–7.35 (complex, 6H), 7.90 (s, 1H), 8.68 (br s, 1H); ^{13}C NMR (101 MHz, CDCl$_3$, APT pulse sequence) δ d (CH, CH$_3$) 76.1, 126.6, 127.3, 128.4, 128.4, 128.5, 128.6, 128.8, 130.5, 130.9, 146.0; u (C, CH$_2$) 25.9, 28.8, 36.6, 44.6, 51.9, 68.1, 102.2, 117.5, 130.2, 133.2, 134.3, 137.9, 143.7, 154.4; HRMS calcd for $C_{31}H_{31}N_4O$ $[M + H]^+$ 475.2492, found 475.2522; HPLC purity > 99.5%.

3-(4-Imino-7-phenethyl-5,6-diphenyl-4,7-dihydro-3*H*-pyrrolo[2,3-*d*]pyrimidin-3-yl)-*N,N*-dimethylpropan-1-amine (5jj).

—Formimidate **3b** (30.0 mg, 0.072 mmol) and 3-(dimethylamino)-1-propylamine (14.7 mg, 0.144 mmol, 2.0 equiv) were reacted according to General Procedure D and purified by MDF purification to afford **5jj** as an off-white solid (31.7 mg, 0.0666 mmol, 93% yield). ^{1}H NMR (400 MHz, CDCl$_3$) δ 2.10 (t, *J* = 6.7 Hz, 2H), 2.31 (s, 6H), 2.43 (t, *J* = 6.6 Hz, 2H), 2.86–2.93 (m, 2H), 4.34–4.39 (m, 2H), 4.43 (t, *J* = 6.7 Hz, 2H), 6.85–6.91 (m, 2H), 7.02–7.09 (m, 2H), 7.15–7.22 (complex, 5H), 7.25–7.37 (complex, 6H), 8.03 (s, 1H), 8.66 (br s, 1H); ^{13}C NMR (101 MHz, CDCl$_3$, APT pulse sequence) δ d (CH, CH$_3$) 44.7, 126.7, 127.8, 128.5 (× 2 C), 128.7, 128.7, 128.9, 130.4, 130.7, 145.3; u (C, CH$_2$) 25.3, 36.4, 47.0, 54.8, 101.5, 117.2, 129.7, 132.5, 135.6, 137.6, 144.4, 153.2; HRMS calcd for $C_{31}H_{34}N_5$ $[M + H]^+$ 476.2809, found 476.2832; HPLC purity = 96.7%.

3-(4-Imino-7-(4-methoxybenzyl)-5,6-diphenyl-4,7-dihydro-3*H*-pyrrolo[2,3-*d*]pyrimidin-3-yl)propan-1-ol (5kk).

—Formimidate **3c** (63.6 mg, 0.146

mmol) and 3-aminopropanol (21.9 mg, 0.292 mmol, 2.0 equiv)

were reacted according to General Procedure D and purified by MDF purification

to afford **5kk** as an off-white solid (61.0 mg, 0.131 mmol, 90% yield). ^{1}H NMR (500 MHz, CDCl$_3$) δ 2.02–2.07 (m, 2H), 3.63 (t, J = 5.3 Hz, 2H), 4.46 (t, J = 6.7 Hz, 2H), 5.27 (s, 2H), 6.69–6.74 (m, 2H), 6.83 (d, J = 8.7 Hz, 2H), 7.03–7.08 (m, 2H), 7.16–7.21 (m, 2H), 7.22–7.34 (m, 6H), 8.04 (s, 1H), 8.56 (s, 1H); ^{13}C NMR (126 MHz, CDCl$_3$, APT pulse sequence) δ d (CH, CH$_3$) 55.2, 113.9, 127.9, 128.4, 128.6, 128.8, 128.9, 130.4, 131.0, 144.9; u (C, CH$_2$) 32.3, 41.0, 46.0, 57.4, 101.4, 117.3, 128.9, 129.5, 132.3, 136.1, 144.7, 153.9, 159.0; HRMS calcd for C$_{29}$H$_{29}$N$_4$O$_2$ [M + H]$^+$ 465.2285, found 465.2277; HPLC purity = 99.1%.

3-(4-Imino-7-(4-methoxybenzyl)-5,6-diphenyl-4,7-dihydro-3*H*-pyrrolo[2,3-*d*]pyrimidin-3-yl)propan-1-ol (5ll).—212-37C2 Formimidate *3c* (50.0

mg, 0.115 mmol) and 2-aminoethanol (14.0 mg, 0.230 mmol,

2.0 equiv) were reacted according to General Procedure D

and purified by flash chromatography to afford **5ll** as a beige solid (22.3 mg, 0.0495 mmol, 43% yield). ^{1}H NMR (400 MHz, CDCl$_3$) δ 3.75 (s, 3H), 3.93–4.04 (m, 2H), 4.38 (t, J = 4.5 Hz, 2H), 5.25 (s, 2H), 6.74 (d, J = 8.7 Hz, 2H), 6.85 (d, J = 8.7 Hz, 2H), 7.06 (dt, J = 1.5, 6.8 Hz, 2H), 7.17–7.35 (complex, 8H), 7.88 (s, 1H); ^{13}C NMR (101 MHz, CDCl$_3$, APT pulse sequence) δ d (CH, CH$_3$) 55.2, 113.9, 127.4, 128.3, 128.4, 128.5, 128.6, 130.4, 131.1, 145.5; u (C, CH$_2$) 46.2, 53.1, 62.8, 102.4, 117.6, 129.4, 130.0, 133.1, 134.7, 144.0, 156.0, 158.9; HRMS calcd for C$_{28}$H$_{27}$N$_4$O$_2$ [M + H]$^+$ 451.2129, found 451.2118; HPLC purity > 99.5%.

(*trans*)-4-(4-Imino-7-(4-methoxybenzyl)-5,6-diphenyl-4,7-dihydro-3*H*-pyrrolo[2,3-*d*]pyrimidin-3-yl)cyclohexan-1-ol (5mm).—Formimidate **3c**

(69.0 mg, 0.158 mmol), *trans*-4-aminocyclohexanol hyrochloride

(72.1 mg, 0.475 mmol, 3.0 equiv) and triethylamine (32.1 mg, 0.317 mmol, 2.0 equiv)

were reacted according to General Procedure E and purified by MDF purification to afford **5mm** as an off-white solid (73.1 mg, 0.145 mmol, 92% yield). ^{1}H NMR (500 MHz, CDCl$_3$) δ 1.73–1.75 (m, 4H), 2.14 (d, J = 8.5 Hz, 4H), 3.67–3.72 (m, 1H), 3.76 (s, 3H), 5.12–5.22 (m, 1H), 5.24 (s, 2H), 6.74–6.80 (m, 2H), 6.89 (d, J = 8.7 Hz, 2H), 7.05–7.10 (m, 2H), 7.20–7.33 (complex, 8H), 7.85 (s, 1H); ^{13}C NMR (126 MHz, CDCl$_3$, APT pulse sequence) δ d (CH, CH$_3$) 41.0, 55.2, 69.7, 113.9, 127.2, 128.2, 128.3, 128.4, 128.5, 130.5, 131.1, 142.1; u (C, CH$_2$) 30.7, 34.6, 45.6, 102.7, 118.0, 129.7, 130.4, 133.4, 142.8, 154.8, 158.8; HRMS calcd for C$_{32}$H$_{33}$N$_4$O$_2$ [M + H]$^+$ 505.2598, found 505.2591; HPLC purity > 99.5%.

7-(4-Methoxybenzyl)-5,6-diphenyl-3-(tetrahydro-2*H*-pyran-4-yl)-3,7-dihydro-4*H*-pyrrolo[2,3-*d*]pyrimidin-4-imine (5nn).—Formimidate **3c** (60.0 mg, 0.138 mmol) and

4-aminotetrahydropyran (27.9 mg, 0.276 mmol, 2.0 equiv were reacted according to General

Procedure D and purified by flash chromatography to afford **5nn** as an off-white solid (18.5 mg, 0.0377 mmol, 27% yield). ^{1}H NMR (400 MHz, CDCl$_3$) δ 1.86–2.08 (m, 4H), 3.61 (td, J = 2.3, 11.7 Hz, 2H), 3.75 (s, 3H), 4.12 (dd, J = 4.2, 11.6 Hz, 2H), 5.22 (s, 2H), 5.30–5.43 (m, 1H), 6.72–6.80 (m, 2H), 6.86–6.91 (m, 2H), 7.06 (dd, J = 1.6, 8.0 Hz, 2H), 7.18–7.29 (complex, 8H), 7.81 (s, 1H); ^{13}C NMR (101 MHz, CDCl$_3$, APT pulse sequence) δ d (CH, CH$_3$) 55.2, 113.9, 126.9, 128.0, 128.2, 128.3, 128.3, 130.6, 131.2, 142.5; u (C,

CH$_2$) 32.9, 45.5, 67.7, 103.1, 118.2, 130.0, 130.7, 133.8, 142.2, 155.3, 158.8; HRMS calcd for C$_{31}$H$_{31}$N$_4$O$_2$ [M + H]$^+$ 491.2442, found 491.2446; HPLC purity > 99.5%.

7-(4-Methoxybenzyl)-5,6-diphenyl-3-((tetrahydro-2*H*-pyran-4-yl)methyl)-3,7-dihydro-4*H*-pyrrolo[2,3-*d*]pyrimidin-4-imine (5oo).—

Formimidate **3c** (46.0 mg, 0.106 mmol) and 4-(aminomethyl)tetrahydropyran (18.3 mg, 0.158 mmol, 1.5 equiv) were reacted according to General Procedure D and purified by flash chromatography to afford **5oo** as a tan solid (41.8 mg, 0.083 mmol, 78% yield). ^{1}H NMR (400 MHz, CDCl$_3$) δ 1.39 (qd, *J* = 4.5, 12.2 Hz, 2H), 1.64–1.75 (m, 2H), 2.34 (ddp, *J* = 3.7, 7.3, 11.3 Hz, 1H), 3.37 (td, *J* = 2.0, 11.8 Hz, 2H), 3.75 (s, 3H), 3.91–4.12 (m, 4H), 5.23 (s, 2H), 6.71–6.77 (m, 2H), 6.83–6.90 (m, 2H), 7.04–7.09 (m, 2H), 7.18–7.28 (complex, 8H), 7.68 (s, 1H); ^{13}C NMR (101 MHz, CDCl$_3$, APT pulse sequence) δ d (CH, CH$_3$) 33.0, 55.2, 113.9 (× 2C), 127.1, 128.3, 128.4, 128.5, 130.5, 131.1, 145.7; u (C, CH$_2$) 30.5, 45.7, 54.2, 67.5, 103.3, 118.0, 129.9, 130.6, 133.1, 133.7, 142.9, 155.3, 158.8, 158.9; HRMS calcd for C$_{32}$H$_{33}$N$_4$O$_2$ [M + H]$^+$ 505.2598, found 505.2603; HPLC purity > 99.5%.

7-(4-Methoxybenzyl)-5,6-diphenyl-3-((tetrahydrofuran-2-yl)methyl)-3,7-dihydro-4*H*-pyrrolo[2,3-*d*]pyrimidin-4-imine (5pp).—

Formimidate **3c** (30.0 mg, 0.0689 mmol) and 2-(aminomethyl)tetrahydrofuran (13.9 mg, 0.138 mmol, 2.0 equiv) were reacted according to General Procedure D and purified by MDF purification to afford **5pp** as an off-white solid (29.8 mg, 0.0607 mmol, 88% yield). ^{1}H NMR (400 MHz, CDCl$_3$) δ 1.62 (ddt, *J* = 7.5, 8.6, 12.4 Hz, 1H), 1.86–1.96 (m, 2H), 2.05–2.17 (m, 1H), 3.67–3.82 (m, 2H), 3.73 (s, 3H), 3.88 (dt, *J* = 6.8, 8.3 Hz, 1H), 4.32 (qd, *J* = 2.6, 7.6 Hz, 1H), 4.52 (dd, *J* = 2.6, 13.9 Hz, 1H), 5.21 (s, 2H), 6.71–6.76 (m, 2H), 6.85–6.90 (m, 2H), 7.02–7.07 (m, 2H), 7.15–7.26 (complex, 8H), 7.81 (s, 1H); ^{13}C NMR (101 MHz, CDCl$_3$, APT pulse sequence) δ d (CH, CH$_3$) 55.2, 76.3, 113.8, 126.8, 128.0, 128.2, 128.3, 128.4, 130.5, 131.2, 146.7; u (C, CH$_2$) 25.8, 28.9, 45.5, 50.6, 68.0, 103.1, 118.0, 130.1, 130.8, 132.7, 134.0, 143.0, 155.6, 158.8; HRMS calcd for C$_{31}$H$_{31}$N$_4$O$_2$ [M + H]$^+$ 491.2442, found 491.2462; HPLC purity > 99.5%.

3-(4-Imino-5,6-diphenyl-7-(4-(trifluoromethoxy)benzyl)-4,7-dihydro-3*H*-pyrrolo[2,3-*d*]pyrimidin-3-yl)propan-1-ol (5qq).—

Formimidate **3d** (60.4 mg, 0.123 mmol) and 3-aminopropanol (18.5 mg, 0.247 mmol, 2.0 equiv) were reacted according to General Procedure D and purified by MDF purification to afford **5qq** as a tan solid (41.1 mg, 0.0793 mmol, 64% yield). ^{1}H NMR (500 MHz, CDCl$_3$) δ 1.98–2.06 (m, 2H), 3.61 (t, *J* = 5.6 Hz, 2H), 4.39 (t, *J* = 6.4 Hz, 2H), 5.32 (s, 2H), 6.94 (d, *J* = 8.7 Hz, 2H), 7.02–7.09 (m, 4H), 7.18–7.22 (m, 2H), 7.23–7.34 (complex, 6H), 7.92 (s, 1H), 8.56 (br s, 1H); ^{13}C NMR (126 MHz, CDCl$_3$, APT pulse sequence) δ d (CH, CH$_3$) 41.0, 121.0, 127.7, 128.5, 128.6, 128.7, 128.8, 130.4, 130.9, 145.3; u (C, CH$_2$) 32.8, 45.1, 45.6, 57.2, 102.0, 117.9, 120.4 (q, *J* = 257.7 Hz), 129.6, 132.5, 134.9, 135.7, 144.1, 148.5, 155.0; ^{19}F NMR (376 MHz, CDCl$_3$) δ −57.9; IR (neat) 1625, 1563, 1507 cm^{-1}; HRMS calcd for C$_{29}$H$_{26}$F$_3$N$_4$O$_2$ [M + H]$^+$ 519.2002, found 519.2007; HPLC purity = 98.7%.

(*trans*)-4-(4-Imino-5,6-diphenyl-7-(4-(trifluoromethoxy)benzyl)-4,7-dihydro-3*H*-pyrrolo[2,3-*d*]pyrimidin-3-yl)cyclohexan-1-ol (5rr).—

Formimidate **3d** (41.6 mg,

0.085 mmol), *trans*-4-aminocyclohexanol hydrochloride (38.7 mg, 0.255 mmol, 3.0 equiv) and triethylamine (17.2 mg, 0.170 mmol, 2.0 equiv) were reacted according to General Procedure E and purified by MDF purification to afford **5rr** as an off-white solid (38.8 mg, 0.0695 mmol, 82% yield). ^{1}H NMR (500 MHz, CDCl$_3$) δ 1.67–1.88 (m, 4H), 2.13–2.21 (m, 4H), 3.66–3.74 (m, 1H), 5.22–5.32 (m, 1H), 5.31 (s, 2H), 6.97 (d, *J* = 8.6 Hz, 2H), 7.03–7.06 (m, 2H), 7.07–7.11 (m, 2H), 7.21–7.33 (complex, 8H), 7.91 (s, 1H); ^{13}C NMR (101 MHz, CDCl$_3$) δ 30.5, 34.8, 45.3, 51.7, 69.9, 103.2, 118.4, 120.4 (q, *J* = 258.8 Hz), 120.9, 127.0, 128.1, 128.3, 128.3, 128.4, 130.4, 130.5, 131.0, 132.6, 133.6, 136.5, 142.2, 142.6, 148.3, 155.3; ^{19}F NMR (376 MHz, CDCl$_3$) δ −57.9; IR 1625, 1563, 1507 cm^{-1}; HRMS calcd for C$_{32}$H$_{30}$F$_3$N$_4$O$_2$ [M + H]$^+$ 559.2315, found 559.2299; HPLC purity = 98.5%.

(*cis*)-4-(4-lmino-5,6-diphenyl-7-(4-(trifluoromethoxy)benzyl)-4,7-dihydro-3*H*-pyrrolo[2,3-*d*]pyrimidin-3-yl)cyclohexan-1-ol (5ss).

—Formimidate **3d** (78.9 mg, 0.161 mmol), *cis*-4-aminocyclohexanol hydrochloride (73.3 mg, 0.484 mmol, 3.0 equiv) and triethylamine (32.6 mg, 0.322 mmol, 2.0 equiv) were reacted according to General Procedure E and purified by MDF purification to afford **5ss** as an off-white solid (31.5 mg, 0.0564 mmol, 35% yield). ^{1}H NMR (400 MHz, DMSO-*d*$_6$) δ 1.32–1.77 (complex, 8H), 3.59–3.68 (m, 1H), 3.68–3.78 (m, 1H), 5.01 (s, 2H), 6.96 (d, *J* = 8.6 Hz, 2H), 7.02–7.36 (complex, 11H), 7.94 (s, 1H), 8.17 (d, *J* = 4.0 Hz, 1H); ^{13}C NMR (101 MHz, DMSO-*d*$_6$) δ 26.3, 30.8, 45.3, 47.5, 64.8, 118.9, 120.0 (q, 257.4 Hz), 120.9, 121.2, 126.1, 126.3, 128.2, 128.2, 128.5, 128.7, 130.8, 130.9, 133.3, 137.6, 147.1, 151.5; ^{19}F NMR (376 MHz, DMSO-*d*$_6$) δ −56.9; HRMS calcd for C$_{32}$H$_{30}$F$_3$N$_4$O$_2$ [M + H]$^+$ 559.2315, found 559.2304; HPLC purity = 98.8%.

3-((*trans*)-4-Methoxycyclohexyl)-5,6-diphenyl-7-(4-(trifluoromethoxy)benzyl)-3,7-dihydro-4*H*-pyrrolo[2,3-*d*]pyrimidin-4-imine (5tt).

—Formimidate **3d** (49.0 mg, 0.100 mmol), *trans*-4-methoxycyclohexan-1-amine (25.9 mg, 0.200 mmol, 2.0 equiv) and potassium *tert*-butoxide (11.2 mg, 0.100 mmol, 1.0 equiv) were reacted according to General Procedure E and purified by flash chromatography to afford **5tt** as light yellow solid (38.9 mg, 0.0679 mmol, 68% yield). ^{1}H NMR (400 MHz, CDCl$_3$) δ 1.43–1.73 (m, 4H), 2.19 (dd, *J* = 31.6, 11.7 Hz, 4H), 3.23 (tt, *J* = 11.2, 4.2 Hz, 1H), 3.37 (s, 3H), 5.10 (t, *J* = 12.5 Hz, 1H), 5.26 (s, 2H), 6.48 (br s, 1H), 6.87–7.09 (m, 6H), 7.15–7.30 (m, 8H), 7.77 (s, 1H); ^{13}C NMR (101 MHz, CDCl$_3$) δ 30.5, 31.1, 45.3, 51.9, 56.0, 78.4, 103.2, 118.4, 120.7 (q, *J* = 258.6 Hz), 120.9, 121.7, 127.0, 128.1, 128.3, 128.3, 128.3, 130.4, 130.5, 131.0, 133.5, 136.5, 142.2, 142.6, 148.3, 155.2; ^{19}F NMR (376 MHz, CDCl$_3$) δ −57.9; IR (neat) 1628, 1559, 1507, 1259 cm^{-1}; HRMS calcd for C$_{33}$H$_{32}$F$_3$N$_4$O$_2$ [M + H]$^+$ 573.2472, found 573.2466; HPLC purity = 99.7%.

5,6-Diphenyl-3-(tetrahydro-2*H*-pyran-4-yl)-7-(4-(trifluoromethoxy)benzyl)-3,7-dihydro-4*H*-pyrrolo[2,3-*d*]pyrimidin-4-imine (5uu).

—Formimidate **3d** (61.0 mg, 0.125 mmol) and 4-amintetrahydropyran (25.2 mg, 0.249 mmol, 2.0 equiv) were reacted according to General Procedure D and purified by MDF purification to afford **5uu** as a tan solid (42.6 mg, 0.0782 mmol, 63% yield). ^{1}H NMR (500 MHz, CDCl$_3$) δ 1.98 (qd, *J* = 4.4, 12.0 Hz, 2H), 2.08 (d, *J* = 13.6 Hz, 2H), 3.65–3.83 (m, 2H), 4.10–4.17 (m, 2H), 5.31 (s, 2H), 5.45–5.59 (m, 1H), 6.97 (d, *J* = 8.6 Hz, 2H), 7.01–7.06 (m, 2H), 7.06–7.11

(m, 2H), 7.20–7.33 (complex, 8H), 7.93 (s, 1H); ^{13}C NMR (126 MHz, CDCl$_3$) δ 32.9, 34.6, 44.5, 45.5, 66.6, 67.3, 102.3, 118.1, 120.3 (q, J = 258.6 Hz), 121.0, 124.2, 127.5, 128.4, 128.5, 128.6, 128.7, 129.8, 130.4, 130.9, 132.7, 135.9, 142.1, 148.5, 154.1, 160.4; HRMS calcd for C$_{31}$H$_{28}$F$_3$N$_4$O$_2$ [M + H]$^+$ 545.2159, found 545.2151; HPLC purity > 99.5%.

4-((3-(3-Hydroxypropyl)-4-imino-5,6-diphenyl-3,4-dihydro-7H-pyrrolo[2,3-d]pyrimidin-7-yl)methyl)benzenesulfonamide (5vv).—Formimidate **3e** (34.1 mg, 0.07 mmol) and 2-aminobutanol (10.6 mg, 0.141 mmol, 2.0 equiv) were reacted according to General Procedure D and purified by MDF purification to afford **5vv** as a tan solid (19.4 mg, 0.0378 mmol, 54% yield). ^{1}H NMR (400 MHz, DMSO-d$_6$) δ 1.82 (p, J = 6.0 Hz, 2H), 3.35–3.40 (m, 2H), 4.03 (t, J = 6.5 Hz, 2H), 5.31 (s, 2H), 6.09 (br s, 1H), (d, J = 8.3 Hz, 2H), 7.14 (dd, J = 7.1, 2.4 Hz, 2H), 7.23–7.33 (complex, 8H), 7.68 (d, J = 8.3 Hz, 2H), 7.98 (s, 1H); ^{13}C NMR (101 MHz, DMF-d$_7$, APT pulse sequence) δ d (CH, CH$_3$) 32.4, 44.2, 45.6, 57.7, 102.9, 118.0, 126.4, 127.2, 127.5, 128.6, 128.7, 128.7, 130.6, 130.9, 131.4, 133.5, 134.2, 142.3, 143.8, 147.4, 155.5; u (C, CH$_2$) 32.4, 44.2, 45.6, 57.7, 102.9, 118.0, 130.6, 133.5, 134.2, 142.3, 143.8, 155.5; IR 1624, 1486, 1444, 1331 cm^{-1}; HRMS calcd for C$_{28}$H$_{28}$N$_5$O$_3$S[M + H]$^+$ 514.1907, found 514.1899; HPLC purity = 98.2%.

4-((4-Imino-5,6-diphenyl-3-(tetrahydro-2H-pyran-4-yl)-3,4-dihydro-7H-pyrrolo[2,3-d]pyrimidin-7-yl)methyl)benzenesulfonamide (5ww).—Formimidate **3e** (47.0 mg, 0.097 mmol) and 4-aminotetrahydropyran (19.6 mg, 0.194 mmol, 2.0 equiv) were reacted according to General Procedure D and purified by MDF purification to afford **5ww** as a tan solid (22.3 mg, 0.0414 mmol, 43% yield). ^{1}H NMR (500 MHz, DMSO-d$_6$) δ 1.75–1.82 (m, 2H), 1.89–2.03 (m, 2H), 3.30–3.43 (m, 2H), 3.98 (dd, J = 11.1, 3.9 Hz, 2H), 5.13 (tt, J = 12.1, 3.7 Hz, 1H), 5.30 (s, 2H), 6.23 (br s, 1H), 7.06 (d, J = 8.5 Hz, 2H), 7.12–7.16 (m, 2H), 7.21–7.33 (complex, 8H), 7.67–7.72 (m, 2H), 8.09 (s, 1H); ^{13}C NMR (126 MHz, DMSO-d$_6$) δ 31.8, 45.1, 49.8, 67.0, 102.5, 117.5, 125.9, 126.7, 127.1, 128.3, 128.4, 130.1, 130.5, 130.8, 132.0, 133.8, 141.7, 141.9, 142.9, 143.2, 144.4, 154.3; IR (neat) 1625, 1601, 1445, 1336 cm^{-1}; HRMS calcd for C$_{30}$H$_{30}$N$_5$O$_3$S[M + H]$^+$ 540.2064, found 540.2054; HPLC purity > 99.5%.

4-((4-Imino-5,6-diphenyl-3-((tetrahydro-2H-pyran-4-yl)methyl)-3,4-dihydro-7H-pyrrolo[2,3-d]pyrimidin-7-yl)methyl)benzenesulfonamide (5xx).—Formimidate **3e** (42.6 mg, 0.088 mmol) and 4-(aminomethyl)tetrahydropyran (10.1 mg, 0.088 mmol, 1.0 equiv) were reacted according to General Procedure D and purified by MDF purification to afford **5xx** as an off-white foam (32.2 mg, 0.0582 mmol, 66% yield). ^{1}H NMR (500 MHz, CDCl$_3$) δ 1.38 (qd, J = 4.4, 12.2 Hz, 2H), 1.60–1.70 (m, 2H), 2.34 (dqt, J = 3.8, 7.4, 11.3 Hz, 1H), 3.36 (td, J = 2.0, 11.8 Hz, 2H), 3.93–3.99 (m, 2H), 4.08 (d, J = 7.2 Hz, 2H), 5.35 (s, 2H), 6.94–7.11 (m, 4H), 7.17–7.41 (m, 8H), 7.66–7.87 (m, 3H); ^{13}C NMR (126 MHz, CDCl$_3$, APT pulse sequence) δ d (CH, CH$_3$) 32.9, 40.9, 126.7, 127.4, 127.6, 128.6, 128.8, 130.4, 130.8, 145.8, 168.4; u (C, CH$_2$) 30.3, 45.9, 54.7, 67.4, 102.6, 118.1, 129.5, 132.6, 134.6, 141.7, 142.0, 143.9, 154.1; HRMS calcd for C$_{31}$H$_{32}$N$_5$O$_3$S[M + H]$^+$ 554.2220, found 554.2213; HPLC purity > 99.5%.

3-(7-(Cyclohexylmethyl)-4-imino-5,6-diphenyl-4,7-dihydro-3*H*-pyrrolo[2,3-*d*]pyrimidin-3-yl)propan-1-ol (5yy).—Formimidate **3f** (33.9 mg, 0.082 mmol) and 3-aminopropanol (12.4 mg, 0.165 mmol, 2.0 equiv) were reacted according to General Procedure D and purified by MDF purification to afford **5yy** as a tan residue (6.7 mg, 0.015 mmol, 19% yield). ^{1}H NMR (500 MHz, CDCl$_3$) δ 0.75 (dq, *J* = 3.3, 11.6 Hz, 2H), 0.96–1.11 (m, 3H), 1.36 (dd, *J* = 6.8, 10.2 Hz, 2H), 1.57 (tdd, *J* = 4.0, 7.5, 14.9 Hz, 4H), 2.09 (t, *J* = 6.0 Hz, 2H), 3.69 (t, *J* = 5.5 Hz, 2H), 4.03 (d, *J* = 7.5 Hz, 2H), 4.47–4.55 (m, 2H), 7.16–7.21 (m, 4H), 7.26–7.37 (m, 6H), 7.92 (s, 1H); ^{13}C NMR (126 MHz, CDCl$_3$) δ 25.5, 26.1, 30.4, 32.7, 38.2, 49.2, 57.6, 63.3, 101.2, 117.2, 127.1, 127.8, 128.5, 128.6, 128.9, 129.0, 129.9, 130.4, 130.9, 132.5, 144.2, 144.6; HRMS calcd for $C_{28}H_{33}N_4O$ [M + H]$^+$ 441.2649, found 441.2645; HPLC purity = 96.3%.

(*trans*)-4-(7-(Cyclohexylmethyl)-4-imino-5,6-diphenyl-4,7-dihydro-3*H*-pyrrolo[2,3-*d*]pyrimidin-3-yl)cyclohexan-1-ol (5zz).—Formimidate **3f** (47.5 mg, 0.115 mmol), *trans*-4-aminocyclohexanol hydrochloride (52.5 mg, 0.346 mmol, 3.0 equiv) and triethylamine (23.4 mg, 0.231 mmol, 2.0 equiv) were reacted according to General Procedure E and purified by MDF purification to afford **5zz** as a tan residue (7.9 mg, 0.016 mmol, 14% yield). ^{1}H NMR (500 MHz, CDCl$_3$) δ 0.74 (qd, *J* = 3.5, 11.5 Hz, 2H), 0.98–1.10 (m, 3H), 1.38 (d, *J* = 12.9 Hz, 2H), 1.58 (ddt, *J* = 3.8, 7.6, 15.0 Hz, 4H), 1.75 (tt, *J* = 6.6, 13.3 Hz, 2H), 1.81–1.97 (m, 2H), 2.11–2.25 (m, 4H), 3.70 (tt, *J* = 4.1, 10.7 Hz, 1H), 4.01 (d, *J* = 7.5 Hz, 2H), 5.30–5.41 (m, 1H), 7.14–7.22 (m, 4H), 7.24–7.31 (m, 3H), 7.31–7.35 (m, 3H), 7.96 (s, 1H); ^{13}C NMR (101 MHz, CDCl$_3$) δ 25.6, 26.1, 30.4, 30.5, 34.7, 38.3, 48.7, 51.6, 69.9, 102.8, 117.7, 126.8, 127.8, 128.2, 128.2, 130.6, 131.1, 133.2, 133.9, 141.7, 142.3, 155.3; HRMS calcd for $C_{31}H_{37}N_4O$ [M + H]$^+$ 481.2962, found 481.2957; HPLC purity = 97.8%.

7-(Cyclohexylmethyl)-5,6-diphenyl-3-(tetrahydro-2*H*-pyran-4-yl)-3,7-dihydro-4*H*-pyrrolo[2,3-*d*]pyrimidin-4-imine (5aaa).—Formimidate **3f** (31.6 mg, 0.077 mmol) and 4-aminotetrahydropyran (15.5 mg, 0.154 mmol, 2.0 equiv) were reacted according to General Procedure D and purified by MDF purification to afford **5aaa** as an tan residue (4.6 mg, 0.010 mmol, 13% yield). ^{1}H NMR (400 MHz, CDCl$_3$) δ 0.65–0.79 (m, 2H), 0.96–1.12 (m, 2H), 1.39 (d, *J* = 12.6 Hz, 2H), 1.48–1.64 (m, 4H), 1.72 (br s, 2H), 1.86–2.12 (m, 4H), 3.66 (br s, 2H), 3.96 (d, *J* = 7.5 Hz, 2H), 4.11 (dd, *J* = 11.5, 3.9 Hz, 2H), 7.09–7.36 (complex, 10H), 7.83 (s, 1H); ^{13}C NMR (101 MHz, CDCl$_3$) δ 25.6, 26.1, 30.4, 32.9, 38.3, 48.8, 67.6, 76.7, 77.0, 77.3, 102.5, 117.7, 126.9, 128.0, 128.2, 128.3, 130.5, 130.9, 131.0, 133.7, 141.7, 142.4, 155.0; IR (neat) 1628, 1560, 1445, 1358, 1237 cm^{-1}; HRMS calcd for $C_{30}H_{35}N_4O$ [M + H]$^+$ 467.2805, found 467.2799; HPLC purity = 99.0%.

3-(7-(Cyclopropylmethyl)-4-imino-5,6-diphenyl-4,7-dihydro-3*H*-pyrrolo[2,3-*d*]pyrimidin-3-yl)propan-1-ol (5bbb).—Formimidate **3g** (43.2 mg, 0.117 mmol) and 3-aminopropanol (17.6 mg, 0.234 mmol, 2.0 equiv) were reacted according to General Procedure D and purified by MDF purification to afford **5bbb** as a tan residue (42.8 mg, 0.107 mmol, 92% yield). ^{1}H NMR (500 MHz, CDCl$_3$) δ −0.01 (dt, *J* = 4.7, 6.0 Hz, 2H), 0.20–0.31 (m, 2H), 0.75–0.88 (m, 1H), 1.85–1.98 (m, 2H), 3.49 (dd, *J* = 4.9, 6.1 Hz, 2H), 3.88 (d, *J* = 7.1 Hz, 2H), 4.33 (t, *J* = 6.8 Hz, 2H), 7.03–7.09

(complex, 4H), 7.11–7.23 (complex, 6H), 7.88 (s, 1H), 8.42 (br s, 1H); ^{13}C NMR (126 MHz, CDCl$_3$, APT pulse sequence) δ d (CH, CH$_3$) 11.7, 127.9, 128.6, 128.8, 128.9, 130.4, 130.9, 144.4; u (C, CH$_2$) 4.2, 32.2, 46.3, 47.6, 57.4, 101.1, 117.1, 129.8, 132.3, 136.2, 144.7, 153.6; HRMS calcd for C$_{25}$H$_{27}$N$_4$O [M + H]$^+$ 399.2179, found 399.2174; HPLC purity = 98.7%.

7-(Cyclopropylmethyl)-5,6-diphenyl-3-(tetrahydro-2*H*-pyran-4-yl)-3,7-dihydro-4*H*-pyrrolo[2,3-*d*]pyrimidin-4-imine (5ccc).—Formimidate **3g**

(37.1 mg, 0.100 mmol) and 4-aminotetrahydropyran (20.3 mg, 0.201
mmol, 2.0 equiv) were reacted according to General Procedure D and purified by MDF
purification to afford **5ccc** as a tan residue (27.4 mg, 0.0645 mmol, 65% yield). ^{1}H NMR
(400 MHz, CDCl$_3$) δ 0.06–0.15 (m, 2H), 0.31–0.38 (m, 2H), 0.96 (tt, *J* = 7.9, 4.8 Hz, 1H),
1.85–2.01 (m, 4H), 3.60 (td, *J* = 6, 2.1 Hz, 2H), 3.96 (d, *J* = 7.0 Hz, 2H), 4.11 (dd, *J* = 11.3,
3.9 Hz, 2H), 5.28–5.42 (m, 1H), 6.43 (br s, 1H), 7.13–7.25 (complex, 7H), 7.25–7.33 (m,
3H), 7.78 (s, 1H). ^{13}C NMR (101 MHz, CDCl$_3$) δ 4.0, 11.8, 32.8, 46.9, 49.5, 67.6, 102.9,
117.9, 126.7, 128.0, 128.2, 128.2, 130.5, 131.1, 132.6, 133.9, 141.8, 142.0, 155.3, 160.3;
HRMS calcd for C$_{27}$H$_{29}$N$_4$O [M + H]$^+$ 425.2336, found 425.2334; HPLC purity > 99.5%.

7-(Cyclopropylmethyl)-5,6-diphenyl-3-((tetrahydro-2*H*-pyran-4-yl)methyl)-3,7-dihydro-4*H*-pyrrolo[2,3-*d*]pyrimidin-4-imine (5ddd).—Formimidate **3g** (45.7 mg,

0.124 mmol) and (tetrahydro-2Hpyran-4-yl)methanamine (28.5 mg, 0.247 mmol, 2.0 equiv)
were reacted according to General Procedure D and purified by MDF purification to afford
5ddd as a tan residue (36.3 mg, 0.0828 mmol, 67% yield). ^{1}H NMR (500 MHz, CDCl$_3$) δ
−0.06–0.04 (m, 2H), 0.17–0.33 (m, 2H), 0.77–0.88 (m, 1H), 1.18–1.35 (m, 2H), 1.55 (ddd, *J*
= 2.0, 4.1, 12.7 Hz, 2H), 2.22 (ttt, *J* = 3.8, 7.3, 11.2 Hz, 1H), 3.23 (td, *J* = 2.0, 11.8 Hz, 2H),
3.79–3.85 (m, 2H), 3.87 (d, *J* = 7.0 Hz, 2H), 3.98 (d, *J* = 7.2 Hz, 2H), 7.05–7.17 (complex,
7H), 7.17–7.24 (m, 3H), 7.57 (s, 1H), 8.51 (br s, 1H); ^{13}C NMR (126 MHz, CDCl$_3$,
APT pulse sequence) δ d (CH, CH$_3$) 11.7, 33.0, 127.4, 128.5, 128.5, 128.7, 130.5, 131.0,
145.0; u (C, CH$_2$) 4.1, 30.3, 47.4, 54.8, 67.4, 102.2, 117.5, 130.3, 132.9, 134.7, 143.6, 154.0;
HRMS calcd for C$_{28}$H$_{31}$N$_4$O [M + H]$^+$ 439.2492, found 439.2486; HPLC purity > 99.5%.

2-(7-Benzyl-4-imino-5,6-bis(4-methoxyphenyl)-4,7-dihydro-3H-pyrrolo[2,3-d]pyrimidin-3-yl)ethanol (5eee).—Formimidate **3h** (42 mg, 0.090 mmol)

and ethanolamine (11 mg, 0.18 mmol, 2.0 equiv) were reacted
according to General Procedure D and purified by MDF purification
to afford **5eee** as a light yellow solid (36 mg, 0.075 mmol, 83% yield). Mp =
131–144 °C; *I*H NMR (500 MHz, CDCl$_3$) δ 3.78 (s, 3 H), 3.79 (s, 3 H), 4.00 (t, *J* = 4.0 Hz,
2 H), 4.94 (t, *J* = 4.0 Hz, 2 H), 5.34 (s, 2 H), 6.77 (d, *J* = 6.8 Hz, 2 H), 6.84 (d, *J* = 6.8 Hz, 2
H), 6.95 (m, 2 H), 6.97 (d, *J* = 7.2 Hz, 2 H), 7.12 (d, *J* = 6.8 Hz, 2 H), 7.24 (m, 3 H), 7.94 (s,
1 H), 8.65 (s, 1 H); ^{13}C NMR (126 MHz, CDCl$_3$, APT pulse sequence) δ d (CH, CH$_3$) 40.9,
55.2, 113.9, 114.5, 126.8, 127.6, 128.6, 131.4, 132.1, 144.2; u (C, CH$_2$) 46.5, 52.9, 61.7,
101.2, 116.6, 121.1, 136.7, 144.6, 154.0, 159.2, 159.8, 169.3; IR 1669, 1622, 1609 cm^{-1};
HRMS calcd for C$_{29}$H$_{29}$N$_4$O$_3$ [M + H]$^+$ 481.2240, found 481.2231; HPLC purity = 99.8%.

2-(7-Benzyl-4-imino-5,6-bis(4-methoxyphenyl)-4,7-dihydro-3H-pyrrolo[2,3-d]pyrimidin-3-yl)propanol (5fff).—Formimidate **3h** (44 mg, 0.095 mmol)

and 3-amino-1-propanol (14 mg, 0.19 mmol, 2.0 equiv) were reacted
according to General Procedure D and purified by MDF purification to afford **5fff** as
a light yellow solid (35 mg, 0.070 mmol, 74% yield). Mp = 53–59 °C; ^{1}H NMR (500 MHz,
CDCl$_3$) δ 2.04 (t, J = 4.4 Hz, 2 H), 3.63 (t, J = 4.4 Hz, 2 H), 3.78 (s, 3 H), 3.79 (s, 3 H), 4.42
(t, J = 5.2 Hz, 2 H), 5.32 (s, 2 H), 6.77 (d, J = 6.8 Hz, 2 H), 6.84 (d, J = 6.8 Hz, 2 H), 6.95
(m, 3 H), 6.97 (m, 1 H), 7.12 (d, J = 6.8 Hz, 2 H), 7.23 (m, 3 H), 7.94 (s, 1 H), 8.62 (s, 1 H);
^{13}C NMR (126 MHz, CDCl$_3$, APT pulse sequence) δ d (CH, CH$_3$) 40.9, 55.1, 113.8, 114.2,
126.8, 127.5, 128.5, 131.4, 132.1, 168.3; u (C, CH$_2$) 32.5, 45.5, 46.3, 57.2, 101.6, 116.8,
121.6, 124.5, 135.5, 137.0, 144.1, 154.3, 159.2, 158.9, 159.6; IR 1667, 1623, 1610 cm^{-1};
HRMS calcd for C$_{30}$H$_{31}$N$_4$O$_3$ [M + H]$^+$ 495.2396, found 495.2391; HPLC purity > 99.5%.

(*trans*)-4-(7-Benzyl-4-imino-5,6-bis(4-methoxyphenyl)-4,7-dihydro-3*H*-pyrrolo[2,3-*d*]pyrimidin-3-yl)cyclohexan-1-ol (5ggg).—Formimidate **3h**

(81.0 mg, 0.174 mmol) and (*trans*)-2-aminocyclohexanol
(40.1 mg, 0.348 mmol, 2.0 equiv) were reacted according to General
Procedure D and purified by MDF purification to afford **5ggg** as an off-white solid (7.0 mg,
0.013 mmol, 4% yield). ^{1}H NMR (500 MHz, CDCl$_3$) δ 1.62–1.71 (m, 4H), 2.09–2.19 (m,
4H), 3.63–3.71 (m, 1H), 3.77 (s, 3H), 3.78 (s, 3H), 5.11–5.22 (m, 1H), 5.27 (s, 2H), 6.75 (d,
J = 8.7 Hz, 2H), 6.81 (d, J = 8.7 Hz, 2H), 6.96 (td, J = 2.0, 6.7 Hz, 4H), 7.13 (d, J = 8.7 Hz,
2H), 7.21–7.33 (m, 3H), 7.84 (s, 1H); ^{13}C NMR (126 MHz, CDCl$_3$, APT pulse sequence) δ
d (CH, CH$_3$) 55.20, 55.23, 69.8, 113.8, 114.1, 126.8, 127.4, 128.6, 131.6, 132.2, 141.7; u (C,
CH$_2$) 30.8, 34.5, 46.1, 102.5, 117.3, 122.3, 125.3, 134.1, 137.6, 142.8, 154.6, 158.8, 159.4;
HRMS calcd for C$_{33}$H$_{35}$N$_4$O$_3$ [M + H]$^+$ 535.2704, found 535.2710; HPLC purity = 96.2%.

(*1R,2R*) and (*1S,2S*)-2-(7-Benzyl-4-imino-5,6-bis(4-methoxyphenyl)-4,7-dihydro-3*H*-pyrrolo[2,3-*d*]pyrimidin-3-yl)cyclohexan-1-ol (5hhh).—Formimidate

3h (41.2 mg, 0.088 mmol), (*trans*)-2-aminocyclohexanol hydrochloride (20.4 mg, 0.177
mmol, 2.0 equiv) and triethylamine (17.9 mg, 0.177 mmol, 2.0 equiv) were reacted
according to General Procedure E and purified by MDF purification to afford **5hhh** as a
tan solid (20.1 mg, 0.0376 mmol, 43% yield). ^{1}H NMR (500 MHz, CDCl$_3$) δ 1.36 (dddd, J
= 3.7, 8.6, 13.1, 16.6 Hz, 1H), 1.55 (tdd, J = 3.4, 11.1, 13.2 Hz, 1H), 1.82 (dtt, J = 4.8, 12.3,
39.4 Hz, 4H), 2.09–2.18 (m, 1H), 2.22–2.31 (m, 1H), 3.67 (td, J = 4.6, 10.4 Hz, 1H), 3.79
(s, 3H), 3.80 (s, 3H), 5.14 – 5.22 (m, 1H), 5.32, 5.36 (ABq, J_{AB} = 12.5 Hz, 2H), 6.78 (d, J =
8.7 Hz, 2H), 6.84 (d, J = 8.8 Hz, 2H), 6.93–6.99 (m, 4H), 7.13 (d, J = 8.1 Hz, 2H), 7.24–7.30
(m, 3H), 8.13 (s, 1H), 8.65 (br s, 1H); ^{13}C NMR (126 MHz, CDCl$_3$, APT pulse sequence) δ
d (CH, CH$_3$) 40.9, 55.1, 113.8, 114.2, 126.8, 127.5, 128.5, 131.4, 132.1, 168.3; u (C, CH$_2$)
32.5, 45.5, 46.3, 57.2, 101.6, 116.8, 121.6, 124.5, 135.5, 137.0, 144.1, 154.3, 159.2, 158.9,
159.6; HRMS calcd for C$_{33}$H$_{35}$N$_4$O3 [M + H]$^+$ 535.2704, found 535.2693; HPLC purity =
99.8%.

7-Benzyl-3-((*trans*)-4-methoxycyclohexyl)-5,6-bis(4-methoxyphenyl)-3,7-dihydro-4*H*-pyrrolo[2,3-*d*]pyrimidin-4-imine (5iii).—Formimidate **3h** (43.7

mg, 0.094 mmol) and (*trans*)-4- methoxycyclohexylamine (24.3
mg, 0.188 mmol, 2.0 equiv) were reacted according to General Procedure D and
purified by MDF purification to afford **5iii** as a tan solid (8.2 mg, 0.0149 mmol, 16% yield).

^{1}H NMR (500 MHz, CDCl$_3$) δ 1.68 (d, J = 13.6 Hz, 4H), 2.16–2.27 (m, 4H), 3.18–3.29 (m, 1H), 3.37 (s, 3H), 3.77 (s, 3H), 3.78 (s, 3H), 5.24–5.33 (m, 1 H), 5.29 (s, 2H), 6.76 (d, J = 8.7 Hz, 2H), 6.82 (d, J = 8.6 Hz, 2H), 6.94–6.98 (complex, 5H), 7.10–7.15 (m, 2H), 7.22–7.28 (m, 2H), 7.91 (s, 1H); ^{13}C NMR (126 MHz, CDCl$_3$, APT pulse sequence) δ d (CH, CH$_3$) 41.0, 55.21, 55.24, 55.8, 78.2, 113.1, 113.8, 114.3, 126.8, 127.5, 128.6, 131.6, 132.2; HRMS calcd for C$_{34}$H$_{37}$N$_4$O$_3$ [M + H]$^+$ 549.2860, found 549.2853; HPLC purity = 95.5%.

7-Benzyl-5,6-bis(4-methoxyphenyl)-3-(tetrahydro-2H-pyran-4-yl)-3,7-dihydro-4H-pyrrolo[2,3-d]pyrimidin-4-imine (5jjj).—Formimidate **3h** (80.0 mg, 0.172 mmol) and 4-aminotetrahydropyran (34.8 mg, 0.344 mmol, 2.0 equiv) were reacted according to General Procedure D and purified by MDF purification to afford **5jjj** as an off-white foam (53.2 mg, 0.102 mmol, 59% yield). ^{1}H NMR (500 MHz, CDCl$_3$) δ 1.92 (qd, J = 4.4, 12.1 Hz, 2H), 2.00 (ddd, J = 1.8, 4.1, 12.1 Hz, 2H), 3.61 (td, J = 2.1, 11.6 Hz, 2H), 3.75 (s, 3H), 3.76 (s, 6H), 4.05–4.19 (m, 2H), 5.25 (s, 2H), 5.35 (tt, J = 4.1, 12.1 Hz, 1H), 6.47 (br s, 1H), 6.70–6.77 (m, 2H), 6.78–6.84 (m, 2H), 6.93–7.01 (m, 3H), 7.12–7.17 (m, 2H), 7.18–7.29 (m, 4H), 7.78 (s, 1H); ^{13}C NMR (126 MHz, CDCl$_3$, APT pulse sequence) δ d (CH, CH$_3$) 49.6, 55.17, 55.21, 113.7, 113.8, 126.7, 127.3, 128.5, 131.6, 132.3, 142.3; u (C, CH$_2$) 32.9, 46.0, 67.7, 103.1, 117.6, 122.8, 126.1, 132.8, 138.1, 141.9, 155.4, 158.5, 159.2; HRMS calcd for C$_{32}$H$_{33}$N$_4$O$_3$ [M + H]$^+$ 521.2547, found 521.2537; HPLC purity > 99.5%.

7-Benzyl-5,6-bis(4-methoxyphenyl)-3-((tetrahydrofuran-3-yl)methyl)-3,7-dihydro-4H-pyrrolo[2,3-d]pyrimidin-4-imine (5kkk).—Formimidate **3h** (32.0 mg, 0.069 mmol) and 3-aminomethyltetrahydrofuran (13.9 mg, 0.137 mmol, 2.0 equiv) were reacted according to General Procedure D and purified by MDF purification to afford **5kkk** as a tan solid (22.6 mg, 0.0434 mmol, 63% yield). ^{1}H NMR (500 MHz, CDCl$_3$) δ 1.69–1.78 (m, 1H), 2.12 (dtd, J = 5.4, 8.0, 13.2 Hz, 1H), 3.09 (qq, J = 2.5, 4.0, 7.8 Hz, 1H), 3.66 (dd, J = 4.6, 9.1 Hz, 1H), 3.75–3.81 (m, 2H), 3.78 (s, 3H), 3.79 (s, 3H), 3.98 (td, J = 5.4, 8.2 Hz, 1H), 4.11 (dd, J = 8.1, 13.8 Hz, 1H), 4.26 (dd, J = 7.0, 13.8 Hz, 1H), 5.30 (d, J = 5.7 Hz, 2H), 6.75–6.80 (m, 2H), 6.81–6.86 (m, 2H), 6.94–7.01 (m, 4H), 7.12–7.17 (m, 2H), 7.22–7.29 (m, 3H), 7.75 (s, 1H), 8.67 (br s, 1H); ^{13}C NMR (126 MHz, CDCl$_3$, APT pulse sequence) δ d (CH, CH$_3$) 37.4, 55.21, 55.23, 113.8, 114.2, 126.8, 127.5, 128.6, 131.5, 132.2, 145.0; u (C, CH$_2$) 29.7, 46.3, 51.3, 67.5, 70.5, 102.5, 117.2, 122.1, 125.1, 134.5, 137.5, 143.4, 154.3, 158.8, 159.5; HRMS calcd for C$_{32}$H$_{33}$N$_4$O$_3$ [M + H]$^+$ 521.2547, found 521.2539; HPLC purity > 99.5%.

5,6-Bis(benzo[d][1,3]dioxol-5-yl)-7-benzyl-3-(tetrahydro-2H-pyran-4-yl)-3,7-dihydro-4H-pyrrolo[2,3-d]pyrimidin-4-imine (5lll).—Formimidate **3i** (65.0 mg, 0.132 mmol), sodium methoxide (14.2 mg, 0.263, 2.0 equiv) and 4-aminotetrahydropyran (26.6 mg, 0.263 mmol, 2.0 equiv) were reacted according to General Procedure E and purified by MDF purification to afford **5lll** as a tan solid (19.6 mg, 0.0357 mmol, 27% yield). ^{1}H NMR (500 MHz, CDCl$_3$) δ 1.92 (qd, J = 4.4, 12.1 Hz, 2H), 1.99–2.05 (m, 2H), 3.63 (t, J = 11.6 Hz, 2H), 4.06–4.15 (m, 2H), 5.26 (s, 2H), 5.32–5.42 (m, 1H), 5.93 (s, 2H), 5.94 (s, 2H), 6.49 (d, J = 1.6 Hz, 1H), 6.53 (dd, J = 1.7, 7.9 Hz, 1H), 6.65–6.70 (m, 2H), 6.72–6.76 (m, 2H), 6.97 (dd, J = 1.5, 8.0 Hz, 2H), 7.20–7.29 (m, 4H), 7.80 (br s, 1H); ^{13}C NMR (126 MHz, CDCl$_3$) δ δ 32.9, 36.6,

46.2, 47.7, 66.8, 67.3, 101.2, 101.3, 108.3, 108.6, 110.7, 111.0, 117.4, 123.2, 123.9, 125.0, 126.2, 126.8, 127.6, 128.6, 137.2, 141.8, 147.2, 147.2, 147.5, 147.7, 147.8, 147.9, 153.9; HRMS calcd for $C_{32}H_{29}N_4O_5$ [M + H]$^+$ 549.2132, found 549.2136; HPLC purity = 97.5%.

2-(7-Benzyl-4-imino-5-phenyl-4,7-dihydro-3*H*-pyrrolo[2,3-*d*]pyrimidin-3-yl)ethan-1-ol (11a).—Formimidate **10** (46.0 mg, 0.140 mmol) and ethanolamine (25.6 mg, 0.419 mmol, 3.0 equiv) were reacted according to General Procedure D and purified by MDF purification to afford **11a** as a tan solid (19.5 mg, 0.0566 mmol, 40% yield). ^{1}H NMR (400 MHz, CDCl$_3$) δ 3.91–4.00 (m, 2H), 4.16–4.23 (m, 2H), 5.29 (s, 2H), 6.74 (s, 1H), 7.21–7.25 (m, 2H), 7.27–7.36 (m, 4H), 7.37–7.45 (m, 4H), 7.65 (s, 1H); ^{13}C NMR (101 MHz, CDCl$_3$, APT pulse sequence) δ d (CH, CH$_3$) 121.0, 127.2, 127.5, 127.9, 128.8, 128.9, 129.1, 146.0; u (C, CH$_2$) 48.2, 53.1, 63.4, 102.4, 120.6, 134.1, 136.9, 143.5, 157.6; HRMS calcd for $C_{21}H_{21}N_4O$ [M + H]$^+$ 345.1710, found 345.1710; HPLC purity = 96.2%.

7-Benzyl-5-phenyl-3-(tetrahydro-2*H*-pyran-4-yl)-3,7-dihydro-4*H*-pyrrolo[2,3-*d*]pyrimidin-4-imine (11b).—Formimidate **10** (23.0 mg, 0.070 mmol) and 4-aminotetrahydropyran (21.2 mg, 0.209 mmol, 3.0 equiv) were reacted according to General Procedure D and purified by MDF purification to afford **11b** as a tan solid (9.3 mg, 0.0242 mmol, 35% yield). ^{1}H NMR (400 MHz, CDCl$_3$) δ 1.87–2.06 (m, 4H), 3.61 (td, J = 2.3, 11.7 Hz, 2H), 4.07–4.18 (m, 2H), 5.29 (s, 2H), 5.36 (tt, J = 4.2, 12.0 Hz, 1H), 6.71 (s, 1H), 7.23–7.45 (complex, 10H), 7.78 (s, 1H); HRMS calcd for $C_{24}H_{25}N_4O$ [M + H]$^+$ 385.2023, found 385.2022; HPLC purity > 99.5%.

7-Benzyl-3-(furan-2-ylmethyl)-5-phenyl-3,7-dihydro-4*H*-pyrrolo[2,3-*d*]pyrimidin-4-imine (11c).—Formimidate **10** (38.0 mg, 0.115 mmol) and 2-aminomethylfuran (33.5 mg, 0.345 mmol, 3.0 equiv) were reacted according to General Procedure D and purified by flash chromatography to afford **11c** as a tan solid (33.0 mg, 0.0867 mmol, 75% yield). ^{1}H NMR (400 MHz, CDCl$_3$) δ 5.24 (s, 2H), 5.27 (s, 2H), 6.33 (dd, J = 1.9, 3.3 Hz, 1H), 6.44–6.47 (m, 1H), 6.69 (s, 1H), 7.20–7.45 (complex, 11H), 7.80 (s, 1H); ^{13}C NMR (101 MHz, CDCl$_3$, APT pulse sequence) δ d (CH, CH$_3$) 109.6, 110.7, 120.6, 127.1, 127.6, 127.9, 128.7, 128.9 (× 2C), 142.8, 145.5; u (C, CH$_2$) 42.7, 48.2, 102.7, 120.9, 134.3, 137.0, 143.0, 149.5, 155.1; HRMS calcd for $C_{24}H_{21}N_4O$ [M + H]$^+$ 381.1710, found 381.1715; HPLC purity = 95.7%.

7-Benzyl-3-(3,4-dimethoxyphenethyl)-5-phenyl-3,7-dihydro-4*H*-pyrrolo[2,3-*d*]pyrimidin-4-imine (11d).—Formimidate **10** (28.0 mg, 0.085 mmol) and 2-(3,4-dimethoxyphenyl)ethan-1-amine (15.4 mg, 0.085 mmol, 1.0 equiv) were reacted according to General Procedure D and purified by MDF purification to afford **11d** as a tan solid (30.4 mg, 0.0653 mmol, 77% yield). ^{1}H NMR (400 MHz, CDCl$_3$) δ 3.07 (t, J = Hz, 2H), 3.72 (s, 3H), 3.85 (s, 3H), 4.26 (t, J = 6.8 Hz, 2H), 5.25 (s, 2H), 6.65 (d, J = 1.9 Hz, 1H), 6.68–6.74 (m, 2H), 6.78 (d, J = 8.1 Hz, 1H), 7.17–7.36 (complex, 7), 7.37–7.50 (m, 4H); HRMS calcd for $C_{29}H_{29}N_4O_2$ [M + H]$^+$ 465.2285, found 465.2287; HPLC purity = 99.2%.

3-(7-Benzyl-4-imino-5,6-dimethyl-4,7-dihydro-3*H*-pyrrolo[2,3-*d*]pyrimidin-3-yl)propan-1-ol (5mmm).—Formimidate **3j** (41.0 mg, 0.146 mmol) and

3-amino-1-propanol (32.8 mg, 0.437 mmol, 3.0 equiv) were reacted according to General Procedure D and purified by flash chromatography to afford **5mmm** as a colorless oil (41.6 mg, 0.134 mmol, 92% yield). ^{1}H NMR (400 MHz, CDCl$_3$) δ 1.91 (tt, J = 5.0, 7.4 Hz, 3H), 2.10 (s, 3H), 2.34 (s, 3H), 3.50–3.60 (m, 2H), 4.20 (dd, J = 5.0, 6.8 Hz, 2H), 5.27 (s, 2H), 6.98–7.06 (m, 2H), 7.18–7.38 (m, 3H), 7.54 (s, 1H); ^{13}C NMR (101 MHz, CDCl$_3$, APT pulse sequence) δ d (CH, CH$_3$) 9.6, 10.7, 126.4, 127.4, 128.8, 144.4; u (C, CH$_2$) 33.6, 42.8, 45.2, 56.7, 103.6, 109.3, 127.7, 137.5, 142.5, 158.0; HRMS calcd for C$_{18}$H$_{23}$N$_4$O [M + H]$^+$ 311.1866, found 311.1894; HPLC purity = 98.4%.

(*trans*)-4-(7-Benzyl-4-imino-5,6-dimethyl-4,7-dihydro-3*H*-pyrrolo[2,3-*d*]pyrimidin-3-yl)cyclohexan-1-ol (5nnn).—

Formimidate **3j** (41.0 mg, 0.146 mmol), (*trans*)-4-aminocyclohexanol hydrochloride (66.3 mg, 0.437 mmol, 3.0 equiv) and sodium methoxide (15.8 mg, 0.291 mmol, 2 equiv) were reacted according to General Procedure E and purified by flash chromatography to afford **5nnn** as a colorless oil (16.5 mg, 0.047 mmol, 32% yield). ^{1}H NMR (400 MHz, CDCl$_3$) δ 1.69–1.95 (m, 4H), 2.14–2.28 (m, 4H), 2.19 (s, 3H), 2.45 (s, 3H), 3.70 (td, J = 5.3, 10.6 Hz, 1H), 5.07 (t, J = 11.5 Hz, 1H), 5.36 (s, 2H), 7.00–7.08 (m, 2H), 7.23–7.38 (m, 3H), 7.99 (s, 1H), 8.71 (s, 1H); ^{13}C NMR (101 MHz, CDCl$_3$, APT pulse sequence) δ d (CH, CH$_3$) 9.9, 10.7, 56.2, 69.0, 126.5, 127.9, 128.9, 139.8; u (C, CH$_2$) 31.1, 34.0, 45.7, 102.0, 109.3, 132.2, 136.3, 144.7, 152.3; HRMS calcd for C$_{21}$H$_{27}$N$_4$O [M + H]$^+$ 351.2179, found 351.2199; HPLC purity = 98.7%.

7-Benzyl-5,6-dimethyl-3-(tetrahydro-2*H*-pyran-4-yl)-3,7-dihydro-4*H*-pyrrolo[2,3-*d*]pyrimidin-4-imine (5ooo).—

Formimidate **3j** (41.0 mg, 0.146 mmol) and 4-aminotetrahydropyran (44.2 mg, 0.437 mmol, equiv) were reacted according to General Procedure D and purified by flash chromatography to afford **5ooo** as a colorless oil (43.1 mg, 0.128 mmol, 88% yield). ^{1}H NMR (500 MHz, CDCl$_3$) δ 1.86–2.04 (m, 4H), 2.09 (s, 3H), 2.36 (s, 3H), 3.65 (td, J = 2.1, 11.7 Hz, 2H), 4.07–4.20 (m, 2H), 5.26 (s, 2H), 5.39 (tt, J = 4.1, 12.2 Hz, 1H), 6.97–7.08 (m, 2H), 7.16–7.36 (m, 3H), 7.66 (s, 1H); ^{13}C NMR (126 MHz, CDCl$_3$, APT pulse sequence) δ d (CH, CH$_3$) 9.5, 10.7, 49.4, 126.4, 127.3, 128.7, 141.3; u (C, CH$_2$) 32.8, 45.1, 67.7, 103.8, 109.3, 127.1, 137.6, 141.5, 156.4; HRMS calcd for C$_{20}$H$_{25}$N$_4$O [M + H]$^+$ 337.2023, found 337.2052; HPLC purity = 98.0%.

3-(9-Benzyl-4-imino-4,5,6,7,8,9-hexahydro-3H-pyrimido[4,5-b]indol-3-yl)propan-1-ol (5ppp).—

Formimidate **3k** (63.0 mg, 0.196 mmol) and 3-amino-1-propanol (44.2 mg, 0.588 mmol, 3.0 equiv) were reacted according to General Procedure D and purified by flash chromatography to afford **5ppp** as a colorless oil (64.2 mg, 0.183 mmol, 93% yield). ^{1}H NMR (400 MHz, CDCl$_3$) δ 1.73 (tdd, J = 2.2, 4.0, 8.9 Hz, 4H), 1.87–2.00 (m, 2H), 2.19–2.26 (m, 2H), 2.76–2.83 (m, 2H), 2.97 (t, J = 7.2 Hz, 2H), 3.51–3.59 (m, 2H), 4.16 (t, J = 7.2 Hz, 2H), 4.20–4.24 (m, 2H), 6.95–7.09 (m, 2H), 7.16–7.33 (m, 3H), 7.54 (s, 1H); ^{13}C NMR (101 MHz, CDCl$_3$, APT pulse sequence) δ d (CH, CH$_3$) 126.7, 128.5, 128.9, 143.8; u (C, CH$_2$) 21.5, 22.27, 22.35, 23.0, 33.6, 37.1, 42.8, 43.5, 56.6, 103.1, 111.2, 126.7, 128.5, 128.9, 130.8, 138.4, 142.2, 143.8, 157.7; HRMS calcd for C$_{21}$H$_{27}$N$_4$O [M + H]$^+$ 351.2179, found 351.2211; HPLC purity = 99.1%.

(*trans*)-4-(4-lmino-9-phenethyl-4,5,6,7,8,9-hexahydro-3H-pyrimido[4,5-b]indol-3-yl)cyclohexan-1-ol (5qqq).—Formimidate **3k** (69.0 mg, 0.215 mmol), (*frans*)-4-aminocyclohexanol hydrochloride (74.2 mg, 0.644 mmol, 3.0 equiv) and sodium methoxide (23.2 mg, 0.429, 2 equiv) were reacted according to General Procedure E and purified by flash chromatography followed by reverse-phase flash chromatography to afford **5qqq** as an off-white solid (18.4 mg, 0.047 mmol, 22% yield). ^{1}H NMR (400 MHz, CDCl$_3$) δ 1.69–1.97 (complex, 6H), 2.14–2.33 (complex, 8H), 2.85–2.93 (m, 2H), 3.00 (t, *J* = 7.1 Hz, 2H), 3.67–3.76 (m, 1H), 4.27 (t, *J* = 7.1 Hz, 2H), 4.99–5.12 (m, 1H), 6.91–7.04 (m, 2H), 7.16–7.36 (m, 3H), 7.96 (s, 1H), 8.72 (s, 1H); ^{13}C NMR (101 MHz, CDCl$_3$, APT pulse sequence) δ d (CH, CH$_3$) 56.4, 69.0, 126.9, 128.6, 128.8, 139.0; u (C, CH$_2$) 21.6, 21.9, 22.0, 22.6, 31.1, 34.0, 36.7, 43.9, 101.3, 111.1, 135.3, 137.7, 144.5, 151.8; HRMS calcd for C$_{24}$H$_{31}$N$_4$O [M + H]$^+$ 391.2492, found 391.2518; HPLC purity = 99.5%.

9-Phenethyl-3-(tetrahydro-2*H*-pyran-4-yl)-3,5,6,7,8,9-hexahydro-4*H*-pyrimido[4,5-*b*]indol-4-imine (5rrr).—Formimidate **3k** (68.0 mg, 0.212 mmol) and 4-aminotetrahydropyran (64.6 mg, 0.635 mmol, 3.0 equiv) were reacted according to General Procedure D and purified by flash chromatography to afford **5rrr** as a colorless oil (63.7 mg, 0.169 mmol, 80% yield). ^{1}H NMR (400 MHz, CDCl$_3$) δ 1.73 (ddtt, *J* = 3.1, 6.1, 9.2, 12.5 Hz, 4H), 1.86–2.08 (m, 4H), 2.21 (dt, *J* = 3.1, 5.6 Hz, 2H), 2.82 (q, *J* = 4.1, 5.8 Hz, 2H), 2.97 (t, *J* = 7.3 Hz, 2H), 3.57–3.78 (m, 2H), 4.13 (dt, *J* = 5.7, 8.5 Hz, 4H), 5.38 (tt, *J* = 4.2, 11.8 Hz, 1H), 6.98–7.11 (m, 2H), 7.16–7.35 (m, 3H), 7.65 (s, 1H); ^{13}C NMR (101 MHz, CDCl$_3$, APT pulse sequence) δ d (CH, CH$_3$) 49.4, 126.6, 128.5, 128.9, 140.8; u (C, CH$_2$) 21.5, 22.3, 22.4, 23.1, 32.8, 37.2, 43.5, 67.7, 103.3, 111.2, 130.1, 138.5, 141.0, 156.2; HRMS calcd for C$_{23}$H$_{29}$N$_4$O [M + H]$^+$ 377.2336, found 377.2361; HPLC purity = 97.2%.

(E)-*N'*-(1-benzyl-3-cyano-4,5-diphenyl-1*H*-pyrrol-2-yl)-*N*-((*trans*)-4-hydroxycyclohexyl)formimidamide (4f).—Formimidate **3a** (267 mg, 0.0.659 mmol) and (*trans*)4- aminocyclohexanol hydrochloride (500 mg, 3.30 mmol, 5.0 equiv) were reacted according to General Procedure D except temperature kept at rt and purified by flash chromatography to afford **4f** as a tan solid (191.4 mg, 0.403 mmol, 61% yield). ^{1}H NMR (400 MHz, DMSO-d6) δ 1.09–1.25 (m, 4H), 1.73–1.84 (m, 2H), 1.85–1.93 (m, 2H), 3.33–3.43 (m, 1H), 3.57–3.68 (m, 1H), 4.52 (d, *J* = 4.4 Hz, 1H), 5.00 (s, 2H), 6.78–6.89 (m, 2H), 7.08–7.27 (m, 10H), 7.24–7.33 (m, 2H), 7.83 (dd, *J* = 7.3, 4.4 Hz, 1H), 8.13 (dd, *J* = 4.3, 0.9 Hz, 1H); LRMS calcd for C$_{31}$H$_{30}$N$_4$O [M + H]$^+$ 475.6, found 475.2; HPLC purity 99.5%.

3-((7-Benzyl-5,6-diphenyl-7*H*-pyrrolo[2,3-*d*]pyrimidin-4-yl)amino)propan-1-ol (13a).—Pyrrolopyrimidine **5** (25.0 mg, 0.058 mmol) was slurried in isopropanol (1 mL) and water (1 mL). The microwave vial was sealed and heated at 180 °C for 2 h. Upon cooling the solvents were removed and the residue purified by flash chromatography to afford **13a** as a colorless oil (24.2 mg, 0.055 mmol, 96% yield). ^{1}H NMR (400 MHz, CDCl$_3$) δ 1.58 (p, *J* = 5.6 Hz, 2H), 3.48–3.59 (m, 4H), 5.31 (s, 2H), 6.83–6.92 (m, 2H), 6.94–7.03 (m, 2H), 7.08–7.37 (complex, 11H), 8.31 (s, 1H); ^{13}C NMR (101 MHz, CDCl$_3$, APT pulse sequence) δ d (CH, CH$_3$) 127.0, 127.1, 127.2, 128.2, 128.3, 128.4, 128.6, 130.5, 131.1, 151.9; u (C, CH$_2$) 33.5, 36.8, 46.1, 58.0, 101.3, 113.9, 130.5, 134.4, 134.7, 137.9,

149.9, 157.2; IR 1592, 1565, 1467 cm^{-1}; HRMS calcd for $C_{28}H_{27}N_4O$ [M + H]$^+$ 435.2179, found 435.2176; HPLC purity > 99.5%.

trans-4-((7-Benzyl-5,6-diphenyl-7H-pyrrolo[2,3-d]pyrimidin-4-yl)amino)cyclohexan-1-ol (13b).—Pyrrolopyrimidine **5f** (271.7 mg, 0.573 mmol) was slurried in isopropanol (3 mL) and water (2 mL). The microwave vial was sealed and heated at 160 °C for 2.5 h. Upon cooling the solvents were removed and the residue purified by reverse-phase flash chromatography and recrystallized from acetone to afford **13b** as a white solid (218.7 mg, 0.461 mmol, 80% yield). ^{1}H NMR (400 MHz, CDCl$_3$) δ 1.00 (tdd, J = 3.5, 10.6, 13.0 Hz, 2H), 1.43 (tdd, J = 3.6, 10.2, 13.0 Hz, 2H), 1.79–1.90 (m, 2H), 2.05 (ddt, J = 3.9, 8.1, 12.6 Hz, 2H), 3.53 (tt, J = 4.1, 10.1 Hz, 1H), 4.07 (dtd, J = 3.9, 7.2, 10.8 Hz, 1H), 5.36 (s, 2H), 6.91 (dd, J = 2.1, 7.4 Hz, 2H), 7.03–7.08 (m, 2H), 7.12–7.30 (m, 11H), 8.41 (s, 1H); ^{13}C NMR (101 MHz, CDCl$_3$, APT pulse sequence) δ d (CH, CH$_3$) 48.2, 69.4, 126.9, 127.1, 127.1, 128.2, 128.4, 128.4, 130.6, 131.0, 152.2; u (C, CH$_2$) 30.6, 33.5, 46.0, 101.6, 113.9, 130.5, 134.2, 134.5, 138.0, 150.0, 155.8; IR 1589, 1564, 1466 cm^{-1}; HRMS calcd for $C_{31}H_{31}N_4O$ [M + H]$^+$ 475.2492, found 475.2489; HPLC purity = 98.0%.

Supplementary Material

Refer to Web version on PubMed Central for supplementary material.

Acknowledgements

Abbreviations Used:

PNC	perinucleolar compartment
MMPI	metalloproteinase inhibitors
RNP	ribonucleoprotein particles
LLPS	liquid–liquid phase separation
lncRNA	long noncoding RNA
hnRNP	heterogeneous nuclear ribonucleoproteins
PTBP1	polypyrimidine tract-binding protein 1
PTB	polypyrimidine tract-binding
PTBP	polypyrimidine tract-binding protein
MLSMR	Molecular Libraries Small Molecule Repository

HCA	high-content assay
MLM	mouse liver microsomes
RPMI	Roswell Park Memorial Institute
FBS	fetal bovine serum
IACUC	institutional animal care and use committee
HESI	heated electrospray source ionization
MDF	mass-directed fraction collection

REFERENCES

1. Jiang WG; Sanders AJ; Katoh M; Ungefroren H; Gieseler F; Prince M; Thompson SK; Zollo M; Spano D; Dhawan P; Sliva D; Subbarayan PR; Sarkar M; Honoki K; Fujii H; Georgakilas AG; Amedei A; Niccolai E; Amin A; Ashraf SS; Ye L; Helferich WG; Yang X; Boosani CS; Guha G; Ciriolo MR; Aquilano K; Chen S; Azmi AS; Keith WN; Bilsland A; Bhakta D; Halicka D; Nowsheen S; Pantano F; Santini D Tissue invasion and metastasis: Molecular, biological and clinical perspectives. Semin. Cancer Biol 2015, 35, S244–S275. [PubMed: 25865774]

2. Fares J; Fares MY; Khachfe HH; Salhab HA; Fares Y Molecular principles of metastasis: a hallmark of cancer revisited. Signal Transduction and Targeted Ther. 2020, 5 (1), 28.

3. Chaffer CL; Weinberg RA A perspective on cancer cell metastasis. Science 2011, 331 (6024), 1559–1564. [PubMed: 21436443]

4. Hayes E; Nicholson RI; Hiscox S Acquired endocrine resistance in breast cancer: implications for tumour metastasis. Front Biosci (Landmark Ed) 2011, 16, 838–848. [PubMed: 21196206]

5. Costanzo ES; Sood AK; Lutgendorf SK Biobehavioral influences on cancer progression. Immunol. Allergy Clin. North Am 2011, 31 (1), 109–132. [PubMed: 21094927]

6. Kraljevic Pavelic S; Sedic M; Bosnjak H; Spaventi S; Pavelic K Metastasis: New perspectives on an old problem. Mol. Cancer 2011, 10 (1), 22. [PubMed: 21342498]

7. Hoon DSB; Ferris R; Tanaka R; Chong KK; Alix-Panabières C; Pantel K Molecular mechanisms of metastasis. J. Surg. Oncol 2011, 103 (6), 508–517. [PubMed: 21480243]

8. Anderson RL; Balasas T; Callaghan J; Coombes RC; Evans J; Hall JA; Kinrade S; Jones D; Jones PS; Jones R; Marshall JF; Panico MB; Shaw JA; Steeg PS; Sullivan M; Tong W; Westwell AD; Ritchie JWA A framework for the development of effective anti-metastatic agents. Nature Reviews Clinical Oncology 2019, 16 (3), 185–204.

9. Fontebasso Y; Dubinett SM Drug development for metastasis prevention. Crit. Rev. Oncog 2015, 20 (5-6), 449–473. [PubMed: 27279241]

10. Lyu Y; Xiao Q; Yin L; Yang L; He W Potent delivery of an MMP inhibitor to the tumor microenvironment with thermosensitive liposomes for the suppression of metastasis and angiogenesis. Signal Transduction and Targeted Ther. 2019, 4 (1), 26.

11. Clézardin P Mechanisms of action of bisposphonates in oncology: a scientific concept evolving from antiresorptive to anticancer activities. Bonekey reports 2013, 2, 267–267. [PubMed: 24422040]

12. Lee JJ; Chu E Sequencing of antiangiogenic agents in the treatment of metastatic colorectal cancer. Clin. Colorectal Cancer 2014, 13 (3), 135–144. [PubMed: 24768040]

13. Norton JT; Wang C; Gjidoda A; Henry RW; Huang S The perinucleolar compartment is directly associated with DNA. J. Biol. Chem 2009, 284 (7), 4090–4101. [PubMed: 19015260]

14. Yap K; Mukhina S; Zhang G; Tan JSC; Ong HS; Makeyev EV A Short tandem repeat-enriched RNA assembles a nuclear compartment to control alternative splicing and promote cell survival. Mol. Cell 2018, 72 (3), 525–540 e13. [PubMed: 30318443]

15. Pollock C; Huang S The perinucleolar compartment. J. Cell. Biochem 2009, 107 (2), 189–193. [PubMed: 19288520]

16. Slusarczyk A; Kamath R; Wang C; Anchel D; Pollock C; Lewandowska MA; Fitzpatrick T; Bazett-Jones DP; Huang S Structure and function of the perinucleolar compartment in cancer cells. Cold Spring Harb. Symp. Quant. Biol 2010, 75, 599–605. [PubMed: 21289045]

17. Kamath RV; Thor AD; Wang C; Edgerton SM; Slusarczyk A; Leary DJ; Wang J; Wiley EL; Jovanovic B; Wu Q; Nayar R; Kovarik P; Shi F; Huang S Perinucleolar compartment prevalence has an independent prognostic value for breast cancer. Cancer Res. 2005, 65 (1), 246–253. [PubMed: 15665301]

18. Frankowski KJ; Wang C; Patnaik S; Schoenen FJ; Southall N; Li D; Teper Y; Sun W; Kandela I; Hu D; Dextras C; Knotts Z; Bian Y; Norton J; Titus S; Lewandowska MA; Wen Y; Farley KI; Griner LM; Sultan J; Meng Z; Zhou M; Vilimas T; Powers AS; Kozlov S; Nagashima K; Quadri HS; Fang M; Long C; Khanolkar O; Chen W; Kang J; Huang H; Chow E; Goldberg E; Feldman C; Xi R; Kim HR; Sahagian G; Baserga SJ; Mazar A; Ferrer M; Zheng W; Shilatifard A; Aubé J; Rudloff U; Marugan JJ; Huang S Metarrestin, a perinucleolar compartment inhibitor, effectively suppresses metastasis. Sci. Transl. Med 2018, 10 (441).

19. Metarrestin (ML-246) in Subjects With Metastatic Solid Tumors. https://ClinicalTrials.gov/show/NCT04222413: 2020.

20. Huang S High content assay for compounds that inhibit the assembly of the perinucleolar compartment. https://pubchem.ncbi.nlm.nih.gov/bioassay/2417.

21. Norton JT; Titus SA; Dexter D; Austin CP; Zheng W; Huang S Automated high-content screening for compounds that disassemble the perinucleolar compartment. J. Biomol. Screen 2009, 14 (9), 1045–1053. [PubMed: 19762548]

22. Roth HJ; Eger K Synthese von 2-Amino-3-cyano-pyrrolen. Arch. Pharm 1975, 308 (3), 179–185.

23. Girgis NS; Jørgensen A; Pedersen EB Phosphorus pentoxide in organic synthesis, VII. Synthesis of 3-aryl-3,7-dihydro-4H-pyrrolo[2,3-d]pyrimidin-4-imines. Liebigs Ann. Chem 1983, 1983 (12), 2066–2072.

24. Yumoto M; Kawabuchi T; Sato K; Takashima M 2-Aminopyrrole derivatives and method for their preparation. 1998, Japanese Patent JP 10316654.

25. Fischer RW; Misun M Large-scale synthesis of a pyrrolo[2,3-d]pyrimidine via Dakin–West reaction and Dimroth rearrangement. Org. Process Res. Dev 2001, 5 (6), 581–586.

26. https://dtp.cancer.gov/databases_tools/compare.htm.

27. Vilimas T; Wang AQ; Patnaik S; Hughes EA; Singleton MD; Knotts Z; Li D; Frankowski K; Schlomer JJ; Guerin TM; Springer S; Drennan C; Dextras C; Wang C; Gilbert D; Southall N; Ferrer M; Huang S; Kozlov S; Marugan J; Xu X; Rudloff U Pharmacokinetic evaluation of the PNC disassembler metarrestin in wild-type and Pdx1-Cre;LSL-KrasG12D/+; Tp53R172H/+ (KPC) mice, a genetically engineered model of pancreatic cancer. Cancer Chemother. Pharmacol 2018, 82 (6), 1067–1080. [PubMed: 30306263]

28. Padilha EC; Shah P; Wang AQ; Singleton MD; Hughes EA; Li D; Rice KA; Konrath KM; Patnaik S; Marugan J; Rudloff U; Xu X Metabolism and pharmacokinetics characterization of metarrestin in multiple species. Cancer Chemother. Pharmacol 2020, 85 (4), 805–816. [PubMed: 32185484]

29. Shah P; Siramshetty VB; Zakharov AV; Southall NT; Xu X; Nguyen DT Predicting liver cytosol stability of small molecules. J. Cheminform 2020, 12 (1), 21. [PubMed: 33431020]

30. Shah P; Kerns E; Nguyen DT; Obach RS; Wang AQ; Zakharov A; McKew J; Simeonov A; Hop CE; Xu X An automated high-throughput metabolic stability assay using an integrated high-resolution accurate mass method and automated data analysis software. Drug. Metab. Dispos 2016, 44 (10), 1653–1661. [PubMed: 27417180]

31. Sun H; Nguyen K; Kerns E; Yan Z; Yu KR; Shah P; Jadhav A; Xu X Highly predictive and interpretable models for PAMPA permeability. Bioorg. Med. Chem 2017, 25 (3), 1266–1276. [PubMed: 28082071]
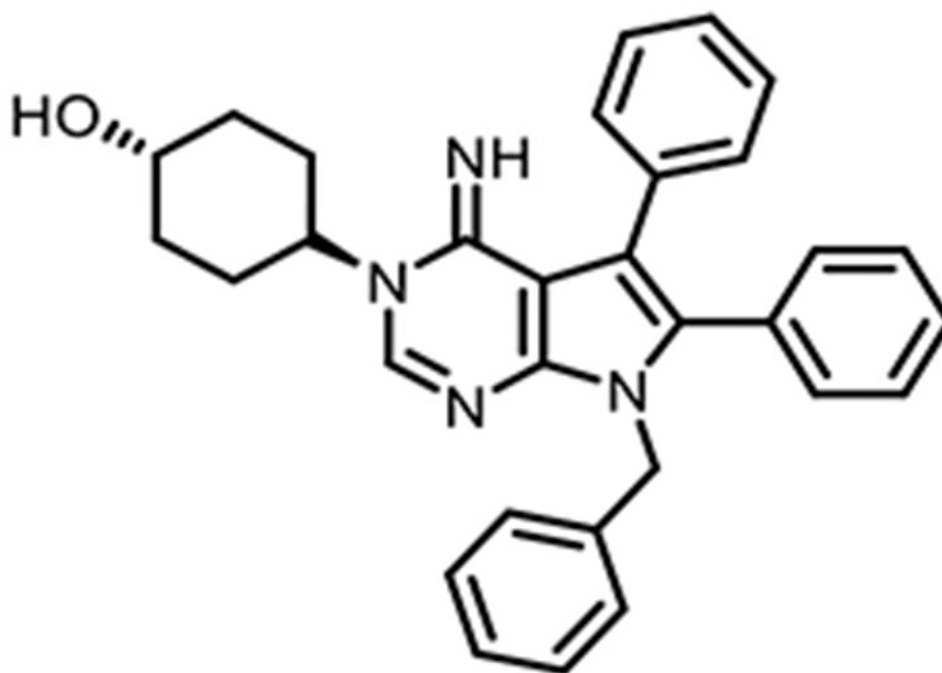
Figure 1.
The structure of metarrestin (NCATS-SM0590).
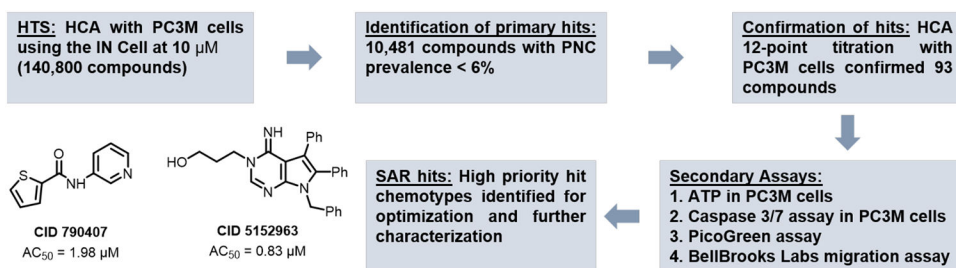
Figure 2.
Workflow for identification of novel, non-cytotoxic small molecules that cause PNC reduction.
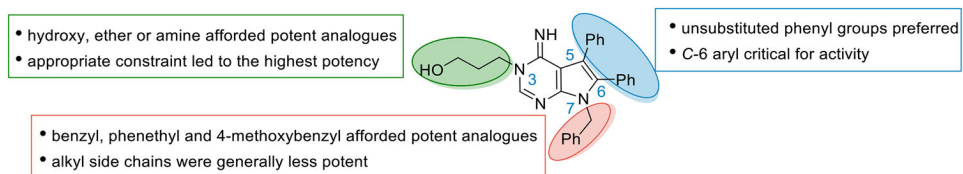
Figure 3.
Structure–activity relationship summary and notable trends identified.
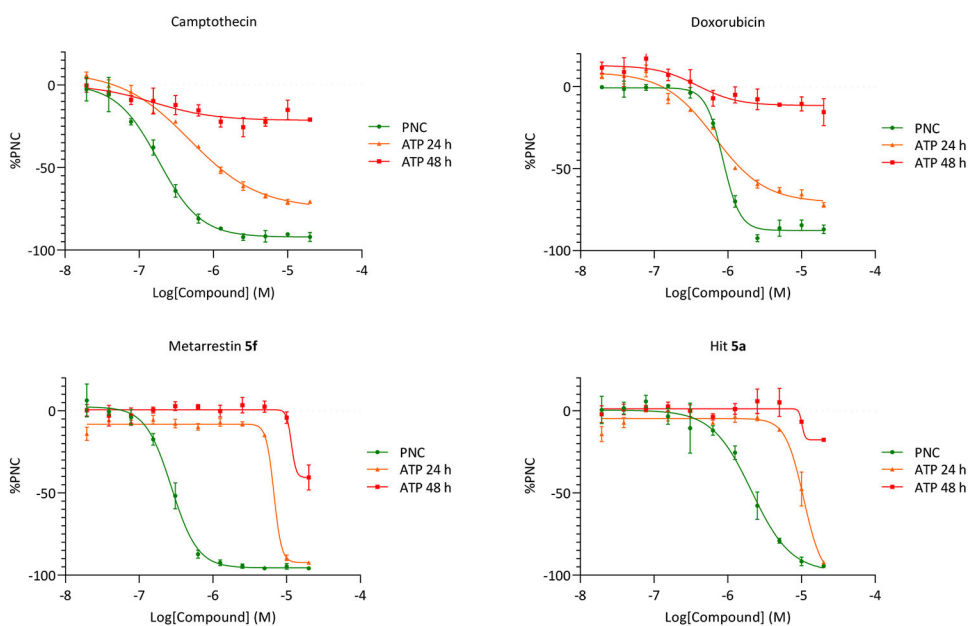
Figure 4.
Concentration-dependent % PNC reduction by analogues **5f, 5a**, camptothecin and doxorubicin in PC3M-GFP cells at 24 h. Overlaid are concentration-dependent effect on ATP levels at 24 h and 48 h in the same cells.
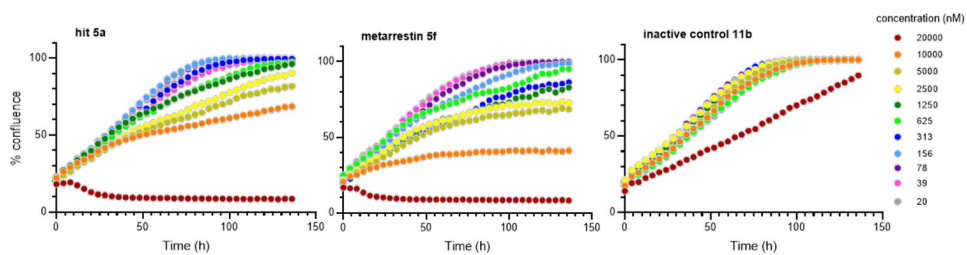
Figure 5.
Effect of compounds hit **5a**, lead **5f** (metarrestin) and PNC inactive control **11b** on the growth of PC3M-PTB-GFP cells at 12 doses from 20 nM to 20 μM (1:2 dilutions) plotted every 4 h over a period of 130 h.
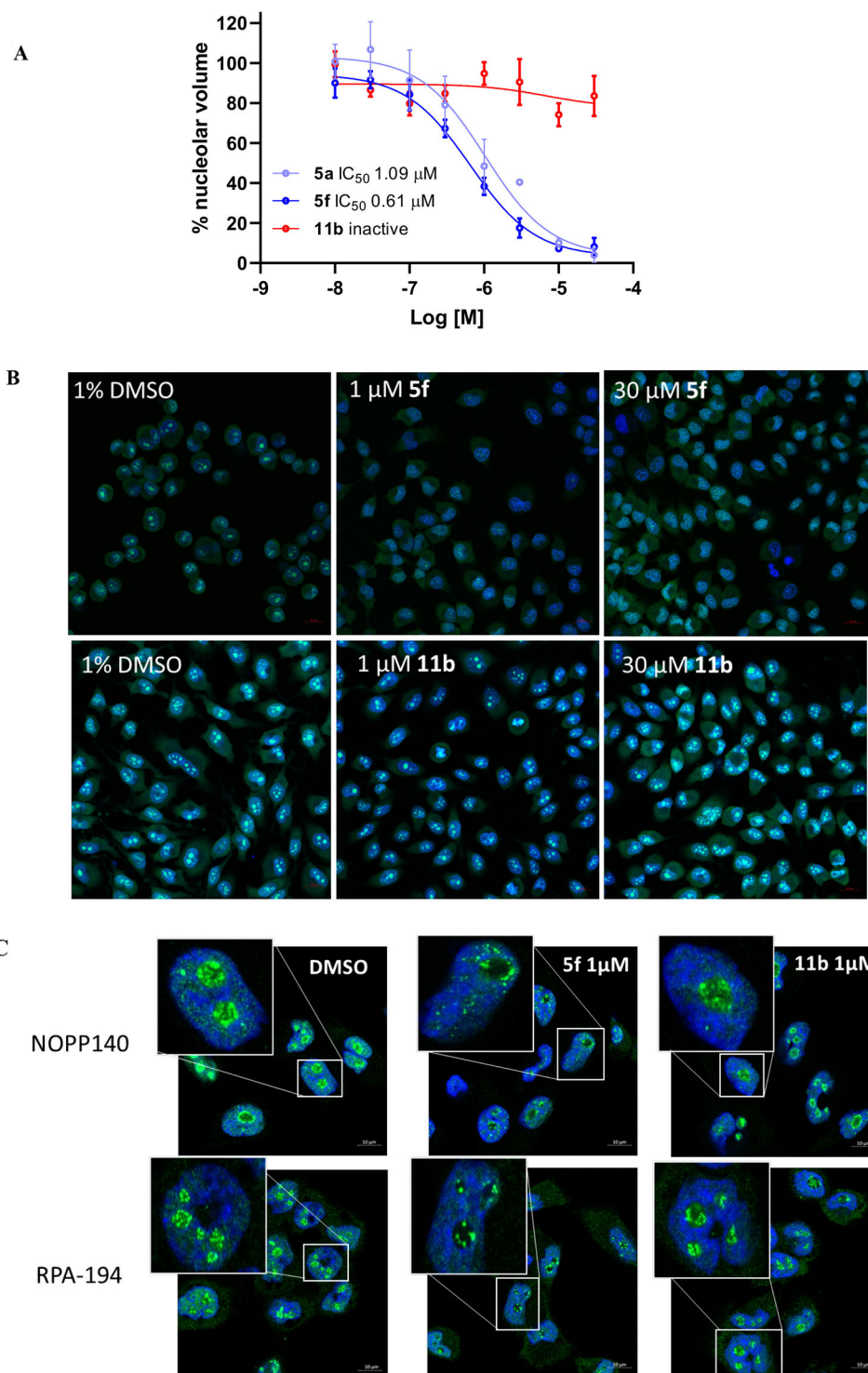
Figure 6.

A. Concentration-dependent reduction of nucleolar volume in PC3M cells with hit **5a**, **5f** (metarrestin) and inactive control **11b**. **B**. Images of nucleoli using Nucleolar-ID® Green Detection Kit (Enzo) after treatment with **5f** (metarrestin) and inactive control **11b** at 1 and 30 μM compared to control (1% DMSO). **C. 5f** (metarrestin) selectively alters nucleolar

architecture in PC3M cells. Confocal microscopy images of the PC3M cells treated with 1 μM of **5f** and PNC inactive analog **11b** for 1 hour and stained with RNA synthesis marker RP-194 (large subunit of polymerase I; bottom in green) and ribosomal pre-assembly regulator NOPP140 (top in green). The nucleus is in blue. Scale bar indicates 10 μm.
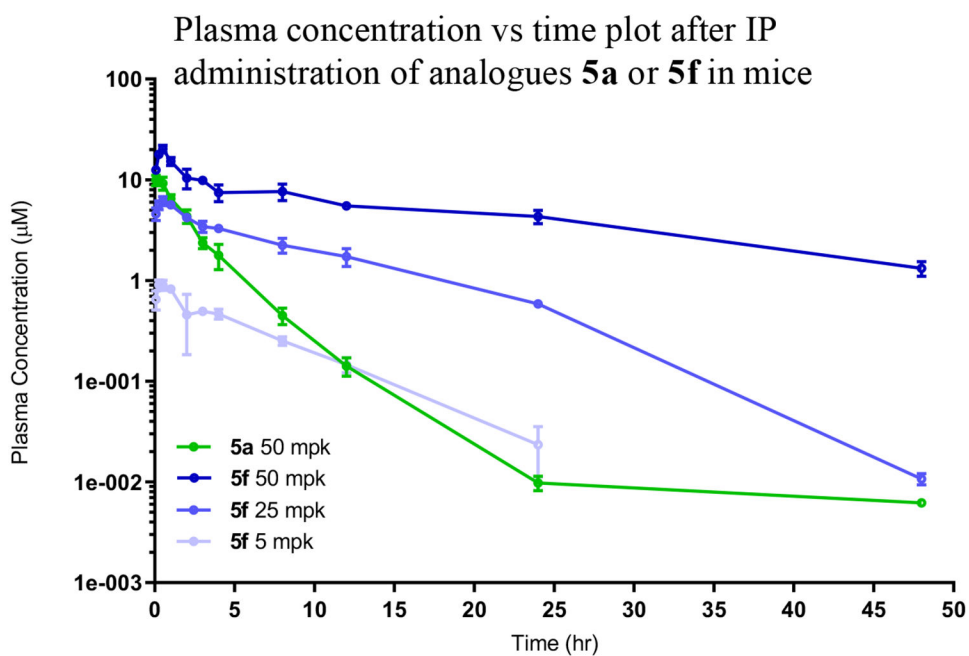
Figure 7.
Plasma concentration vs time plot after IP administration of analogues **5a** or **5f** in male C57BL/6 @ 50 mpk; and analogue **5f** in 5 and 25 mpk in female BALB/c mice. **5f** was formulated at 2.5/0.5 mg/mL with 5-10% NMP + 20% PEG400 + 70-75% (25%HP-β-CD in water). **5a** was formulated at 5 mg/mL with 10% DMAC+5% Solutol HS 15+ 85% Saline.
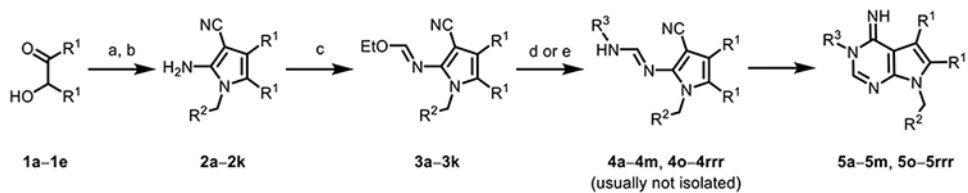
Scheme 1. General synthetic sequence to fully substituted pyrrole analogues.[a]

[a] Reagents and conditions: (a) $R^2CH_2NH_2$ (1.0 or 1.5 equiv), HCl (12 mol %) or triflouroacetic acid (5 mol %), toluene, reflux; (b) malononitrile (2.0–3.0 equiv), toluene or EtOH, reflux, 33–75% yield over two steps; (c) triethylorthoformate (10.0–15.0 equiv), neat, 70 °C, 20–81% yield; (d) R^3NH_2 (1.0–5.0 equiv), MeOH, 65 °C, 13–98% yield; (e) R^3NH_2 (2.0–5.0 equiv), KOt-Bu or NaOt-Bu or Et$_3$N (1.0–3.0 equiv), MeOH, 65 °C, 14–92% yield.
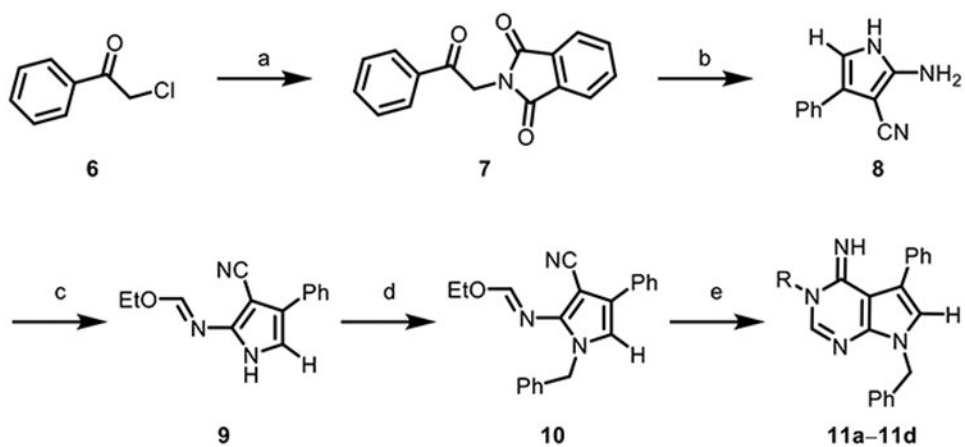
Scheme 2. Synthetic sequence to monophenylpyrrole analogues.[a]
[a] Reagents and conditions: (a) potassium phthalimide (1.0 equiv), DMF, rt, 83% yield; (b) malononitrile (1.3 equiv), NaOH, MeOH:H₂O (3:1), rt, 62% yield; (c) triethylorthoformate (15.0 equiv), neat, 70 °C, 84% yield; (d) K₂CO₃ (2 equiv), benzyl bromide (1.3 equiv), acetone, 65 °C, 75% yield; (e) RNH₂ (1.0–3.0 equiv), MeOH, 65 °C, 35–77% yield.
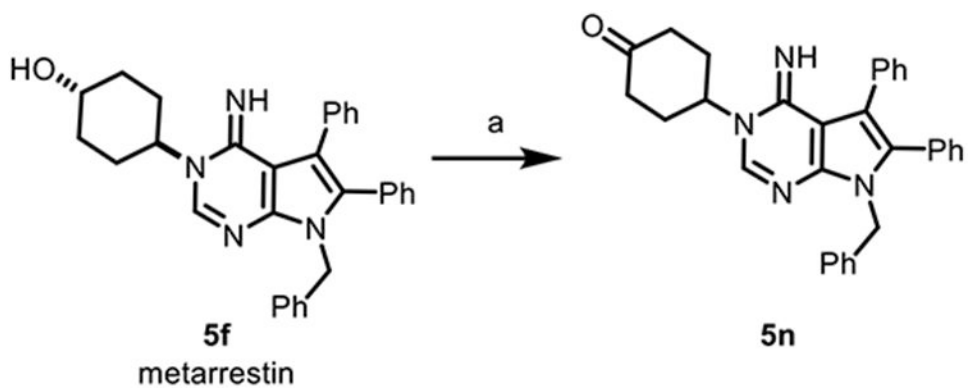
Scheme 3. Conversion of metarrestin 5f to ketone analogue 5n.[a]

[a]Reagents and conditions: (a) Burgess reagent (1.3 equiv), 4 Å molecular sieve, DMSO, rt, 6% yield.
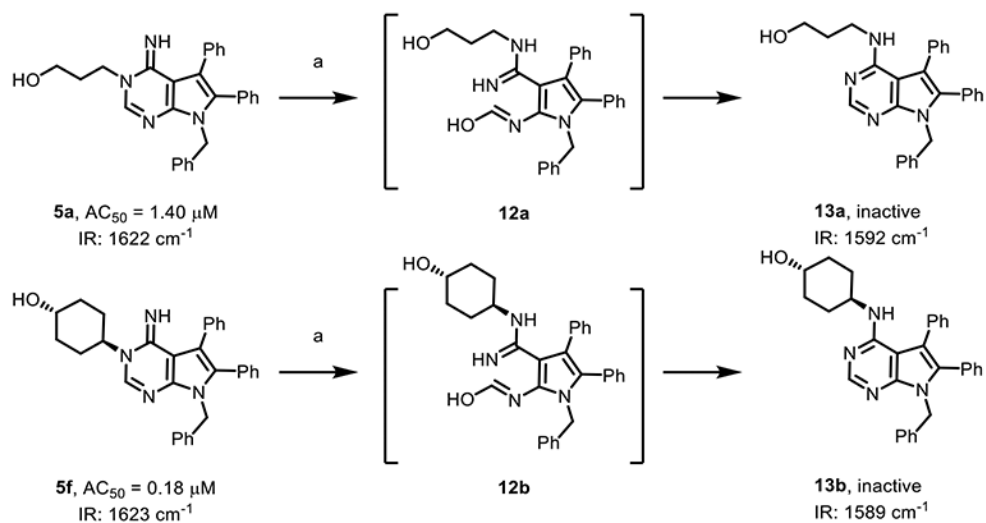
Scheme 4. Conversion of the HTS hit 5a and lead analogue 5f (metarrestin) to the inactive analogues 13a and 13b through a Dimroth rearrangement reaction sequence and characteristic IR absorption bands.

[a]Reagents and conditions: (a) *i*-PrOH/water, 160–180 °C, 2–2.5 h, 80–96% yield.

Table 1.
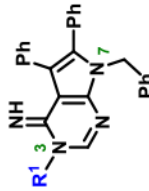
Positive control and key compounds with corresponding PNC inhibitory activity and cytotoxicity.
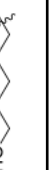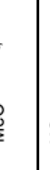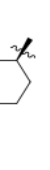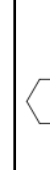
Compound	PNC reduction[a] IC$_{50}$ μM	ATP[b] IC$_{50}$ μM	ATP IC$_{50}$/PNC IC$_{50}$ (window)
Camptothecin	0.19	0.48	2.5
Doxorubicin	0.86	0.66	0.76
5a	1.88	10.86	5.8
5f	0.20	7.65	38.3

[a] PNC reduction in PC3M cells, average of n = 3;

[b] cytotoxicity assessment using the ATPlite[TM] luminescence assay, average of n = 3

Table 2.

Survey of *N-3* substitutions on the *N-7* benzyl substituted pyrrole scaffold.

Compound	R¹	PNC reduction[a]		cLogP[d]	Permeability ($\times 10^{-6}$ cm/sec)[e]	MLM $T_{1/2}$ (mins ± SD)
		IC$_{50}$ (μM)	pIC$_{50}$ ± SD			
5a	HO~	1.88[b]	5.73 ± 0.07[b]	4.04	>1000	25 ± 3.6
5b	HO~	0.83	6.08 ± 0.03	3.82	>1000	25.1 ± 11.8
5c	HO~	4.30	5.37 ± 0.03	4.00	>1000	7.7 ± 0.8
5d	HO~	3.22	5.50 ± 0.10	4.53	>1000	9 ± 0.6
5e	MeO~	9.31	5.03 ± 0.06	4.58	>1000	9.5 ± 0.5
5f (metarrestin)	HO	0.20[b]	6.75 ± 0.24[b]	4.34	>1000	120 ± 0
5g	HO	0.83[b]	6.08 ± 0.0[b]	4.34	>1000	52.3 ± 8.3
5h	OH	0.51	6.30 ± 0.06	5.22	>1000	28.8 ± 3.9
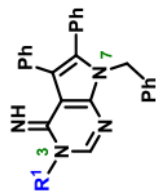
Compound	R[1]	PNC reduction[a]		cLogP[d]	Permeability ($\times 10^{-6}$ cm/sec)[e]	MLM $T_{1/2}$ (mins ± SD)
		IC_{50} (μM)	pIC_{50} ± SD			
5i		2.00	5.70 ± 0.05	5.54	>1000	2.4 ± 0.8
5j		0.93	6.03 ± 0.03	5.58	>1000	17.4 ± 2.2
5k		>20	—	5.70	<1	5.5 ± 0.8
5l		>20	—	5.71	606	6.4 ± 0.3
5m		0.25	6.60 ± 0.06	5.06	ND[f]	ND[f]
5n		0.30	6.52 ± 0.03	3.94	>1000	38.2 ± 3.7
5o		0.32[b]	6.50 ± 0.03[b]	4.03	>1000	29.6 ± 3.5
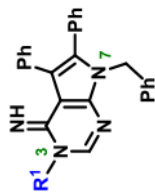
Compound	R¹	PNC reduction[a]		cLogP[d]	Permeability (× 10⁻⁶ cm/sec)[e]	MLM T$_{1/2}$ (mins ± SD)
		IC$_{50}$ (μM)	pIC$_{50}$ ± SD			
5p		10.86	4.97 ± 0.06	4.65	>1000	7.1 ± 0.7
5q		10.86	4.97 ± 0.06	4.22	>1000	5.3 ± 0.3
5r		9.31	5.03 ± 0.06	4.81	>1000	6.5 ± 0.6
5s		>20	—	3.53	7.2	113.4 ± 11.5
5t		23.40	4.63 ± 0.06	5.17	>1000	4.3 ± 1
5u		6.59	5.18 ± 0.06	5.56	445.1	29.9 ± 2.2
5v		>20	—	3.9	164.7	ND[f]
5w		2.95	5.53 ± 0.06	4.77	1358	14.3 ± 0.6
5x		12.59	4.90 ± 0[c]	4.94	319.6	120 ± 0

Compound	R¹	PNC reduction[a]		cLogP[d]	Permeability ($\times 10^{-6}$ cm/sec)[e]	MLM T$_{1/2}$ (mins ± SD)
		IC$_{50}$ (μM)	pIC$_{50}$ ± SD			
5y		5.01	5.30 ± 0[c]	6.25	ND[f]	32.2 ± 6.8
5z		23.40	4.63 ± 0.06	6.83	>1000	14 ± 1.6
5aa		25.12	4.60 ± 0[c]	6.15	1196.9	12.1 ± 3.2

[a]PNC reduction in PC3M cells, average of n = 3 unless noted otherwise

[b]n = 6

[c]identical IC50 value in all three runs

[d]calculated using ChemDraw 12.0

[e]PAMPA Pion Lipid at pH = 7.4

[f]ND Not Determined.

Table 3.

Survey of *N-3* substitutions on the *N-7* phenethyl substituted pyrrole scaffold.

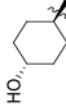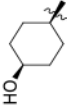| Compound	R[1]	PNC reduction[a]		cLogP	Permeability (× 10^{-6} cm/sec)[d]	MLM T$_{1/2}$ (mins ± SD)
		IC$_{50}$ (µM)	pIC$_{50}$ ± SD			
5bb		1.31	5.88 ± 0.03	4.40	>1000	32.6 ± 1.7
5cc		4.47	5.35 ± 0[b]	4.58	>1000	6.6 ± 0.4
5dd		0.34	6.47 ± 0.03	4.92	>1000	120 ± 0
5ee		2.72	6.02 ± 0.03	6.11	ND[e]	4.3 ± 0.1
5ff		0.96	5.00 ± 0	4.61	>1000	14.5 ± 1.7
5gg		10.00	5.00 ± 0	5.23	1229.2	7.3 ± 1.3
5hh		10.86	4.97 ± 0.06	4.80	>1000	6.9 ± 0.6
5ii		7.94	5.10 ± 0	5.39	>1000	8.4 ± 2.3
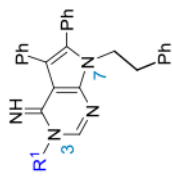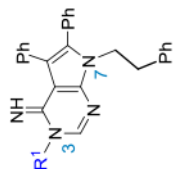
| Compound | R[1] | PNC reduction[a] | | cLogP | Permeability ($\times$ 10^{-6} cm/sec)[d] | MLM $T_{1/2}$ (mins ± SD) |
		IC$_{50}$ (μM)	pIC$_{50}$ ± SD			
5jj		12.59	4.9 ± 0	5.51	294.4	77.9 ± 12.4

[a] PNC reduction in PC3M cells, average of n = 3;
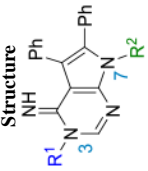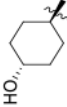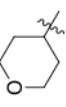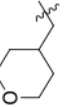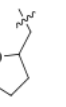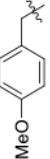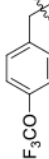
[b] identical IC$_{50}$ value in all three runs
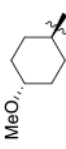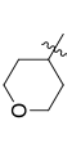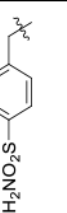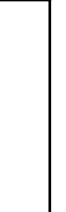
[c] calculated using ChemDraw 12.0

[d] PAMPA Pion Lipid at pH = 7.4

[e] ND Not Determined.

Table 4.

Survey of *N*-3 substitutions on the *N*-7(*p*-substituted benzyl)-substituted pyrrole scaffold.

Compound	R¹	R²	PNC reduction [a] IC₅₀ (μM)	PNC reduction [a] pIC₅₀ ± SD	cLogP	Permeability (× 10⁻⁶ cm/sec) [c]	MLM T₁/₂ (mins ± SD)
5kk	HO	MeO-benzyl	2.17	5.67 ± 0.06	3.96	>1000	19.9 ± 0.5
5ll	HO		2.83	5.55 ± 0.05	3.74	>1000	31.1 ± 2.1
5mm	HO (cyclohexyl)		0.16	6.80 ± 0.06	4.26	>1000	120 ± 0
5nn	(tetrahydropyran)		0.17	6.76 ± 0	3.95	ND [d]	ND [d]
5oo	(tetrahydropyran)		9.31	5.03 ± 0.06	4.57	1266.09	13 ± 0.3
5pp	(tetrahydrofuran)		8.63	5.07 ± 0.06	4.73	>1000	9.4 ± 0.8
5qq	HO	F₃CO-benzyl	4.40	5.36 ± 0.10	5.07	>1000	ND [d]
5rr	HO (cyclohexyl)		0.64	6.20 ± 0.06	5.37	1246.89	120 ± 0
5ss	HO (cyclohexyl)		3.42	5.47 ± 0.03	5.37	1246.89	120 ± 0

Compound	Structure R^1	R^2	PNC reduction[a] IC$_{50}$ (µM)	pIC$_{50}$ ± SD	cLogP	Permeability (× 10^{-6} cm/sec)[c]	MLM T$_{1/2}$ (mins ± SD)
5tt	MeO cyclohexyl		1.09	5.96 ± 0	6.09	ND[d]	ND[d]
5uu	oxane-methyl	H$_2$NO$_2$S-benzyl	0.96	6.02 ± 0.03	5.06	>1000	72 ± 6
5vv	HO-propyl		>20	—	2.21	<1	26.7 ± 2.3
5ww	oxane		1.18	5.93 ± 0.06	2.19	1	70 ± 3
5xx	oxane		25.56	4.60 ± 0.10	2.81	<1	8.3 ± 1.5

[a] PNC reduction in PC3M cells, average of n = 3

[b] calculated using ChemDraw 12.0

[c] PAMPA Pion Lipid at pH = 7.4

[d] ND Not Determined.

Table 5.

Survey of active *N-3* substitutions combined with an investigation of *N-7* alkyl substitution.

Compound	Structure		PNC reduction[a]		cLogP[b]	Permeability (× 10⁻⁶ cm/sec)[c]	MLM T₁/₂ (mins ± SD)
	R¹	R²	IC₅₀ (μM)	pIC₅₀ ± SD			
5yy			27.73	4.57 ± 0.12	5.18	>1000	ND[d]
5zz			2.73	5.56 ± 0	5.48	ND[d]	ND[d]
5aaa			2.02	5.70 ± 0.06	5.16	ND[d]	ND[d]
5bbb			6.31	5.20 ± 0	3.5	>1000	25.4 ± 1.7
5ccc			0.83	6.08 ± 0.03	3.49	>1000	68 ± 20
5ddd			34.35	4.47 ± 0.06	4.11	>1000	16.3 ± 0.9

[a] PNC reduction in PC3M cells, average of n = 3

[b] calculated using ChemDraw 12.0

[c] PAMPA Pion Lipid at pH = 7.4

[d] ND Not Determined.

Table 6.

Survey of diphenylpyrrole replacement SAR.

Compound	R[1]	Structure Pyrrolopyrimidine scaffold	PNC reduction[a] IC$_{50}$ (μM)	PNC reduction[a] pIC$_{50}$ ± SD	cLogP[b]	Permeability (× 10^{-6} cm/sec)[c]	MLM T$_{1/2}$ (mins ± SD)
5eee			>20	—	3.67	>1000	73.2 ± 14.6
5fff			>20	—	3.9	>1000	21.6 ± 6.2
5ggg			>20	—	4.2	196	ND[d]
5hhh			>20	—	5.08	>1000	29.2 ± 6.9
5iii			>20	—	4.91	>1000	ND[d]
5jjj			>20	—	3.88	>1000	58.7 ± 2.9
5kkk			>20	—	4.07	>1000	16.5 ± 1.5
5lll			>20	—	3.97	ND[d]	ND[d]

Compound	Structure		PNC reduction[a]		cLogP[b]	Permeability (× 10⁻⁶ cm/sec)[c]	MLM T₁/₂ (mins ± SD)
	R¹	Pyrrolopyrimidine scaffold	IC₅₀ (µM)	pIC₅₀ ± SD			
11a			>20	—	2.32	1270.9	9.2 ± 1.7
11b			>20	—	2.53	1729	5.2 ± 0.7
11c			>20	—	3.64	1737	3 ± 0.1
11d			>20	—	4.66	>1000	2.9 ± 0.3
5mmm			>20	—	1.61	609.3	120 ± 0
5nnn			>20	—	1.91	<1	120 ± 0
5ooo			>20	—	1.59	1683.3	26.9 ± 4.8
5ppp			>20	—	2.81	883.12	4.5 ± 0.1
5qqq			>20	—	3.11	204.6	86.5 ± 4
5rrr			>20	—	2.8	ND[d]	ND[d]

[a] PNC reduction in PC3M cells, average of n = 3

[b] calculated using ChemDraw 12.0

[c]PAMPA Pion Lipid at pH = 7.4

[d]ND Not Determined.

Table 7.

Exploration of core structure modifications.

Compound	Structure	PNC reduction[a]		cLogP[b]	Permeability ($\times 10^{-6}$ cm/sec)[c]	MLM T$_{1/2}$ (mins ± SD)
		IC$_{50}$ (μM)	pIC$_{50}$ ± SD			
4f		>20	—	5.29	327.5	11.2 ± 1.2
3a		>20	—	5.9	ND[d]	ND[d]
2a		>20	—	5.12	62	13.3 ± 0.7
13a		>20	—	5.69	ND[d]	ND[d]
13b		>20	—	6.02	ND[d]	ND[d]

[a]PNC reduction in PC3M cells, average of n = 3

[b] calculated using ChemDraw 12.0

[c] PAMPA Pion Lipid at pH = 7.4

[d] ND Not Determined.

Table 8.

Profiling of lead compound **5f** (metarrestin) in the Psychoactive Drug Screening Program's comprehensive binding affinity panel.[a]

Target	Ki (nM)	Target	Ki (nM)	Target	Ki (nM)	Target	Ki (nM)	Target	Ki (nM)	Target	Ki (nM)
5-HT1A	NA	5-HT3	NA	Alpha2A	NA	D1	NA	GABAA	NA	M4	NA
5-HT1B	NA	5-HT5A	NA	Alpha2B	NA	D2	NA	H1	3,557	M5	NA
5-HT1D	NA	5-HT6	NA	Alpha2C	1,215	D3	NA	H2	NA	MOR	NA
5-HT1E	NA	5-HT7	NA	Beta1	NA	D4	NA	KOR	NA	NET	NA
5-HT2A	NA	Alpha1A	NA	Beta2	NA	D5	NA	M1	NA	SERT	NA
5-HT2B	NA	Alpha1B	NA	Beta3	NA	DAT	3,411	M2	NA	Sigma1	NA
5-HT2C	NA	Alpha1D	3,260	BZP rat Brain	NA	DOR	NA	M3	NA	Sigma2	244

[a] Numerical entries are Ki values (nM), NA = no significant activity in primary binding assay (< 50% radioligand displacement at 10,000 nM test compound concentration).

Table 9.

In vitro ADME data for HTS hit **5a**, lead **5f** (metarrestin), and analogues **5n**, **5o** and **5dd**.

Compound	PNC IC$_{50}$	MLM T$_{1/2}$	PAMPA pH 7.4	Aqueous kinetic solubility
unit	μM	min	10^{-6} cms^{-1}	μg/mL (μM)
hit **5a**	1.88	25	>1000	>64 (>147)
5f (metarrestin)	0.20	>120	>1000	>47 (>99)
5n	0.30	38	>1000	36 (75)
5o	0.32	30	>1000	8.3 (18)
5dd	0.34	>120	>1000	>65 (>132)

Table 10.

Summary of PK parameters[a] for **5a** and **5f**.

Compound Dose	species	C_{max} (μM)	T_{max} (hr)	C_{48h} (μM)	Terminal $T_{1/2}$ (min)	AUC_{48h} (hr•μM)
5a @ 50mpk	male C57BL/6	9.90	0.08	0.006	4.10	26.00
5f @ 50mpk	male C57BL/6	20.26	0.5	1.32	16.4	231.77
5f @ 5 mpk	female BALB/c	0.91	0.25	BLQ[b]	4.64	6.08
5f @ 25 mpk	female BALB/c	6.17	0.5	0.011	5.52	57.64

[a]Comparison of mouse pharmacokinetic parameters of hit **5a** and lead **5f** (metarrestin) after IP dose of 50 mpk in male C57BL/6 mice (experiments were carried out in triplicate).

[b]BLQ = below the limit of quantification.